NATIONAL UNIVERSITY OF IRELAND, CORK

Time in Quantum Mechanics and the Page–Wootters Formalism

by

Guido De Rosa

Thesis submitted for the degree of
Master of Science
in the Department of Physics

Supervisor: Dr. Andreas Ruschhaupt
Head of Department: Prof. John McInerney

2023

Time in Quantum Mechanics and the Page–Wootters Formalism

Guido De Rosa

gderosa@umail.ucc.ie

Contents

List of Figures

List of Tables

Declaration of Authorship

This is to certify that the work I am submitting is my own and has not been submitted for another degree, either at University College Cork or elsewhere. All external references and sources are clearly acknowledged and identified within the contents. I have read and understood the regulations of University College Cork concerning plagiarism.

Student: Guido De Rosa
Date: 5th October 2023

External Examiner:
Prof. J. Gonzalo Muga – Universidad del País Vasco
Internal Examiner:
Dr. Bryan Kelleher – University College Cork and Tyndall National Institute

I owe *Alice* a lot!

Bob

Abstract

This work relates to the *problem of time*, the difficulties of which represent a classic problem in the foundations of quantum mechanics. It can be traced back to the argument, by Wolfgang Pauli, on the impossibility of defining time as a quantum observable, due to contradictions related to the spectrum of energy (1933).

A number of models, aimed at overcoming such difficulties, have been developed over the decades, and are reviewed in the present work.

Particular attention is paid to the theoretical framework first proposed by Page and Wootters in 1983 (later improved by Lloyd, Giovannetti and Maccone and others), where time and unitary evolution only emerge in terms of *entanglement* between non-interacting subsystems of an otherwise stationary "universe", and where one of the subsystems acts as a "clock" for the "rest" of it.

Discrete clocks, within the framework, are implemented, using existing results related to quantum systems described by finite-dimensional Hilbert spaces. The formalism is then applied to some simple quantum systems, and a numerical comparison is performed between the Page–Wootters model and the predictions of "ordinary" quantum mechanics. The Page and Wootters formalism is also applied to *non-unitary* systems, such as those modeled in absorption theories of time-of-arrival at a particle detector. A comparison is made between the predictions of the two models as well. The case of a differing result opens the way to the potential of an experimental verification. Future lines of research may cover a broader phenomenology, and include a relativistic extension, which is briefly introduced.

Acknowledgements

I have been working towards a Master's degree in Physics while continuing a full-time career as a software engineer and IT professional. I want to thank my colleagues, friends, mentors, managers, in that industry, for their encouragement and intellectual curiosity about my endeavor.

I want to thank my family, friends, adored ones, back in Italy and beyond. Thanks to all those who have supported this journey, beyond my imagination.

Thanks to my fellow postgraduate students, with whom I have shared an office, and long, fruitful conversations; as well as research Staff, and our Senior Collaborator in a special way.

Thanks to my Supervisor, for his extended patience, among other qualities! Thanks to the Examiners.

Also thanks to all those involved in the teaching lab, for the experience as a first-year demonstrator that, if not strictly connected to the topic of this thesis, does remind me where all modern physics ultimately comes from.

I am grateful to Nicole, Paul, Irfan, Antonello, Andreas, Mirek, Paolo, Marco, Jalal, Clarissa, Mark, David, Sergio, Rocco, Bryan, Fedele, Rosario, Trevor, Mossie, Noel, Chris, Tiziano, Ofelia, Sandra, Anthony, Tom, Gonzalo, Paola, Stephen, Lukas, Antonio, Elena, Cian, Beatriz, Jing, John, Nasir, Tamara, Deborah, KC, Nico, Margherita. The list is in no particular order and some names may refer to more than one person. Apologies to all those I may have forgotten.

Chapter 1

Introduction

1.1 Time and the Quantum: an invitation

Time is a fundamental concept in physics, together with space (or *position* within space), matter (or *mass*) and energy.

In quantum mechanics, at least in first quantization, defining the *position* as an observable is unproblematic and somewhat basic. Indeed, representing the quantum state of a particle in terms of coefficients with respect to eigenstates of position is extremely common. Almost always when a *wavefunction* ψ for a state $|\psi\rangle$ is written down, the position representation is assumed, unless otherwise (explicitly) noted:

$$|\psi\rangle = \int \mathrm{d}x' \, \psi(x') \, |x'\rangle \, , \tag{1.1}$$

where[1] $\psi(x') = \langle x'|\psi\rangle$.

As per *mass*, a quantum mechanism that explains how particle acquire mass was theorized by Peter Higgs and others in 1964, and confirmed experimentally in 2012 (ATLAS 2012; CMS 2012; Englert and Brout 1964; Guralnik et al. 1964; Higgs 1964).

Energy, as an observable, is associated with arguably the most important

[1] Here a one-dimensional system is considered, for simplicity: it can be easily verified that more dimensions, and degeneracy, may be taken into account without altering the key concepts.

operator in quantum dynamics: the Hamiltonian.

Time is missing from this picture. As of writing of the present work, there is no general consensus in the physics community on the definition of a quantum operator associated to a time observable, or even only on a particular quantum mechanism that would allow time to "emerge", for example, as an effective quantity.

One may argue that the urge of a consistent quantum description for *all* fundamental measurable quantities, including time, is essentially (if not purely) philosophical, until experiments show (or at least are proposed to show) "wave-like" or other nonclassical features of time, possibly with analogies to what is already observed along the "position axis". Interestingly, accounts exist of experiments, with atomic beams through temporal double-slits, showing diffraction patterns in time (Szriftgiser et al. 1996). Moreover, signatures of *time-crystalline order* in solids and trapped ions have been recently observed (Choi et al. 2017; Rovny et al. 2018a,b; Zhang et al. 2017).

With all the above in mind, the relation between time and other quantities (whether they are "quantum observables" in the formal sense or not) is explored in the rest of this section, with reminders about some basic properties that will be useful for the rest of the discussion.

1.1.1 Time and position

Rigorously speaking, the position observable has no special role in quantum mechanics. Eq. (1.1) can be also expanded to

$$|\psi\rangle = \int \mathrm{d}x' \, \psi(x') \, |x'\rangle = \int \mathrm{d}p' \, \tilde{\psi}(p') \, |p'\rangle \ , \tag{1.2}$$

with p and $|p\rangle$ being respectively eigenvalues and eigenvectors of the momentum operator.

By multiplying on the left by $\langle x|$, Eq. (1.1) yields

$$\psi(x) = \int \mathrm{d}x'\, \psi(x')\delta(x - x')\,. \tag{1.3}$$

In general, for an observable with continuous spectrum, in its own eigenbasis, eigenstates are represented as a Dirac deltas (for discrete spectra, the integral is replaced by a discrete sum, and Dirac deltas by Kronecker deltas).

Applying the position operator $\hat{X}$ to the (1.1), then taking the inner product on the left by $\langle x|$, there has

$$\begin{aligned}\left[\hat{X}\psi\right](x) \coloneqq \langle x|\hat{X}|\psi\rangle &= \int \mathrm{d}x'\, \psi(x')x' \langle x|\hat{X}|x'\rangle \\ &= \int \mathrm{d}x'\, \psi(x')\delta(x - x') = x\psi(x)\,. \end{aligned} \tag{1.4}$$

The position (and an observable in general) is represented, in its own eigenbasis, simply as the multiplication of the original wavefunction by the respective variable.

1.1.2 Time and evolution

As a matter of experience, if not anything else, the state of a physical system, either classical or quantum, with all its observable quantities, can be regarded as a function of the instant in *time* (let us call that independent variable t). The same cannot be stated, in general, for any other pair of measurable quantities: the x coordinate is not a function of the y coordinate (or their respective statistical amplitudes, in the quantum realm), and so on. This status of time as the universally independent variable has shaped classical mathematical physics: Galilean transformations do not change time, which remains as an absolute quantity. The Hamiltonian formalism itself is based on this assumption, and the Hamiltonian formalism is at the foundation of quantum mechanics too, which thus inherits — one may argue— all the consequences of treating time as "external" with respect to the other quantities under study. "[The] Hamiltonian method [...] marks out a particular time variable as the canonical conjugate of the Hamiltonian function"

(Dirac 1933).

Emphasizing time as a parameter, the value of a wavefunction (in position representation, for example) can therefore be expressed as $\psi_t(x)$ at each position x and at each time t. Still, it can be regarded as a function of two variables and one may wonder why (after an inessential change of notation), in the identity

$$\psi(x;t) = \int \mathrm{d}x'\,\mathrm{d}t'\,\delta(x-x')\delta(t-t')\psi(x';\,t')\,, \tag{1.5}$$

the term $\delta(t-t')$ cannot be interpreted as the eigenfunction of some time operator, which in turn acts as a simple multiplication by t on this wavefunction $\psi(x;t)$ —which would be, therefore, a wavefunction in "time–position representation".

The fact that $\delta(t-t')$ would be an *improper* eigenfunction is not the blocking issue in this case (it is not, for the position eigenfunction), and the mathematical intricacies related to the continuous spectrum are elegantly resolved by the spectral theory, mainly by Von Neumann (Neumann 1955), which is an integral part of the standard, commonly accepted formulation of quantum mechanics, almost since the early years of the theory.

The main obstacle is instead the *Pauli's objection*, which is only indirectly related to the special status of time as independent variable of "evolution", and directly related to the properties of the spectrum of the Hamiltonian, as will be illustrated in Section 3.1.

1.1.3 Time and energy

In the quest for a quantum time observable, it is tempting to leverage the dualism between position and momentum, evoked in Eq. (1.2). It is well known that the momentum is the infinitesimal generator of spatial translations:

$$\psi(x-\Delta x;\,t) = e^{-\mathrm{i}\Delta x\hat{P}/\hbar}\psi(x;t)\,, \tag{1.6}$$

where the momentum operator is $\hat{p} \equiv -\mathrm{i}\hbar\frac{\partial}{\partial x}$, in position representation.

It is also well known that the Schrödinger equation is equivalent to stating

that the Hamiltonian is the infinitesimal generator of *temporal* translation:

$$\psi(x; t + \Delta t) = e^{-\mathrm{i}\Delta t \hat{H}/\hbar}\psi(x; t)\,. \tag{1.7}$$

The analogy between the two equations above, among other considerations, motivates the requirement that an hypothetical *self-adjoint* time operator should be the canonically conjugate of the Hamiltonian, just like the momentum operator is canonically conjugate to the position one. This would involve a commutation relation between time and energy that is analogous to the one between position and momentum, $[\hat{X}, \hat{P}] = \mathrm{i}\hbar$, and consequently a time–energy uncertainty relation.

Several formulations of such time–energy uncertainty relations have been proposed, although most of them do not rigorously refer to a time operator $\hat{T}$ in their definition of ΔT.

On another note, it is worth stressing that, while equations (1.6) and (1.7) do offer some conceptual motivation towards defining a time observable that is conjugate to the Hamiltonian, they are not sufficient to logically imply its existence. Both Δx and Δt —which quantify the spatial and temporal translations at the core of this discussion— are, once again, mere *parameters* for the *displacement* and *time evolution* operators respectively:

$$\langle x|\mathcal{D}_{\Delta x}|\psi(t)\rangle = \langle x - \Delta x|\psi(t)\rangle, \quad \text{with } \mathcal{D}_{\Delta x} = e^{-\mathrm{i}\Delta x \hat{P}/\hbar} \tag{1.8}$$

$$\langle x|\mathcal{U}_{\Delta t}|\psi(t)\rangle = \langle x|\psi(t + \Delta t)\rangle, \quad \text{with } \mathcal{U}_{\Delta t} = e^{-\mathrm{i}\Delta t \hat{H}/\hbar}\,. \tag{1.9}$$

Even in terms of *position*, Δx is not to be intended as the the spread of the $\hat{X}$ operator in this case. Hence, the analogy between the roles of *parameters* Δx and Δt, with respect to *operators* $\hat{P}$ and $\hat{H}$, cannot be used, alone, to rigorously prove the same analogy between the position operator $\hat{X}$ and some time operator $\hat{T}$, although it is somewhat suggestive.

Whether a quantum time observable can be in principle defined as a self-adjoint operator, or other mathematical frameworks exist that are suitable, possibly satisfying the above conjugation properties, is indeed one of the fundamental

questions within the entire topic of the quantization of time.

Uncertainty relations

The Heisenberg uncertainty principle is at the core of quantum mechanics. It was first introduced in 1927 (Heisenberg 1927), in the form of a position–momentum relation: $p_1 q_1 \sim h$, in his notation. Interestingly, in the same paper, Heisenberg also introduced a *time–energy* uncertainty relation, $E_1 t_1 \sim h$, related to the time at which a transition between two energy levels occurs.

What did Heisenberg mean by t_1? Was that an early formalization of (the "spread" of) a time observable (or "matrix", in the language of Heisenberg's first formulation of quantum mechanics)? In fact, the same question can be raised for the position–momentum relation too. The original formulation of the uncertainty principle was not expressed in terms of standard deviations and mean values of Hermitian operators as we know it today. Heisenberg approach was semi-empirical and, while it turned unsatisfactory from a formal perspective, in some aspects, it had the merit of explicitly dealing with the physics of the disturbance of a measurement device to the measurement itself. Therefore, regardless of the mathematical maturity of its model, the paper did provide convincing phenomenological arguments towards the existence of an uncertainty principle for both the position–momentum *and* the time–energy pair.

As observed in Muga et al. 2007, s. 1.1.3, Heisenberg introduced the equation $\mathbf{Et} - \mathbf{tE} = -\mathrm{i}\hbar$ as "familiar", without really specifying the nature of the matrix $\mathbf{t}$, thus leaving the problem of defining a quantum time observable actually unresolved. Therein, it is argued that the idea of "familiarity" may have originated from the relation between the time span and the frequency[2] width of a signal. Regardless of the status of signal theory in 1927, it is well known, at least in more recent times, that methods like the Fourier analysis are used in Information and Communication engineering to associate a function in the time domain to another

[2]Of course, energy and frequency will be often used interchangeably, being simply related by the the Planck relation $E = h\nu = \hbar\omega$; formulated as early as 1900, and incorporated in all the following research that brought to the foundation of quantum mechanics, including Heisenberg's work.

in the frequency domain; while, in quantum mechanics, the same mathematical operation is generally used to associate a wavefunction in position representation to the corresponding one in momentum representation. This is another suggestive analogy.[3]

Later in 1927, the uncertainty principle was derived in terms of statistical interpretation of quantum observables by Kennard and others (see e.g. Kennard 1927). The clarification of all formal issues has continued until recently (Appleby 1998). However, all this formalization process has regarded position and momentum only —not time and energy.

Mandelstam and Tamm

The formulation of the time–energy uncertainty relations by Mandelstam and Tamm (Mandelstam and Tamm 1945) is considered the least controversial, to the point of being regularly mentioned in standard textbooks. However, they refer to the characteristic times of each specific observable A i.e. the time at which its mean value changes significantly (where "significantly" here means: in the order of its spread ΔA). So this notion of time is *observable-dependent* and does not refer to the time (or the statistical spread of time) at which a particular event happens —as opposed to the Heisenberg paper, which aimed at answering the question: when does a "quantum jump" occur?

In formulas, the characteristic time is defined by Mandelstam and Tamm as

$$\tau_A = \frac{\Delta A}{\mathrm{d}\langle \hat{A} \rangle \Big/ \mathrm{d}t}\,, \tag{1.10}$$

and the uncertainty relation reads:

$$\tau_A \Delta E \geq \frac{\hbar}{2}\,. \tag{1.11}$$

Some limitations of the Mandelstam–Tamm approach will be tackled in Chap-

[3] In Chapter 4, a discrete Fourier transformation will be used indeed to associate a time operator to a frequency operator, in a modified model of quantum mechanics.

ter 4 by further developing models where time–energy relations have to be intended in the sense of "time of occurrence" (of particle detection) and time is represented by a self-adjoint operator.

1.1.4 Time evolution, relativity, photons

The idea of a perfect analogy between position–momentum and time–energy uncertainty relations might naturally lead one to ask whether position and time (or space and time coordinates), as well as momentum and energy, can be treated on equal footing. This is what (classically) happens within Einstein's theory of relativity. Thus, one may further wonder: would a theory combining quantum mechanics and relativity be the suitable framework which would allow a rigorous and logically consistent definition of a time observable, possibly exposing some analogy with the position operator?

None of the proposed models comprehending both quantum theory and *general* relativity have reached general consensus, or the remote possibility of experimental verification (Esposito 2011); but *quantum field theory* (QFT) is an established framework that does combine some principles of quantum mechanics with the *special* theory of relativity.

Unfortunately, QFT does not promote time t to some quantum operator $\hat{t}$; instead, it achieves equal treatment of space and time only by "demoting" the *position* operator to a mere classical parameter.[4] It treats time and space equally only in the sense that they are all classical, which appears as the necessary trade-off in order to quantize other quantities in some mathematically tractable way (Srednicki 2007, s. I.1).

It is no surprise that one of the most successful applications of QFT, the Standard Model, describes all fundamental interactions except gravity: while electroweak and strong interactions can be described within a field theory which treats time and space as a "background" (or *labels* to mark the relevant oper-

[4] More on this in Section 5.2, where the Klein-Gordon equation is reformulated with time as an Hermitian operator in an appropriate Hilbert space —based on the Page–Wootters model, which is introduced in Chapter 4.

ators), time and space are expected to be the main mathematical objects (observables), and transform appropriately, in a theory of gravity which has general relativity as its classical counterpart. Whether the definition of a quantum time operator is an useful step towards a quantum theory of gravity is, of course, beyond the scope of the present work.

The fact that QFT "externalizes" time and position to the rank of classical parameters is particularly true in quantum electrodynamics, also within the phenomenology of quantum optics. Thus it is impossible to define a *photon* position within standard quantum optics (see, for example, Scully and Zubairy 1997, sec. 1.5.4 'Wave function for photons'), and the problem of defining a quantum position observable for a photon shows an interesting analogy with time for a quantum massive particle. It is, in fact, a matter of active research (Hawton 2019; Hawton and Dabierre 2015).

While there is not a wave function for photons, the wave function for massive particles, as seen in the Shrödinger equation, only exists as a function of position (or momentum, etc.) but not as a function of time, i.e. the variable t in Eq. (1.5) cannot be regarded as spanning the spectrum of a time operator.

Nevertheless, we have provided an explanation as to why (even without considering the Pauli objection) relativistic field theories, as currently accepted, cannot provide a solution to the problem of quantum time, in spite of treating time and space on equal footing, and despite the fact that position in quantum mechanics is an observable with its associated self-adjoint operator.

1.2 Structure of the thesis

After explaining the motivation behind this work in Chapter 1, a review of open quantum systems and non-projective measurement theory is outlined in Chapter 2, as a necessary "toolbox" to understand relational models and other theoretical formulations of time as a quantum observable.

The *Pauli objection* itself is detailed in Chapter 3, together with some models that have been proposed to overcome it, with the exception of relational models,

and in particular the Page–Wootters model of "evolution without evolution", which is presented in Chapter 4, where it is also compared to some detector models. Therein, results are compared in relation to some systems of particular interest, and possible analogies are explored.

Further areas of study and applications are suggested in Chapter 5.

Chapter 2

Quantum Measurement Theory: a review

This chapter is devoted to briefly review some foundations and modern developments of quantum measurement theory. Reference texts include Haroche and Raimond 2006; Nakahara and Ohmi 2008; Nielsen and Chuang 2011; Preskill 2015, where they are presented in the context of open quantum systems and quantum information theory.

2.1 Bipartite systems, separable and entangled states

Consider a *bipartite quantum system* i.e. a composite system S made up of two parts, A and B, described by their respective Hilbert spaces $\mathcal{H}_A$ and $\mathcal{H}_B$.

In Haroche and Raimond 2006, a basis for $\mathcal{H}_A$ and a basis for $\mathcal{H}_B$ are indicated as

$$\{|i_A\rangle\} \text{ and } \{|\mu_B\rangle\}$$

with Latin and Greek indices to label basis vectors in the two spaces. This notation indicates potentially different physical roles for the two spaces, such as the *system of interest* and the surrounding *environment*, or the *system being measured*

and the *measurement apparatus*.

If the two subsystems are prepared independently and do not interact with each other, the system is in a *product state* or *separable state*:

$$|\psi_S\rangle = |\psi_A\rangle \otimes |\psi_B\rangle \ . \tag{2.1}$$

It is worth recalling that in a tensor product space $\mathcal{H}_A \otimes \mathcal{H}_B$ not all vectors can be expressed as a tensor product as in (2.1). However, the following holds:

Proposition 2.1.1. *The set of tensor products of basis vectors of $\mathcal{H}_A$ and $\mathcal{H}_B$, i.e.*

$$\{|i\rangle \otimes |\mu\rangle\}_{i\mu} \, ,$$

is a basis for $\mathcal{H}_A \otimes \mathcal{H}_B$.

Therefore, we can express any (generally not separable) state vector of $\mathcal{H}_S$ as a *superposition* of separable basis vectors

$$|\psi_S\rangle = \sum_{i,\mu} \alpha_{i\mu} \, |i\rangle \otimes |\mu\rangle \, . \tag{2.2}$$

Definition 2.1.1. Non separable states are defined as *entangled*.

Physically, $|\psi_S\rangle$ contains information not only about the results of measurements on A and B separately, but also on correlations between these measurements.

The simplest example of entangled system is given by two two-level systems, namely two spin-$\frac{1}{2}$ particles in a singlet state:

$$|\psi_{\text{singlet}}\rangle = \frac{1}{\sqrt{2}} \left(|\uparrow, \downarrow\rangle - |\downarrow, \uparrow\rangle \right) .$$

2.2 Density operator

A quantum state (either pure or *mixed*), is generally described by a *density* operator (or density matrix) ρ.

The general expression for a density operator ρ is

$$\rho = \sum_k p_k \, |\psi_k\rangle\langle\psi_k|$$

with p_k being non negative and $\sum_k p_k = 1$; where p_k indicates the "classical" probability of the system to be in state $|\psi_k\rangle$.

For a pure state (corresponding to ket $|\psi\rangle$) the density operator reduces to

$$\rho_{(\text{pure})} = |\psi\rangle\langle\psi| \ .$$

The expectation value of an observable represented by the operator A is given by (Blum 2013; Fano 1957)

$$\langle A\rangle = \text{tr}(A\rho) \, . \tag{2.3}$$

Eq. (2.3) is valid for any Hermitian operator A. Particularly, it is also valid if A is a *projector* and we will use this e.g. in Proposition 2.5.1.

We will now look at some properties of the density operator.

We can prove the following

Proposition 2.2.1. *Let A be an Hermitian operator with a discrete spectrum, and let $\{|m\rangle\}$ be a complete set of eigenvectors, such that*

$$\text{tr}(A\rho) = 0$$

for any density operator ρ. It follows that $A = 0$.

Proof. We can choose —to explicitly evaluate the expression of the trace— for each positive integer n, a particular density operator $\rho = |n\rangle\langle n|$, corresponding to a (pure) eigenstate of A.

With this particular choice, for each n,

$$A\rho = \langle n|A|n\rangle \, |n\rangle\langle n| \ .$$

It then follows:

$$0 = \mathrm{tr}(A\rho) = \sum_m \langle m|(\langle n|A|n\rangle |n\rangle\langle n|)|m\rangle$$
$$= \sum_m \langle n|A|n\rangle \langle m|n\rangle \langle n|m\rangle = \langle n|A|n\rangle . \quad (2.4)$$

With respect to the basis $\{|n\rangle\}$ the operator A is represented by a matrix whose elements are given by $a_{nm} = \langle n|A|m\rangle$; but $\{|n\rangle\}$ is an eigenbasis, therefore we are only interested in the diagonal elements (the off-diagonal ones being zero). However, the diagonal elements are $\langle n|A|n\rangle = 0$ for all n, according to Eq. (2.4), therefore the operator itself is $A = 0$. □

The *additivity* property follows immediately:

Corollary 2.2.1.1. *If* $\mathrm{tr}(A\rho) + \mathrm{tr}(B\rho) = \mathrm{tr}(C\rho)$ *for any density operator* ρ*, then* $A + B = C$*.*

2.3 Partial trace and open systems

In a bipartite system, one subsystem considered alone is an *open quantum system*, while the system as a whole is still a closed systems.

Let us consider an observable M_A, acting only on subsystems A. It can be expressed in $\mathcal{H}_A \otimes \mathcal{H}_B$ as

$$M_A \otimes \mathbb{1}_B .$$

Its expectation value is (using the expansion in Eq. (2.2), and the notation of Latin indices for system A and Greek ones for system B)

$$\langle M_A\rangle = \langle \psi_S|M_A \otimes \mathbb{1}_B|\psi_S\rangle$$
$$= \sum_{j,\nu} a^*_{j\nu} \left(\langle j| \otimes \langle \nu|\right) \left(M_A \otimes \mathbb{1}_B\right) \sum_{i,\mu} a_{i\mu} \left(|i\rangle \otimes |\mu\rangle\right)$$
$$= \sum_{j,\nu,i,\mu} a^*_{j\nu} a_{i\mu} \langle j|M|i\rangle \langle \mu|\mathbb{1}|\nu\rangle = \sum_{j,\mu,i} a^*_{j\mu} a_{i\mu} \langle j|M|i\rangle \quad (2.5)$$

The bra $\langle\mu|$, when acting on a ket element of $\mathcal{H}_A \otimes \mathcal{H}_B$, can be defined as a map from $\mathcal{H}_A \otimes \mathcal{H}_B$ to $\mathcal{H}_A$.

A formal definition can be given in terms of how it acts upon a generic basis ket of $\mathcal{H}_A \otimes \mathcal{H}_B$.

Definition 2.3.1.

$$\langle\mu|i\nu\rangle = \langle\mu| \Big(|i\rangle \otimes |\nu\rangle \Big) \coloneqq \delta_{\mu\nu} |i\rangle .$$

Intuitively, $\langle\mu|$ is then a "partial bra" as it only maps the "$|\nu\rangle$" part of "$|i\rangle \otimes |\nu\rangle$" to a number:

$$\begin{array}{rccc} \langle\mu| : & |i\rangle \otimes |\nu\rangle & \to & \delta_{\mu\nu} |i\rangle \\ & \cap & & \cap \\ & \mathcal{H}_A \otimes \mathcal{H}_B & & \mathcal{H}_A . \end{array}$$

This is consistent with the idea of "tracing out the environment" within an interpretation where $\mathcal{H}_B$ is the environment, and ultimately with the goal of studying subsystem A alone in spite of its entanglement with the "environment" (or measurement apparatus etc.) modeled by subsystem B.

Conversely, the ket $|\mu\rangle$, when acting on a bra element of $\mathcal{H}_A \otimes \mathcal{H}_B$, can also be defined as a map from $\mathcal{H}_A \otimes \mathcal{H}_B$ to $\mathcal{H}_A$. The following definition of $|\mu\rangle$ is simply *dual* to Definition 2.3.1:

Definition 2.3.2.

$$\langle i\nu|\mu\rangle = \Big(\langle i| \otimes \langle\nu| \Big) |\mu\rangle \coloneqq \delta_{\mu\nu} \langle i| .$$

Similar considerations apply:

$$\begin{array}{rccc} |\mu\rangle : & \langle i| \otimes \langle\nu| & \to & \delta_{\mu\nu} \langle i| \\ & \cap & & \cap \\ & \mathcal{H}_A \otimes \mathcal{H}_B & & \mathcal{H}_A . \end{array}$$

The operations defined (for basis vectors) in Definition 2.3.1 and 2.3.2 are called *partial inner products* (Jacobs 2014, s. 1.3.3). They can be extended to all vectors of $\mathcal{H}_B$ and $\mathcal{H}_B \otimes \mathcal{H}_B$ simply by linearity.

Similarly, partial inner products with bras and kets of $\mathcal{H}_A$ (and values in $\mathcal{H}_B$) can be defined as well.

We are now in the position to introduce the *partial trace*:

Definition 2.3.3. The *partial trace* is a linear map that takes an operator M_{AB} on $\mathcal{H}_A \otimes \mathcal{H}_B$ to an operator on $\mathcal{H}_A$ defined as

$$\operatorname{tr}_B M_{AB} = \sum_{\mu} \langle \mu | M_{AB} | \mu \rangle \ ,$$

where $\{|\mu\rangle\}$ is a basis of $\mathcal{H}_B$.

The first thing to note is that the *partial* trace is *operator-valued*, its value is not a scalar as opposed to the *trace*.

Next, we can introduce the *reduced density operator* of system A, which is obtained by *tracing out the environment* B, via the partial trace:

Definition 2.3.4. If ρ is the density operator of a whole bipartite system, composed of two parts A and B, the *reduced density operator* related to subsystem A is defined as

$$\rho_A = \operatorname{tr}_B(\rho) \, .$$

We assume now that the total state ρ is a pure state $\rho = |\psi_S\rangle\langle\psi_S|$.

If $\{|\mu\rangle\}$ is a basis of $\mathcal{H}_B$, for each element $|\mu\rangle$, using the definitions 2.3.1 and 2.3.2 and the expansion (2.2), we obtain

$$\begin{aligned} \langle \mu | \psi_S \rangle &= \sum_i \alpha_{i\mu} \, |i\rangle \, , \\ \langle \psi_S | \mu \rangle &= \sum_j \alpha^*_{j\mu} \, \langle j| \, . \end{aligned} \tag{2.6}$$

which allows us to expand the definition of reduced density operator (Defini-

tion 2.3.4) as[1]

$$\rho_A = \mathrm{tr}_B(|\psi_S\rangle\langle\psi_S|) = \sum_\mu \langle\mu|\psi_S\rangle \langle\psi_S|\mu\rangle = \sum_{ij\mu} \alpha_{i\mu}\alpha^*_{j\mu} |i\rangle\langle j| \,. \tag{2.7}$$

Finally, we can see that

$$\begin{aligned}\mathrm{tr}(M_A\rho_A) = \sum_k \langle k|M_A\rho_A|k\rangle &= \sum_k \langle k|M_A \left(\sum_{ij\mu} \alpha_{i\mu}\alpha^*_{j\mu} |i\rangle\langle j|\right)|k\rangle \\ &= \sum_{ijk\mu} \alpha_{i\mu}\alpha^*_{j\mu} \langle k|M_A|i\rangle \langle j|k\rangle = \sum_{ij\mu} \alpha_{i\mu}\alpha^*_{j\mu} \langle j|M_A|i\rangle \,,\end{aligned}$$

which is the same result as (2.5).

This allows us to conclude that

Proposition 2.3.1. *For an observable M_A, acting solely on one subsystem, the expectation value for state ρ can be calculated as*

$$\langle M_A\rangle = \mathrm{tr}(M_A\rho_A) \tag{2.8}$$

where ρ_A is the reduced density operator obtained from ρ by tracing out the environment B (as per Definition 2.3.4).

It is clear from (2.7) that ρ_A is self-adjoint, hence it can be diagonalized:

$$\rho_A = \sum_a p_a |a\rangle\langle a| \,. \tag{2.9}$$

Let $\{|k\rangle\}$ be a basis of $\mathcal{H}_A$. From (2.7) we can also derive that

$$\mathrm{tr}\,\rho_A = \sum_k \langle k|\rho_A|k\rangle = \sum_{ijk\mu} \alpha_{i\mu}\alpha^*_{j\mu} \langle k|i\rangle \langle j|k\rangle = \sum_{k\mu} |\alpha_{k\mu}|^2 = 1, \tag{2.10}$$

where the last equality is justified by the normalization of $|\psi_S\rangle$ in (2.2).

[1]The key point of this reasoning is showing how a pure state of the total system can correspond to mixed states in the two subsystems A and B. Therefore it is not restrictive to assume, in what follows, that the total state $\rho = |\psi_S\rangle\langle\psi_S|$ is pure.

The trace, i.e. the sum of matrix diagonal elements, is independent from the chosen basis, hence $\operatorname{tr} \rho_A = 1$ is valid in particular for the diagonal form (2.9), meaning

$$\sum_a p_a = 1$$

and providing a necessary condition to interpret p_a as a probability.

Eq. (2.9), with p_a as a probability, is often given as a *definition* of the density operator. The probability distribution p_a is described as a "classical" uncertainty in the preparation of the system (for example due to an unknown interaction with the environment).

The reverse also holds true:

Proposition 2.3.2. *A system with uncertainties in the preparation of the* state *("mixed") is equivalent to one part ("A") of a bipartite system entangled with the rest ("B") such that the total system $A + B$ is in a pure state.*

The above is called *purification* (see e.g. Nielsen and Chuang 2011, s. 2.5).

2.4 Comparison of a coherent superposition and a mixed state

Given, for simplicity, a two-level system (a qubit), and an orthonormal basis $\{|0\rangle, |1\rangle\}$, it may be of interest to compare a *coherent superposition* of the two pure states $|0\rangle$ and $|1\rangle$, with equal probability on the outcome of a measurement (but in a well-defined quantum state); with a statistical mixture of states $|0\rangle$ and $|1\rangle$, again with equal probability, but *in the determination of the quantum state.*

A natural example of such coherent superposition is (e.g. Nakahara and Ohmi 2008, Example 2.4)

$$|\psi\rangle = \frac{1}{\sqrt{2}} |0\rangle + \frac{1}{\sqrt{2}} |1\rangle ,$$

and the corresponding density operator is

$$\rho_{\text{pure}} = |\psi\rangle\langle\psi| = \frac{1}{2}\Big(|0\rangle + |1\rangle\Big)\Big(\langle 0| + \langle 1|\Big) = \frac{1}{2}\sum_{ij=0}^{1}|i\rangle\langle j| \equiv \frac{1}{2}\begin{pmatrix} 1 & 1 \\ 1 & 1 \end{pmatrix}. \quad (2.11)$$

On the other hand, for the statistical mixture, the density operator is

$$\rho_{\text{mix}} = \frac{1}{2}|0\rangle\langle 0| + \frac{1}{2}|1\rangle\langle 1| \equiv \frac{1}{2}\begin{pmatrix} 1 & 0 \\ 0 & 1 \end{pmatrix}. \quad (2.12)$$

By comparing the matrices in (2.11) and (2.12) we may conclude that the off-diagonal terms in the coherent superposition case indicate *coherence*, or "quantum purity".

It is of interest to look at mixed states which are not necessarily made up of orthonormal pure states. In fact, an ensemble of orthonormal states has "nothing special", and different ensembles may lead to the same density operator.

For example, let us consider[2] this orthogonal ensemble (diagonal density matrix):

$$\rho_1 = \frac{3}{4}|0\rangle\langle 0| + \frac{1}{4}|1\rangle\langle 1|$$

and

$$\rho_2 = \frac{1}{2}|a\rangle\langle a| + \frac{1}{2}|b\rangle\langle b|.$$

with

$$|a\rangle = \sqrt{\frac{3}{4}}|0\rangle + \sqrt{\frac{1}{4}}|1\rangle$$
$$|b\rangle = \sqrt{\frac{3}{4}}|0\rangle - \sqrt{\frac{1}{4}}|1\rangle$$

It is easy to prove that $\rho_1 = \rho_2$. This is just a particular case of a theorem.

[2] Nielsen and Chuang 2011, *Exercise 2.71: (Criterion to decide if a state is mixed or pure).*

Theorem 2.4.1. *(Unitary freedom in the ensemble for density matrices[3]). The ensembles* $\{p_i, |\psi_i\rangle\}$ *and* $\{q_j, |\phi_j\rangle\}$ *generate the same density operator*

$$\rho = \sum_i p_i \, |\psi_i\rangle\langle\psi_i| = \sum_j q_j \, |\phi_j\rangle\langle\phi_j|$$

if and only if there exists a unitary matrix $U = \{u_{ij}\}$ *such that*

$$|\tilde{\psi_i}\rangle = \sum_j u_{ij} |\tilde{\phi_j}\rangle$$

where $|\tilde{\psi_i}\rangle$ *and* $|\tilde{\phi_j}\rangle$ *are the (not normalized) vectors defined as*

$$|\tilde{\psi_i}\rangle = p_i \, |\psi_i\rangle \;\; \textit{and} \;\; |\tilde{\phi_j}\rangle = q_j \, |\phi_j\rangle$$

2.5 Standard measurement and generalizations

The evolution of the density operator for a closed system is given by the map

$$\rho_S \to \mathcal{E}(\rho_S) = U(t)\rho_S U^\dagger(t) \, .$$

We are looking to describe a more general change $\rho \to \mathcal{E}(\rho_S)$ that may also include changes due to measurement (or noise).

Furthermore, we are looking to describe a generalization of projective measurement (Neumann 1955): when a projective, Von-Neumann measurement is performed on a multipartite system, it does not necessarily correspond to a projective measurement on each subsystem (Preskill 2015, c. 3).

2.5.1 General requirements for quantum measurement

One of the postulates of quantum mechanics (Nielsen and Chuang 2011, s. 2.2.3) states that

[3] The proof can be found, for example, in Nielsen and Chuang 2011, *Theorem 2.6.*

1. quantum measurements are described by a collection $\{M_m\}$ of *measurement operators*.

2. The index m refers to the measurement outcomes that may occur in the experiment.

3. If the state of the quantum system is $|\psi\rangle$ immediately before the measurement then the probability that result m occurs is given by

$$\pi_m = \langle\psi|M_m^\dagger M_m|\psi\rangle\,. \tag{2.13}$$

4. The state of the system after the measurement is

$$\frac{M_m\,|\psi\rangle}{\sqrt{\langle\psi|M_m^\dagger M_m|\psi\rangle}}. \tag{2.14}$$

5. The *completeness* property or *decomposition of the identity* is satisfied:

$$\sum_m M_m^\dagger M_m = \mathbb{1}. \tag{2.15}$$

It is easily shown that the completeness is equivalent to the condition that $\sum_m \pi_m = 1$, i.e. the sum of the probabilities for *all* measurement outcomes is equal to 1.

Both the projective measurement and positive-operator measurement (POVM), which will be discussed in Sections 2.5.3 and 2.5.4, satisfy the above postulate.

2.5.2 Review on projectors

A brief review of *projection operators* or *projectors* is useful before introducing the *projective measurement* in Section 2.5.3.

We shall assume, unless otherwise stated, that all vectors are normalized to unity. Consider an observable represented by a self-adjoint operator A with a *discrete, non degenerate spectrum*. Let a_i by an eigenvalue of A, and $|i\rangle$ its

corresponding eigenvector. The probability of a measurement outcome a_i, on a system in the pure state $|\psi\rangle$ is given by

$$\pi_i = \|\langle i|\psi\rangle\|^2 = \langle\psi|i\rangle\,\langle i|\psi\rangle = \langle\psi|P_i|\psi\rangle$$

where $P_i = |i\rangle\langle i|$ appears as the *projector* on the one-dimensional eigenspace related to eigenvalue a_i.

If a_i is degenerate, $j = 1, \ldots, J$ its degeneracy index, and $|ij\rangle$ the corresponding eigenvectors, such probability shall sum over it:

$$\pi_i = \sum_{j=1}^{J} \|\langle ij|\psi\rangle\|^2 = \sum_{j=1}^{J} \langle\psi|ij\rangle\,\langle ij|\psi\rangle = \langle\psi|P_i|\psi\rangle$$

where $P_i = \sum_{j=1}^{J} |ij\rangle\langle ij|$ still is the projector on the (J-dimensional) eigenspace of a_i.

Generally, the probability that the outcome of a measurement falls in the set of eigenvalues $\sigma = \{a_1, \ldots, a_S\}$ is

$$\pi_\sigma = \sum_{i=1}^{S}\sum_{j=1}^{J_i} \|\langle ij|\psi\rangle\|^2 = \sum_{i=1}^{S}\sum_{j=1}^{J_i} \langle\psi|ij\rangle\,\langle ij|\psi\rangle = \langle\psi|P_\sigma|\psi\rangle\,, \tag{2.16}$$

where $P_\sigma = \sum_{i=1}^{S}\sum_{j=1}^{J_i} |ij\rangle\langle ij|$ is once again a projector — on the "generalized eigenspace" spanned by all eigenvectors $\{|ij\rangle\}$ above.

Looking back at Eq. (2.3), it is valid for *any* Hermitian operator, therefore it is also valid for projectors. Hence we can replace A with the projector P_σ, associated to the set of eigenvalues σ according to (2.16) and (2.19).

This is of particular interest because its mean value equates the probability that the outcome of a measurement falls in a given subset of the spectrum of a given observable. So we have:

Proposition 2.5.1. *The probability π_σ that the outcome of a measurement of the observable A on the system described by the state operator ρ falls in the set σ is*

given by:

$$\pi_\sigma = \langle P_\sigma \rangle = \mathrm{tr}(P_\sigma \rho) \tag{2.17}$$

with P_σ defined as in (2.16) or, more generally, in (2.19).

Being π_σ the *probability* of the outcome of a measurement to fall in a given set σ, it has to be:

1. 0 on the empty set
2. non negative
3. *additive* on disjoint sets
4. equal to 1 if σ includes the whole spectrum of A.

Properties 1...3 are the defining properties of a *measure*[4] (Sazonov 2002), and the map $\sigma \subseteq \mathbb{R} \to P_\sigma$ implicitly defined in (2.16) is a *projector-valued measure*.

This notion of projector-valued measure can be generalized in such a way to include both the cases of discrete and continuous spectra, with the following (Ballentine 1998; Neumann 1955)

Theorem 2.5.2 (spectral resolution)**.** *If A is a self-adjoint operator, there is a unique projector-valued measure E defined on the Borel sets of $\mathbb{R}$ such that* [5]

$$A = \int_{-\infty}^{\infty} a \, dE(a) \tag{2.18}$$

and satisfying:

$$E(\mathbb{R}) = \mathbf{1},$$
$$E(B_1 \cap B_2) = E(B_1)E(B_2)\,.$$

[4] Not to be confused with *measurement*.

[5] In (2.18), a is a real number (not a set), but it's intended E to be evaluated on the *interval* from $-\infty$ to a.

In terms of this theorem, the projector in (2.16) is

$$P_\sigma = E(\sigma) = \int_{a\in\sigma} dE(a) \tag{2.19}$$

and $dE(a)$ is —informally speaking— infinitesimal if a belongs to the continuous spectrum, finite if a is a discrete eigenvalue and zero otherwise.

2.5.3 Projective measurement

Let $\mathcal{H}_A$ and $\mathcal{H}_B$ be the Hilbert spaces describing a system under measurement and the measurement device respectively. For simplicity, let both have finite dimension N. Let $|\Psi\rangle, |\Psi'\rangle \in \mathcal{H}_A \otimes \mathcal{H}_B$ be the overall state of the system *plus* measurement apparatus, respectively before and after the measurement.

Let us also consider a *complete*, *orthogonal* set of N projectors $P_0 \dots P_{N-1}$ on the Hilbert space $\mathcal{H}_A$, i.e. the projectors have the properties

$$\sum_n P_n = \mathbb{1}, \tag{2.20}$$

$$P_i P_j = \delta_{ij} P_i \,. \tag{2.21}$$

On $\mathcal{H}_B$ instead, describing the measurement device, let us consider the basis:

$$\{|0\rangle \dots |N-1\rangle\} \,. \tag{2.22}$$

The coupling between the system and the apparatus can be modeled by a unitary operator transforming the state of system and apparatus before and after the measurement. The following is a possible example (Preskill 2015, s. 3.1.1 "Orthogonal Measurements"):

$$U = \sum_{a,b=0}^{N-1} P_a \otimes |b+a\rangle\langle b| \,, \tag{2.23}$$

where $|b+a\rangle$ and $\langle b|$ are all elements of the basis (2.22) and the sum $b+a$ is

modulo N: intuitively, if the a-th eigenvalue of the observable is measured, a sort of "circular dial" on the measurement device rotates of a positions.

For this reason, $\mathcal{H}_B$ is also called *pointer space*.

If the system and the measurement device are initially in the state $|\psi\rangle$ and $|0\rangle$ respectively (therefore $|\Psi\rangle = |\psi\rangle \otimes |0\rangle$), using the Eq. (2.23), the state after the measurement will be

$$|\Psi'\rangle = U(\Psi) = U\Big(|\psi\rangle \otimes |0\rangle \Big) = \sum_{a,b} P_a \otimes |b+a\rangle\langle b| \, (\, |\psi\rangle \otimes |0\rangle \,). \tag{2.24}$$

Indeed, in Eq. (2.24), only terms with $b = 0$ survive. Therefore

$$\begin{aligned} |\Psi'\rangle &= \sum_a \Big(P_a \otimes |a\rangle\langle 0| \Big) \Big(|\psi\rangle \otimes |0\rangle \Big) \\ &= \sum_a P_a \, |\psi\rangle \otimes |a\rangle \, . \end{aligned} \tag{2.25}$$

The probability of an outcome a is

$$\begin{aligned} \pi_a = \; & \langle \Psi'| \Big(\mathbb{1} \otimes |a\rangle\langle a| \Big) |\Psi'\rangle \\ &= \sum_{b,c} \left(\langle\psi| \, P_b \otimes \langle b| \right) \Big(\mathbb{1} \otimes |a\rangle\langle a| \Big) \left(P_c \, |\psi\rangle \otimes |c\rangle \right) \\ &= \sum_{b,c} \Big(\langle\psi| P_b P_c |\psi\rangle \, \langle b|a\rangle \, \langle a|c\rangle \Big) = \langle\psi| P_a |\psi\rangle \, . \end{aligned} \tag{2.26}$$

Eq. (2.25) clearly shows that the system and the measurement device are completely correlated (entangled). If the measurement apparatus is observed in state $|a\rangle$ —with probability π_a as stated in Eq. (2.26)— then the system being measured is in state $P_a \, |\psi\rangle$ or, in normalized form:

$$|\psi'_a\rangle := \frac{P_a \, |\psi\rangle}{\| P_a \, |\psi\rangle \|} = \frac{P_a \, |\psi\rangle}{\sqrt{\langle\psi| P_a |\psi\rangle}} \, . \tag{2.27}$$

Indeed, $|\psi\rangle$ is transformed into its projection $|\psi'_a\rangle$ onto the eigenspace corresponding to the eigenvalue a of the observable of interest.

Please note the above *is not* a derivation of the Born (probability) rule altogether, as it still needs to be postulated for the measurement apparatus.

Finally, if the measurement apparatus is not observed, therefore an outcome a is not known, the system *after* measurement is in a statistical mixture of "all possible wavefunction collapses" weighted on the probability π_a. By using both (2.26) and (2.27), and the definition of the density operator for the initial pure state $\rho = |\psi\rangle\langle\psi|$:

$$\rho' = \sum_a \Pr(a) \, |\psi'_a\rangle\langle\psi'_a| = \sum_a P_a \, |\psi\rangle\langle\psi| \, P_a = \sum_a P_a \rho P_a \, .$$

So, the initial pure state ρ is transformed by the measurement process into a mixed one. In other words, the initial, coherent superposition of eigenstates represented by $\rho = |\psi\rangle\langle\psi|$ becomes a maximal statistical mixture ρ' (as seen in Section 2.4).

It can be proven that the transformation

$$\rho \to \sum_a P_a \rho P_a \tag{2.28}$$

is also valid in the more general case of ρ being a mixed state before the measurement —in this case, it is transformed into another mixed state, but still described by the (2.28). A generalization to observables with a continuous spectrum is also possible (see e.g. Preskill 2015, s. 3.1.1 for more details).

2.5.4 General measurement and POVM

In a similar fashion to Section 2.5.3, let us again consider a system under measurement and the measurement apparatus, but, for further simplicity, let both their Hilbert spaces have finite dimension $N = 2$. The examples in this Subsection are based on Preskill 2015, s. 3.1.2, with the details of some calculations expanded further.

Let $|0\rangle_A, |1\rangle_A \in \mathcal{H}_A$ be the eigenstates of the observable subject of measurement, and P_0, P_1 their respective projectors. Let $\{|0\rangle_B, |1\rangle_B\}$ be the correspond-

ing orthonormal basis in the pointer space $\mathcal{H}_B$.

Let the initial state in $\mathcal{H}_A$ be $|\psi\rangle_A = \alpha\,|0\rangle_A + \beta\,|1\rangle_A$, and the initial state of the measurement device be $|0\rangle_B$.

Expanding the sums in Eqs. (2.24) and (2.25) —with indices a and b both spanning over values 0, 1 only— the state after measurement will be:

$$\begin{aligned}|\Psi'\rangle &= U(|\psi\rangle_A \otimes |0\rangle_B) = U(\{\alpha\,|0\rangle_A + \beta\,|1\rangle_A\} \otimes |0\rangle_B) \\ &= \alpha\,|0\rangle_A \otimes |0\rangle_B + \beta\,|1\rangle_A \otimes |1\rangle_B = P_0\,|\psi\rangle_A \otimes |0\rangle_B + P_1\,|\psi\rangle_A \otimes |1\rangle_B\,. \quad (2.29)\end{aligned}$$

When we observe the pointer, let us assume we are not able to "measure" it with respect to the basis $\{|0\rangle, |1\rangle\}$, but with respect to another basis, say,

$$\left\{|\pm\rangle_B = \frac{1}{\sqrt{2}}\Big(|0\rangle_B \pm |1\rangle_B\Big)\right\}. \quad (2.30)$$

A natural question is whether the above (projective) measurement of the pointer device will correspond to a projective measurement in $\mathcal{H}_A$, with respect the corresponding basis $\left\{|\pm\rangle_A = \frac{1}{\sqrt{2}}\Big(|0\rangle_A \pm |1\rangle_A\Big)\right\}$. The answer is negative, as it will be shown.

Indeed, we can rewrite (2.29) as

$$\begin{aligned}|\Psi'\rangle &= U(|\psi\rangle_A \otimes |0\rangle_B) \\ &= \frac{1}{\sqrt{2}}\Big(\alpha\,|0\rangle_A \otimes (|+\rangle + |-\rangle) + \beta\,|1\rangle_A \otimes (|+\rangle - |-\rangle)\Big) \\ &= \frac{1}{\sqrt{2}}\Big((\alpha\,|0\rangle_A + \beta\,|1\rangle_A) \otimes |+\rangle + (\alpha\,|0\rangle_A - \beta\,|1\rangle_A) \otimes |-\rangle\Big) \\ &:= M_+\,|\psi\rangle_A \otimes |+\rangle + M_-\,|\psi\rangle_A \otimes |-\rangle\,, \quad (2.31)\end{aligned}$$

where we have defined:

$$M_+ \equiv \frac{1}{\sqrt{2}}\begin{pmatrix}1 & 0\\ 0 & 1\end{pmatrix} \qquad M_- \equiv \frac{1}{\sqrt{2}}\begin{pmatrix}1 & 0\\ 0 & -1\end{pmatrix} \quad (2.32)$$

with respect to the basis $\{|0\rangle_A, |1\rangle_A\}$.

The most important difference between equations (2.31) and (2.29) is that the operators $M_\pm$ are *not* projectors onto $|\pm\rangle_A$. Thus the unitary operation U is not a projective measurement with respect to such basis!

Moreover, M_- in the example is not even idempotent, therefore it is not a projector onto *any* linear subspace of $\mathcal{H}_A$. The lack of idempotency means, physically, that, if we repeat the measurement, we do not generally obtain the same result (and do not leave the system A in the same state).

On the other hand, while $M_\pm$ are not (a complete set of) orthogonal projectors, the operators $E_\pm := M_\pm M_\pm^\dagger$ still satisfy the *decomposition of the identity*:

$$E_+ + E_- = M_+^\dagger M_+ + M_-^\dagger M_- = \mathbb{1}, \tag{2.33}$$

similarly to the projectors P_n in Eq. (2.20).

Operators $\{E_+, E_-\}$ are an example of *POVM* (positive operator-valued measure) i.e. a measure whose values are *positive operators*.

Positive operators are a more general class of operators than projectors. They are defined as Hermitian operators E in an Hilbert space $\mathcal{H}$ satisfying

$$\langle\psi|E|\psi\rangle \geq 0, \quad \forall\psi \in \mathcal{H}.$$

The example we have considered only allows two possible outcomes. More generally, for a discrete set of possible outcomes, Eq. (2.33) can be written:

$$\sum_m E_m = \sum_m M_m^\dagger M_m = \mathbb{1}. \tag{2.34}$$

Looking back at the general measurement postulate (Section 2.5.1), we see that the statistical distribution of measurement outcomes is determined by the product $M_m^\dagger M_m = E_m$ rather than the measurement operator M_m itself. So one can define the positive operators E_m directly. However, the state *after* the measurement, as in Eq. (2.14) *does* depend on M_m.

It is important to note that, given a positive operator E_m, the operator M_m such that

$$E_m = M_m^\dagger M_m \tag{2.35}$$

is not uniquely determined. Indeed, if one replaces M_m with UM_m —where U is any unitary operator— it is easily verified that Eq. (2.35) is still satisfied.

One conclusion that can be drawn is that, taking into consideration (2.13) and (2.14), and the above observation, for a given POVM defined by the positive operators $\{E_m\}$, one can predict the probability of measurement outcomes, but not the state of the system after the measurement.

A more abstract and general definition of POVM is as follows:[6]

Definition 2.5.1. Given a (Borel) σ-algebra $\mathcal{B}(\mathbb{R})$ of subsets of $\mathbb{R}$, and the space $\mathcal{F}(\mathcal{H})$ of positive, self-adjoint operators on a Hilbert space, a *positive operator-valued measure* $(POVM)$ is a map $E : \mathcal{B}(\mathbb{R}) \to \mathcal{F}(\mathcal{H})$ such that

- $E(\mathbb{R}) = \mathbb{1}$ (completeness)
- $E\left(\bigcup_n \Delta_n\right) = \sum_n E(\Delta_n)$ (additivity)

where $\{\Delta_n\}$ is a countable family of disjoint sets in $\mathcal{B}(\mathbb{R})$.

2.6 Quantum channels and Kraus operators

We have seen so far that:

1. Given a bipartite system described by the Hilbert space $\mathcal{H}_A \otimes \mathcal{H}_B$, the subsystem in $\mathcal{H}_A$ is not necessarily in a pure state itself; it may have the properties of a mixed state. (Section 2.3).

2. An orthogonal measurement of the bipartite system can realize a (non-orthogonal) POVM on $\mathcal{H}_A$ alone (Subsection 2.5.4).

[6] See e.g. Beneduci 2014; Berberian 1966 — the level of generalization may vary.

It is therefore of interest to study the evolution (as a density matrix in $\mathcal{H}_A$) of subsystem A alone, while the bipartite system as a whole evolve unitarily. The system A alone is initially described by the density operator $\rho = |\psi\rangle\langle\psi|$. By tracing out B (in the sense of Section 2.3), there has:

$$\rho \to \mathcal{E}(\rho) \coloneqq \sum_a M_a \rho M_a^\dagger \tag{2.36}$$

which generalizes the unitary evolution $\rho \to U\rho U^\dagger$.

The linear map, or "super operator",[7] $\mathcal{E}$ is called *quantum channel*.[8] The word "channel" is drawn from communication theory, as the state ρ can be interpreted as being *transmitted* through a communication link from a sender to another party who receives it modified into the state $\mathcal{E}(\rho)$.

A quantum channel $\mathcal{E}$

1. is linear: $\mathcal{E}(\alpha\rho_1 + \beta\rho_2) = \alpha\mathcal{E}(\rho_1) + \beta\mathcal{E}(\rho_2)$;
2. preserves hermiticity: $\rho = \rho^\dagger \implies \mathcal{E}(\rho) = \mathcal{E}(\rho)^\dagger$;
3. preserves positivity: $\rho = \rho^\dagger \geq 0 \implies \mathcal{E}(\rho) \geq 0$;
4. preserves trace: $\mathrm{tr}(\mathcal{E}(\rho)) = \mathrm{tr}(\rho)$.
5. is *completely positive*.[9] If $\mathcal{H}_R$ is another Hilbert space of arbitrary dimension, then $\mathcal{E} \otimes \mathbb{1}_R$ is also positive in $\mathcal{H}_A \otimes \mathcal{H}_R$.

Expressing $\mathcal{E}$ in terms of operators M_a satisfying the partition of the identity (2.15) is called *operator-sum representation* of the quantum channel.

The operators $\{M_a\}$ are called the *Kraus operators* of the channel.

Similarly to POVM $\{E_a\}$, given a particular channel $\mathcal{E}$, the set $\{M_a\}$ is not uniquely determined, but generally exists.

[7] A *superoperator* is a linear map that associates an operator in a Hilbert space to another operator (instead of a vector to another vector).

[8] Another name for it is *trace-preserving completely positive map*, or *TPCP map* for short. (Preskill 2015, s. 3.2)

[9] Preskill 2015, s. 3.2.6; Nielsen and Chuang 2011, s. 8.2.4.

A fundamental comparison with unitary evolution is that quantum channels can be *composed* too, but *an inverse does not generally exist*. The fact that the existence of an inverse is not guaranteed corresponds, mathematically, to the concept of *semigroup* and, physically, to the *irreversibility* of the process of entanglement of subsystem A with the environment. In other words, there is no quantum channel that will bring back an entangled, mixed state back to its initial pure state; but a generalized evolution from time t_0 to time t_1, described by $\mathcal{E}_1$, and another from t_1 to t_2 described by $\mathcal{E}_2$ can be combined to describe the evolution from t_0 to t_2:

$$\rho \to (\mathcal{E}_1 \circ \mathcal{E}_2)(\rho) = \sum_{\mu,a} N_\mu M_a \rho M_a^\dagger N_\mu^\dagger \,.$$

If we demand that $\mathcal{E}_1 \circ \mathcal{E}_2$ is the identity (or "superidentity", should we say), in other words that $\mathcal{E}_2$ is the *inverse* of $\mathcal{E}_1$, we can prove that the channel must be unitary i.e. $\mathcal{E}_1(\rho) = U\rho U^\dagger$ for some unitary evolution operator U. This excludes decoherence, or entanglement with environment from an initial pure state, from being reversible. See Preskill 2015, s. 3.2 for a detailed proof, and general properties of quantum channels.

Chapter 3

Pauli's objection and historical developments

3.1 Pauli's objection

The existence of a time operator with the properties required in Section 1.1.3 is hindered by a fundamental objection which was raised by W. Pauli for the first time in his *General Principles of Quantum Mechanics*, dated 1933, where he argued that the existence of a self-adjoint operator, conjugate to the Hamiltonian, would lead to absurd consequences on the energy spectrum. He did not provide a formal proof of his argument, and only relegated his observation into a footnote of his work (Pauli 1933); but that was sufficient to lead most physicists to insist that "time is just a parameter" in quantum mechanics since then.

Here we aim at providing a more technical proof of Pauli's "theorem", based on some relatively recent work by E. Galapon (Galapon 2002), while expanding some details further. A preliminary Lemma on commutator algebra follows.

Lemma 3.1.1. *If the commutator* $[T, H]$ *commutes with* T *i.e.*

$$[T, H]T \;=\; T[T, H]\,,$$

then the following holds:

$$[T^k, H] = kT^{k-1}[T, H]\,. \tag{3.1}$$

This is particularly true when $[T, H]$ is a *number* as in (3.4) where T and H are the time and energy operator respectively.

Proof. First of all, the (3.1) is trivially valid for $k = 1$.

For an arbitrary positive integer $k > 1$ there has:

$$\begin{aligned}[T^k, H] &= T^{k-1}TH - HT^{k-1}T \\ &= T^{k-1}TH - T^{k-1}HT + T^{k-1}HT - HT^{k-1}T \\ &= T^{k-1}[T, H] + [T^{k-1}, H]T\end{aligned} \tag{3.2}$$

Now, iterating the result in (3.2),

$$\begin{aligned}[T^k, H] &= T^{k-1}[T, H] + [T^{k-1}, H]T \\ &= T^{k-1}[T, H] + (T^{k-2}[T, H] + [T^{k-2}, H]T)T \\ &= T^{k-1}[T, H] + T^{k-1}[T, H] + [T^{k-2}, H]T^2 \\ &= 2T^{k-1}[T, H] + [T^{k-2}, H]T^2 \\ &= \dots \\ &= nT^{k-1}[T, H] + [T^{k-n}, H]T^n \\ &= \dots\end{aligned} \tag{3.3}$$

where the commutativity hypothesis $[T, H]T = T[T, H]$ has been used to obtain

$$T^{k-2}[T, H]T = T^{k-1}[T, H].$$

Now, (3.3) can be continued until it reaches $n = k$ when the term $[T^{k-n}, H]T^n$ vanishes and a result of $kT^{k-1}[T, H]$ follows. □

Let us now come to the Pauli argument; and assume that there exists a self-adjoint time operator, T, canonically conjugate to the Hamiltonian H, i.e.

$$[T, H] = i\hbar \tag{3.4}$$

Since T is self-adjoint, then for all $\beta \in \mathbb{R}$, $U_\beta = \exp(-i\beta T/\hbar)$ is unitary. A formal expansion of the exponential yields the commutator

$$[U_\beta, H] = \left[\sum_{k=0}^{\infty} \frac{1}{k!}\left(-\frac{i\beta T}{\hbar}\right)^k, H\right] = \sum_{k=0}^{\infty} \frac{1}{k!}\left(-\frac{i\beta}{\hbar}\right)^k [T^k, H]\,. \tag{3.5}$$

As the commutator $[T, H]$ itself commutes with its operator T, the following identity holds (see Lemma 3.1.1):

$$[T^k, H] = kT^{k-1}[T, H]$$

hence:

$$\begin{aligned}[U_\beta, H] &= \sum_{k=0}^{\infty} \frac{1}{k!}\left(-\frac{i\beta}{\hbar}\right)^k kT^{k-1}[T, H] \\ &= \beta \sum_{k=1}^{\infty} \frac{1}{(k-1)!}\left(-\frac{i\beta}{\hbar}\right)^{k-1} T^{k-1} = \beta \sum_{\kappa=0}^{\infty} \frac{1}{\kappa!}\left(-\frac{i\beta T}{\hbar}\right)^{\kappa} = \beta U_\beta \end{aligned} \tag{3.6}$$

where the term for $k = 0$ in the first sum clearly vanishes, hence we can start the sum from $k = 1$ then set $\kappa = k - 1$ in the last step.

Now, given an eigenvector φ_E of H so that $H\varphi_E = E\varphi_E$, using Eq. (3.6), we get

$$HU_\beta\varphi_E = (U_\beta H - [U_\beta, H])\varphi_E = EU_\beta\varphi_E - \beta U_\beta\varphi_E = (E - \beta)U_\beta\varphi_E\,,$$

showing that $U_\beta\varphi_E$ is another eigenvector of H with eigenvalue $E - \beta$. But β is an arbitrary real number and H a *generic* Hamiltonian, hence the spectrum of a generic Hamiltonian H should be the whole real line, which contradicts the discrete and semi-bounded energy spectrum in fact found in most physical systems.

For several decades, Pauli's argument had prevented most theoretical at-

tempts at defining a self-adjoint time operator with the required commutation and uncertainty properties. However, some research effort has been invested into weakening some of those requirements, thus rendering the Pauli objection no longer applicable.

Notable examples of possible approaches involve: renouncing the self-adjointness of the operator $\hat{T}$ (replacing it with a more general symmetric operator); allowing for the corresponding spectral measurement not to be projective (replacing it with a POVM); or including the case of an *imaginary* potential in the Hamiltonian, to model absorption by a detector via loss of normalization (non-unitary evolution).

3.2 Aharonov–Bohm

In their 1961 paper, Aharonov and Bohm (Aharonov and Bohm 1961) showed that "energy can be measured reproducibly in an arbitrarily short time", thus apparently contradicting the time–energy indeterminacy theorized by Mandelstam and Tamm (see also Sec. 1.1.3) and by other authors. As observed by Aharonov and Bohm, in the Mandelstam–Tamm derivation, *time* has a different meaning: it is essentially the lifetime of a system in a particular state and not the duration of the energy measurement process. They also critically reviewed previous works by Landau and Peierls (Landau and Peierls 1965) and by Fock and Krylov (Fock and Krylov 1947), discussed their level of generality and provided counterexamples to their formulation of the time–energy uncertainty relation.

In their model, they considered a free particle as a "clock" and quantize (by symmetrizing the corresponding operators) the classical relation $t = y/v = my/p$ for a particle that is at position $y = 0$ at time $t = 0$ and travels at velocity v along the y axis. The corresponding time operator has then expression:

$$\hat{T}_{AB} = \frac{m}{2}\left(\hat{Y}\frac{1}{\hat{P}_y} + \frac{1}{\hat{P}_y}\hat{Y}\right). \tag{3.7}$$

In the paper, this operator is claimed to be Hermitian, although with a singularity

for $p_y = 0$.[1] With some simple algebra, a commutation relation $[\hat{H}_c, \hat{T}_{AB}] = \mathrm{i}\hbar$ can be proved, where $\hat{H}_c = \hat{P}_y^2/2m$ is the Hamiltonian of the free particle that is used as a "clock".

This seems to contradict Pauli's argument: however, more recent studies (Egusquiza and Muga 1999, 2000; Muga et al. 1998) have shown that $\hat{T}_{AB}$ is not, strictly speaking, self-adjoint but "only" maximally symmetric (a weaker and more general condition). An analogy has been made therein with the momentum on the half-line, a restriction of the well known momentum operator to a subdomain that is defined as $\{\psi \in \mathscr{L}^2(\mathbb{R}) : \psi(x) = 0 \; \forall x < 0\}$ in position representation. It has also been shown that the associated spectral measure is not projector valued, but positive-operator valued (POVM). Projectors are a particular subclass of *positive operators*. Among other applications, suitable positive operators can be used to extend von Neumann decomposition in order to describe open quantum systems and "unsharp" measurements.

Another apparent contradiction is the commutator $[\hat{H}_c, \hat{T}_{AB}] = \mathrm{i}\hbar$ (and the consequent uncertainty relation $\sigma_{H_c}\sigma_{T_{AB}} \geq \frac{\hbar}{2}$) with Aharonov–Bohm's conclusion that energy can be measured, in principle, with arbitrary precision in an arbitrarily short time; but it should be noted that $\hat{H}_c$ is the energy of the clock, not of the system under energy-measurement, thus the contradiction does not hold.

The Aharonov–Bohm model explicitly includes a clock in the description, i.e., a different system to the one under measurement; and this separate system has one of its observables on a well known dependency upon time, so the corresponding eigenvalues can be seen as possible positions of the "hand" of the clock. Aharonov and Bohm infer that $\hat{T}_{AB}$ must commute with all the observables of the main system (and in particular the Hamiltonian, let's call it $\hat{H}_S$), given that they are defined in different Hilbert spaces: therefore, there is no fundamental reason why the system energy represented by $\hat{H}_S$, and the clock time $\hat{T}_{AB}$, could not have, in the same measurement, arbitrarily narrow statistical distributions around some of their eigenvalues.

[1] This is stressed in a footnote of Aharonov–Bohm's paper. The reader might have noticed the irony of fundamental historical papers relegating important information at the level of footnotes —and the present work, in many parts, not even trying to "improve" such a traditional trend.

This idea of a quantum description of time through modeling a "clock" (in other words, the notion of time as "what is shown on a clock" with some suitable properties) has a certain historical relevance because later models, independently developed, have been based on that idea too. In particular, we can mention the Page–Wootters model (Page and Wootters 1983), where a peculiar relation is in place between the clock and the system, of which we will not explore the details at this stage though, as those will be discussed extensively (with numerical applications, experiments, and comparisons with other models) in Chapter 4.

3.3 Allcock and following developments

With three papers dated 1969 (Allcock 1969a,b,c), G. R. Allcock introduced a time-of-arrival quantum observable, along with a first formulation of a detector model based on a non-Hermitian Hamiltonian (by including a *complex potential*). An anti-Hermitian term $-iV_0\theta(x)$ is introduced in the Hamiltonian, to model an absorber aimed at detecting the arrival of a particle in the region $x > 0$ (here θ is the Heaviside *step function*). The particle state evolves in a non-unitary manner, with a transfer of probability from an "incident channel" into "orthogonal and time-labeled measurement channels".

Allcock's initial proposal was in fact based on a *discrete* model, where the wavefunction in the detection region $x > 0$ is periodically removed — i.e. transformed into $\psi(x) = 0\ \forall x > 0$, while it is left unchanged for $x < 0$; then it evolves according to the Schrödinger equation for a time δt when the next "removal" occurs, and so forth.

This suffered mathematical difficulties, which led Allcock to formulate a continuous extension based on the aforementioned complex potential, where the wavefunction norm can continuously decrease as the particle is detected. He showed that the discrete and continuous model can be compared in terms of time resolution, which is δt for the former, and $\hbar/2V_0$ for the latter.

Allcock noticed that when V_0 is large the particle is rather reflected than absorbed; while, when it is small (i.e. the detector has a low absorption rate),

the particle is eventually absorbed but the indetermination $\delta_t \sim \hbar/2V_0$ is, in such case, impractically large.

Overall, Allcock came thus to a negative conclusion and did not overcome the Pauli objection. However, the problem with this complex potential model, either causing reflection or not absorbing sufficiently, was eventually resolved by noting that his results were not general, and potentials can be constructed which absorb the whole wavepacket and avoid reflection (Muga et al. 1995, 2004; Palao et al. 1998).

3.3.1 How a complex potential emerges

Among the methods to define a time-of-arrival quantum observable, the detector model by Allcock (Allcock 1969b), including the following enhancements, is an *operational* one, in that it models a measurement procedure (Muga and Leavens 2000, s. 9) rather than focusing on constructing an operator that satisfies certain requirements (like the Kijowski distribution, see for example Muga and Leavens 2000, s. 8).

The introduction of complex potentials, a non-Hermitian Hamiltonian and the non-unitary time evolution (of what appears formally a pure state) seems artificial and in contradiction with the fundamental rules of quantum mechanics.

While a complex potential can be *postulated* in order to obtain phenomenological laws governing arrival times and detectors, it can also be *obtained* within the established framework of open quantum systems, namely the master equation for an irreversible detector. The core ideas behind this derivation can be —very briefly— summarized as follows (Halliwell 1999).

The detector is modeled by a two-level system with $|1\rangle$ being the state of no-detection and $|0\rangle$ the state of detection. We also introduce the raising and lowering operators $\sigma_+ = |1\rangle\langle 0|$, $\sigma_- = |0\rangle\langle 1|$. The Hamiltonian of the detector is such to have $|0\rangle$ at a lower energy, so the detector "decays" when it "clicks". It is an irreversible transition because of the coupling with the environment. The Hamiltonian encompassing the particle (H_s), the detector (H_d), the environment

(H_E) and the interaction (H_dE) reads

$$H = H_s + H_d + H_E + V(x)H_{dE}\,, \tag{3.8}$$

with H_s being the Hamiltonian of a free particle and

$$H_d = \frac{1}{2}\hbar\omega(|1\rangle\langle 1| - |0\rangle\langle 0|) \tag{3.9a}$$

$$H_E = \sum_n \hbar\omega_n a_n^\dagger a_n \tag{3.9b}$$

$$H_{dE} = \sum_n \hbar\left(\kappa_n^* \sigma_- a_n^\dagger + \kappa_n \sigma_+ a_n\right) \tag{3.9c}$$

$$V(x) = \theta(-x)\,, \tag{3.9d}$$

where a and $a^\dagger$ are the creation and annihilation operator for the electromagnetic field, which constitutes the "environment"; $V(x)$ is chosen to be a step function i.e. the simplest function that makes the detector respond when the particle reaches the region ($x < 0$); and the coupling constants κ_n are to be intended in the same sense of the Jaynes–Cummings model —in fact, the expressions of H_d and H_E also recall it (Walls and Milburn 2008, s. 10.2, Shore and Knight 1993 and many others). This model essentially describes the detector as a Jaynes-Cummings atom with the peculiarity that its coupling with the environment is only activated by the position distribution of another particle.

Tracing out the environment, and with some "standard" assumptions (initial environment at zero temperature, initial separable state "undetected" $\rho(0) = |\psi_0\rangle\langle\psi_0| \otimes |1\rangle\langle 1|$, Markov approximation, weak coupling), the *reduced* dynamics of the particle and the detector is governed by the *master equation*[2]

$$\dot{\rho} = -\frac{\mathrm{i}}{\hbar}[H_s + H_d, \rho] - \frac{\gamma}{2}\left(V^2(x)\sigma_+\sigma_-\rho \; + \rho\sigma_+\sigma_- V^2(x) \; - \; 2V(x)\sigma_-\rho\sigma_+ V(x)\right)\,, \tag{3.10}$$

with γ being "a phenomenological constant determined by the distribution of oscillators in the environment and underlying coupling constants" (Halliwell 1999).

[2]Most details, calculation steps and possible generalizations are clearly skipped here, and can be found in the original article by J. J. Halliwell (Halliwell 1999) and references therein.

A general solution is in the form

$$\rho = \rho_{11} \otimes |1\rangle\langle 1| + \rho_{01} \otimes |0\rangle\langle 1| + \rho_{10} \otimes |1\rangle\langle 0| + \rho_{00} \otimes |0\rangle\langle 0| \,, \tag{3.11}$$

with

$$\dot{\rho}_{11} = -\frac{\mathrm{i}}{\hbar}[H_s, \rho_{11}] - \frac{\gamma}{2}\left(V(x)\rho_{11} + \rho_{11}V(x)\right) \tag{3.12a}$$

$$\dot{\rho}_{01} = -\frac{\mathrm{i}}{\hbar}[H_s, \rho_{01}] - \frac{\gamma}{2}\rho_{01}V(x) + \mathrm{i}\frac{\hbar\omega'}{2}\rho_{01} \tag{3.12b}$$

$$\dot{\rho}_{10} = -\frac{\mathrm{i}}{\hbar}[H_s, \rho_{10}] - \frac{\gamma}{2}V(x)\rho_{10} - \mathrm{i}\frac{\hbar\omega'}{2}\rho_{10} \tag{3.12c}$$

$$\dot{\rho}_{00} = -\frac{\mathrm{i}}{\hbar}[H_s, \rho_{00}] + \gamma V(x)\rho_{11}V(x) \,, \tag{3.12d}$$

and ω' a "renormalized" value for the characteristic frequency ω in H_d.

To give an idea of how the complex potential emerges, let us now focus on ρ_{11} and the corresponding probability of not being detected, which is

$$p_{nd} = \mathrm{Tr}\,\rho_{11}(\tau) = \int_{-\infty}^{\infty} \mathrm{d}x\, \rho_{11}(x, x, \tau) \,, \tag{3.13}$$

where $\rho_{11}(x, x, \tau)$ – or, more generally, $\rho_{ij}(x_1, x_2, \tau)$ for each $i, j = 0, 1$ – are (diagonal) density matrix elements such that, in general:

$$\rho_{ij}(\tau) = \int_{-\infty}^{\infty} \mathrm{d}x_1 \int_{-\infty}^{\infty} \mathrm{d}x_2\, \rho_{ij}(x_1, x_2, \tau)\, |x_1\rangle\langle x_2| \,. \tag{3.14}$$

Now, the solution to the (3.12a) can be written

$$\rho_{11}(t) = e^{-\frac{\mathrm{i}}{\hbar}H_s t - \frac{\gamma}{2}Vt}\rho_{11}(0)e^{\frac{\mathrm{i}}{\hbar}H_s t - \frac{\gamma}{2}Vt} \,. \tag{3.15}$$

If ρ_{11} were in a pure state, say $\rho_{11}(t) = |\psi(t)\rangle\langle\psi(t)|$ (the "undetected wavefunction"), and recalling that $\rho_{11}(0) = |\psi_0\rangle\langle\psi_0|$, Eq. (3.15) can be reformulated as

$$|\psi(t)\rangle = e^{-\frac{\mathrm{i}}{\hbar}H_s t - \frac{\gamma}{2}Vt}\,|\psi_0\rangle = e^{-\frac{\mathrm{i}}{\hbar}\left(H_s - \mathrm{i}\frac{\hbar}{2}\gamma V\right)t}\,|\psi_0\rangle \,, \tag{3.16}$$

showing that the particle evolves as if an "imaginary" (anti-Hermitian) term

$-\mathrm{i}\frac{\hbar}{2}\gamma V$ was added to its otherwise free Hamiltonian H_s. This "proves" the validity of the complex potential model as an *effective* theory, and the consistency with the unitary evolution of the "bigger picture" quantum system.

Another consequence of treating ρ_{11} as a pure state is that the probability of no detection (3.13) can be expressed as

$$p_{nd}(\tau) = \int_{-\infty}^{\infty} \mathrm{d}x \, |\psi(x,\tau)|^2 \,, \tag{3.17}$$

which is the (non conserved) norm $\|\psi\|$ of this effective state vector. Therefore, the probability that the detection *has* happened up to time τ, which is $1-p_{nd}(\tau)$, is equal to the *loss of normalization* $1-\|\psi\|$ at that time. This is the total probability that the detection has happened from the initial time ($t=0$ in our chosen settings) to $t=\tau$. In terms of detection time probability density $\mathbb{P}(t)$, it is therefore

$$\mathbb{P}(t) = -\frac{\mathrm{d}\|\psi\|}{\mathrm{d}t} \,. \tag{3.18}$$

3.4 Detector models

One of the considerations we can gather from the previous Sections is that the problem of arrival time —of a particle at a particular region of space— can be tackled at different "levels".

Operationally, there must be a detector which "clicks" at the arrival of the particle, and the statistical distribution of such click times over repeated measurements is studied. Due the Pauli objection, probabilities in this distribution cannot simply be given in terms of projectors related to eigenspaces of a self-adjoint operator. A more general formulation than projective measurement is therefore necessary.

Detectors can be treated (more or less explicitly) in quantum models of arrival time on different levels:

1. Without making the detector explicit: this is the case of the Kijowski model (Kijowski 1974; Muga and Leavens 2000), which is based on positive-

operator measures (POVM). Given there is no explicit detector in the model, the best candidate statistical distribution and operator are essentially obtained through consistency arguments, including a "reasonable" classical limit. See also the Aharonov–Bohm approach, described in Sec. 3.2.

2. Phenomenological detector models: early attempts to incorporate the measurement apparatus (namely Allcock, Sec. 3.3), which focus on the irreversible process of absorption. Normalization of the quantum state is not preserved, the Hamiltonian is not Hermitian because the potential is not real. The rate of normalization-loss is interpreted as absorption (or detection) probability over time.

3. Full detector models: for example the Atom-Laser model. A two-level atoms in the ground state is sent to a laser-illuminated region (we are interested in the time-of-arrival into this region), is excited, and the first photon which is spontaneously emitted following the excitation is interpreted as detection of the arrival in the region. Problems related to reflection, low absorption rate, and delay in the spontaneous emission are fully taken into account in the model.

A brief, mostly qualitative, illustration of the Atom-Laser model is given below, and references therein can be consulted for more details.

3.4.1 Basics of Atom-Laser Model

As pointed out in Damborenea et al. 2002, the model by Halliwell (Sec. 3.3.1) has the merit of including irreversibility in the detection process, but "remains somewhat abstract since no connection is made with any specific measuring system". The work by Damborenea et al. gives instead an operational description of the notion of *arrival time*.

The model describes an atom sent towards a laser-illuminated region. The arrival time into the region is taken as the time[3] when the first photon is spon-

[3]Please note, while there is an operational definition of detection, there is no operational

taneously emitted by the atom, following its excitation by the laser. The spontaneous photon emission is therefore the "click" of the detector.

There are "delays": 1) in the transition of the atom to the excited state, and 2) in the spontaneous emission. This cannot be addressed by simply increasing the laser intensity (therefore shortening the excitation and decay time) because this would lead to reflection, and the most likely outcome would be no detection and no absorption at all. This is similar to the issue encountered, at a theoretical level, by Allcock when the imaginary absorbing potential was too large.

A suitable detector configuration, therefore, will be based on *weak driving*, but will need to have the delays compensated, which can be achieved by computing the deconvolution with the decay time distribution of an atom at rest.

The weak driving regime is characterized by longer lifetimes. However, in Damborenea et al. 2002, it is shown that, as a limit for shorter lifetimes, the deconvoluted distribution converges to the probability current flux. This is interesting because, on the other hand, in general, the probability current cannot be used to derive a time of arrival distribution, due to the backflow effect —for instance in a one dimensional system, a superposition of only positive momentum eigenfunctions may still lead to a negative current, as it was initially noted by Allcock himself (Allcock 1969c).

A possible experimental implementation can be based on a *3-level* atom, which decades into an intermediate, metastable, "sink" state after emission (Muga et al. 2009; Oberthaler et al. 1996).

The model is based on treating the laser classically while the atom and the spontaneously emitted photons are described with the *quantum jump* or *quantum trajectories* approach: similar to what we have seen in Sec. 3.3.1.

definition of time; in other words, while this model does include an explicit description of the detector, there is still no description or definition of a "clock".

The effective *conditional Hamiltonian* reads:

$$H_c = \frac{\hat{p}^2}{2m} + \frac{\hbar}{2}\begin{pmatrix} 0 & 0 \\ 0 & -\mathrm{i}\gamma \end{pmatrix} + \frac{\hbar}{2}\begin{pmatrix} 0 & \Omega(x) \\ \Omega(x) & -2\Delta \end{pmatrix}, \tag{3.19}$$

where γ is the decay rate or *Einstein coefficient*, $\Omega(x) = \Theta(x)\,\Omega$ is the Rabi frequency (ideally assuming that the half-space $x > 0$ is uniformly illuminated by the laser), and Δ is the effective detuning including Doppler and recoil effects — but the on-resonance case ($\Delta = 0$) can be considered, by setting normal incidence and adjusting the laser frequency (more details in Damborenea et al. 2002 and Muga et al. 2009, s. 4.2).

The Hamiltonian in (3.19) has an imaginary term $\mathrm{i}\gamma$ which makes the Hamiltonian H_c non-Hermitian. Wavefunctions evolve, according to the Schrödinger equation, while *loosing normalization*; the rate $-\frac{\mathrm{d}\|\psi\|^2}{\mathrm{d}t}$ is then interpreted as the probability density of the atom arrival being detected at time t. If the norm $\|\psi\|^2$ vanishes for $t \to +\infty$, that means that the detection will certainly occur at some time. But that limit can be finite, indicating a certain probability of never being detected (for example due to reflection).

The detection (i.e. spontaneous emission of the first photon) is generally delayed with respect to the actual arrival at the laser-illuminated region, due to the finite time required for excitation and de-excitation. That needs to be compensated via deconvolution with the evolution of an atom at rest. Simply adjusting the optical parameters to shorten the excitation and emission times would not be a solution as it would either increase reflection rate dramatically or simply increase the probability that atoms pass through the region undetected.

Nonetheless, one can focus on the state transition of the atom itself i.e. the "arrival" at the excited state of the atom from the ground state, rather than the arrival at a particular region in space. This is the focus of Sec. 3.4.2 below.

The general atom–laser model gives, anyway, an operational justification for the interest in more idealized (and tractable) models too.

3.4.2 Arrival in an excited level

The detection-by-absorption model in Kiukas et al. 2012 is also based on a complex potential that, plugged into the Schrödinger equation, leads to a non-unitary evolution of the state vector (with loss of normalization).

Specifically, the Hamiltonian $\hat{H}$ is replaced by a $\hat{H} - i\hat{D}$ (with $\hat{D}$ self-adjoint, bounded, positive):

$$\left(\hat{H} - i\hat{D}\right) |\psi(t)\rangle = i\hbar \frac{\mathrm{d}}{\mathrm{d}t} |\psi(t)\rangle \,. \tag{3.20}$$

A two-level example is considered to provide a concrete example. Starting from the paper, we now carry on some explicit calculations.

By setting, out of convenience, $\hbar = \omega = 1$ (with ω the characteristic frequency of the system), and directly considering the parameters that minimize the time–energy uncertainty product (ibid.), we have a non-Hermitian "Hamiltonian" $K = \hat{H} - i\hat{D}$ with

$$K = \hat{H} - i\hat{D} \equiv \hbar\omega \left\{ \begin{bmatrix} 0 & 1 \\ 1 & 0 \end{bmatrix} - i \begin{bmatrix} 0 & 0 \\ 0 & \gamma \end{bmatrix} \right\} \tag{3.21}$$

and $\gamma = 2\sqrt{2}$.

We take an initial state of $|0\rangle$ (or $\begin{bmatrix} 1 \\ 0 \end{bmatrix}$ in matrix form).

We then compute, symbolically, the non-unitary evolution $|\psi(t)\rangle = e^{-iKt} |0\rangle$ with the aid of *SymPy* (Meurer et al. 2017) within a *Jupyter* (Kluyver et al. 2016) notebook (see Appendix A.1 for all the details of the calculation).

Simplifying the result in Eq. (A.1), we have:

$$|\psi(t)\rangle \equiv e^{-\frac{\sqrt{2}}{t}} \begin{bmatrix} \cos\left(\frac{\sqrt{2}}{2}t\right) + \sin\left(\frac{\sqrt{2}}{2}t\right) \\ -i\sqrt{2}\sin\left(\frac{\sqrt{2}}{2}t\right) \end{bmatrix} . \tag{3.22}$$

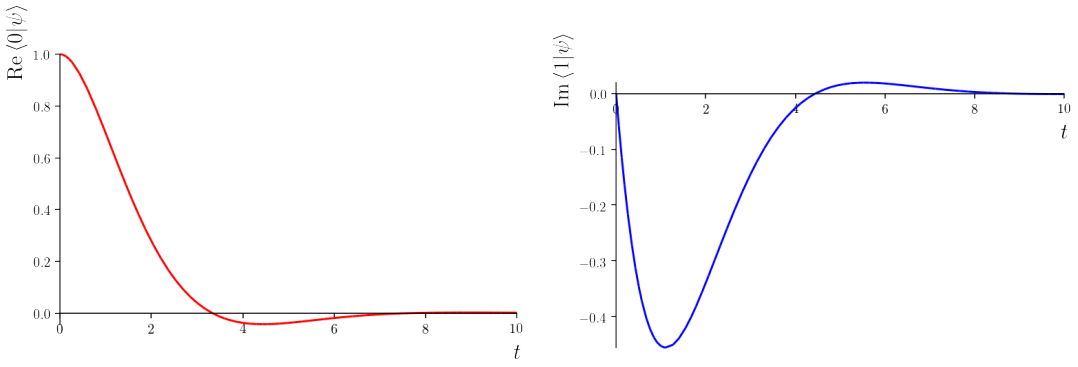

(a) (b)

Figure 3.1: Non-unitary evolution of the absorbed qubit according to the model in Kiukas et al. 2012. The component along $|0\rangle$ is purely real, and the one along $|1\rangle$ is purely imaginary, therefore only their their respective parts are plotted.

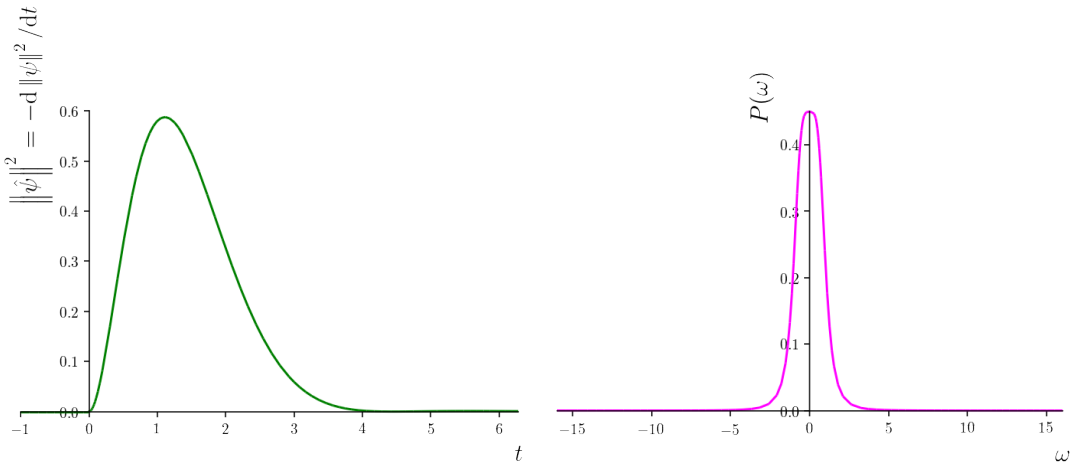

(a) (b)

Figure 3.2: Non-unitary evolution of absorbed qubit. (a) Detection probability in time. It's equal to the loss of normalization $-\frac{\mathrm{d}\|\psi\|^2}{\mathrm{d}t}$ (but also to the squared norm of $\hat{\psi}(t)$ as of Eq. (3.23). (b) Detection probability in the frequency domain. *Note*: The frequency domain, while not essential at this level of treatment, will allow a comparison with the findings of Section 4.6.2, in particular Fig. 4.4b.

The "lossy" evolution, with the two components of the qubit, is shown in Fig. 3.1. The loss of normalization $-\frac{\mathrm{d}\|\psi\|^2}{\mathrm{d}t}$, indicating the probability of arrival in state $|1\rangle$ by absorption, is then derived directly and shown in Fig. 3.2.

This yields the *probability* of detection. One may wonder whether it is possible to derive a corresponding *probability amplitude* vector, whose squared norm across time is equal to the said probability distribution.[4] Within the framework of Kiukas et al. 2012, a "wavefunction in time" in such sense is the $\hat{\psi}$, as in (4.54). It is computed in detail within the notebook in Appendix A.1, Eq. (A.2), simplifying which we obtain:

$$\hat{\psi}(t) = i2^{\frac{5}{4}} e^{-\frac{\sqrt{2}}{2}t} \sin\left(\frac{\sqrt{2}}{2}t\right)\theta(t)\,|1\rangle\,, \tag{3.23}$$

with $\theta(t)$ the Heaviside step function.

[4] The solution is of course not unique, but one may ask whether such functions would lead to quantum interference patterns and other phenomenology which may be subject of further study.

Chapter 4

Page and Wootters Relational Time

This Chapter will be devoted to outlining the Page and Wootters theory of time, also known as the model of "evolution without evolution". Existing literature will be reviewed, with some original considerations, in particular with regards to time–energy uncertainty relations, finite-dimensional systems and discrete clocks (Sections 4.1–4.3).

A second part (Sections 4.4–4.7) will be dedicated to applications of the Page–Wootters model, starting with a discussion of existing experiments (or "experimental illustrations"), then implementing numerical simulations, with a larger number of clock levels. Finally, the Page and Wootters model will be compared to the results of detection and time-of-arrival models based on non-unitary evolution.

4.1 The Model

To introduce the Page–Wootters model, let us first consider a bipartite system $\mathcal{H}_T \otimes \mathcal{H}_S$, and a state vector $|\Psi\rangle\rangle \in \mathcal{H}_T \otimes \mathcal{H}_S$. A "double angle bracket" notation $|\Psi\rangle\rangle$ is used here for vectors in the tensor product space.

Let $|\Psi\rangle\rangle$ be *stationary*, meaning it is an eigenstate of an overall Hamiltonian $\hat{\mathbb{J}}$ in $\mathcal{H}_T \otimes \mathcal{H}_S$:

$$\hat{\mathbb{J}} \, |\Psi\rangle\rangle = 0. \tag{4.1}$$

Finally, we assume that the two subsystems are *non interacting*, meaning that the global Hamiltonian $\mathbb{J}$ can be expressed as a sum of two terms which only act on the respective subspaces $\mathcal{H}_T$ and $\mathcal{H}_S$ (and there is no explicit "interaction term"). In other words, $\hat{\mathbb{J}}$ can be expressed as

$$\hat{\mathbb{J}} = \hat{H}_T \otimes \mathbb{1}_S + \mathbb{1}_T \otimes \hat{H}_S \, . \tag{4.2}$$

Therefore, the evolution of the subsystem described by $\mathcal{H}_S$ will only depend on "its own" Hamiltonian H_S (assumed as time-independent), namely

$$|\psi(t)\rangle_S = e^{-i\hat{H}_S t/\hbar} \, |\psi(0)\rangle_S \, . \tag{4.3}$$

Note the familiar single-bracket notation $|\psi(t)\rangle_S$ for a ket in one of the two parts (subspaces) of $\mathcal{H}_T \otimes \mathcal{H}_S$ ($\mathcal{H}_S$ in this case).

The overall bipartite system is *isolated*. A notable example of isolated system is, of course, the universe. This simple observation is relevant because, in its original formulation (Page and Wootters 1983), $\mathcal{H}_T \otimes \mathcal{H}_S$ is regarded as a partition of the whole universe, which is considered, overall, in a stationary state.

This is known as the "timeless" approach (Marletto and Vedral 2017). A suitable subsystem —described by $\mathcal{H}_T$ within this framework— is chosen in the "universe" so that it acts as *clock* for the *rest* of it, in the sense that there is an observable $\hat{T}$ which can be used to describe the time evolution "without evolution" of the other subsystem[1] $\mathcal{H}_S$.

The operator $\hat{T}$ can be regarded as the *time operator*. It is defined in $\mathcal{H}_T$ (not $\mathcal{H}_S$), and canonically conjugate to the "Hamiltonian" $\hat{H}_T$ (not $\hat{H}_S$). In other words, the time operator is defined in a different Hilbert space than the "system of interest" $\mathcal{H}_S$, therefore the Pauli objection (Sec. 3.1) no longer applies.

[1] A slightly different notation uses indeed $\mathcal{H}_C$ and $\mathcal{H}_R$ (instead of $\mathcal{H}_T$ and $\mathcal{H}_S$) to indicate the Hilbert spaces of the clock (C) and the rest (R) of the "universe" (or isolated system): see, for example, Marletto and Vedral 2017.

As we will see below, in the Page–Wootters model, time evolution is based on an internal *entanglement* relation among elements of subspaces $\mathcal{H}_S$ and $\mathcal{H}_T$ respectively.

An intuitive description may be as follows. From the perspective of the system described by $\mathcal{H}_S$, time is a parameter t; however t can have values which are also eigenvalues of an observable $\hat{T}$ defined in *another* space $\mathcal{H}_T$, with which it is entangled. Such entanglement relation establishes a correspondence between "instants of time" (eigenvalues and eigenstates of observable $\hat{T}$) and ("evolved") states in $\mathcal{H}_S$.

About three decades after the original work by Page and Wootters (Page and Wootters 1983), the formalism was developed further by Giovannetti, Lloyd and Maccone (Giovannetti et al. 2015). Most technical details introduced below are based on that paper.

First of all, the "conventional" state $|\psi(t)\rangle_S$ in $\mathcal{H}_S$ can be obtained from $|\Psi\rangle\rangle$ via partial inner product[2] with a time eigenstate ${}_T\langle t|$:

$$|\psi(t)\rangle_S = {}_T\langle t|\Psi\rangle\rangle \,. \tag{4.4}$$

The function $t \to |\psi(t)\rangle_S$ is the "wavefunction in time representation", in analogy with the wavefunction in position representation of standard quantum mechanics. The state vector $|\Psi\rangle\rangle$ is univocally identified by the "coefficients" $|\psi(t)\rangle_S$ with respect to the basis $\{|t\rangle_T\}$:

$$|\Psi\rangle\rangle = \int \mathrm{d}t \, |t\rangle_T \otimes |\psi(t)\rangle_S \,, \tag{4.5}$$

somewhat similar to the well known expression $|\psi\rangle_S = \int \mathrm{d}x \, \psi_S(x) \, |x\rangle_S$ which defines the position representation.

Under this time representation (or T representation), the operator $\hat{H}_T = \hbar\hat{\Omega}$, canonically conjugate to the time operator $\hat{T}$, is expressed as $-i\hbar\frac{\partial}{\partial t}$, and the commutation relation $[\hat{T}, \hat{H}_T] \underset{T}{\equiv} \left[t, -i\hbar\frac{\partial}{\partial t},\right] = i\hbar$ can be proven immediately, similarly to the well known position-momentum relation $[\hat{x}, \hat{p}] \underset{x}{\equiv} \left[x, -i\hbar\frac{\partial}{\partial x}\right] = i\hbar$.

[2] For the partial inner product, see Definition 2.3.1 and 2.3.2, and Jacobs 2014, s. 1.3.3.

	$\mathcal{H}_T$	$\mathcal{H}_S$
Canonical commutation relation	$\hat{T}$	$\hat{x}$
	$\hat{H}_T \underset{T}{\equiv} -i\hbar\frac{\partial}{\partial t}$	$\hat{p} \underset{x}{\equiv} -i\hbar\frac{\partial}{\partial x}$
Hamiltonian	$\hat{H}_T$	$\hat{H}_S$

Table 4.1: Analogies between observables in the two Hilbert spaces.

Thus, $\hbar\hat{\Omega}$ can be seen as similar to a "linear momentum" in the Hilbert space of time.

Using the T representation in $\mathcal{H}_T$, and comparing (4.2) and (4.1):

$$0 = \left(\hbar\hat{\Omega}\otimes\mathbb{1}_S + \mathbb{1}_T\otimes\hat{H}_S\right)|\Psi\rangle\rangle \equiv -i\hbar\frac{\partial}{\partial t}|\psi(t)\rangle_S + \hat{H}_S|\psi(t)\rangle_S\,, \tag{4.6}$$

we recover the usual form of the Schrödinger equation in H_S (see also Wootters 1984, pp. 709–710).

Here $\hat{\Omega}$ can be seen as a "frequency operator" represented as $-i\frac{\partial}{\partial t}$ and having as eigenfunctions those functions evolving in time with a phase factor $e^{i\omega t}$ only.

From another point of view, $\hat{H}_T = \hbar\hat{\Omega}$ is the "Hamiltonian" of $\mathcal{H}_T$, in that it plays a similar role of H_S in the construction of $\hat{\mathbb{J}}$ in (4.2).

Such analogies among operators in $\mathcal{H}_T$ and $\mathcal{H}_S$ are summarized in Table 4.1.

In the bipartite universe, physical kets $|\Psi\rangle\rangle$ can have a Schmidt decomposition made up of eigenstates $|\omega\rangle_T$ of $\hat{H}_T$ in $\mathcal{H}_T$ entangled with eigenstates $\left|\tilde{\psi}(\omega)\right\rangle_S$ of $\hat{H}_S$ in $\mathcal{H}_S$ (the eigenvalue is $\hbar\omega$ for both $\hat{H}_T$ and $\hat{H}_S$ respectively); or eigenstates $|t\rangle_T$ of $\hat{T}$ in $\mathcal{H}_T$ entangled with time-evolved spatial states $|\psi(t)\rangle_S$ in $\mathcal{H}_S$:

$$|\Psi\rangle\rangle = \int \mathrm{d}\omega\ |\omega\rangle_T\otimes\left|\tilde{\psi}(\omega)\right\rangle_S = \int \mathrm{d}t\ |t\rangle_T\otimes|\psi(t)\rangle_S\,. \tag{4.7}$$

Using the relations ${}_T\langle t|t'\rangle_T = \delta(t-t')$ and $|\omega\rangle_T = \frac{1}{\sqrt{2\pi}}\int \mathrm{d}t\, e^{\mathrm{i}\omega t}|t\rangle_T$ (see also

Giovannetti et al. 2015, p. 2), it follows that[3]

$$ {}_T\langle t|\omega\rangle_T = \frac{1}{\sqrt{2\pi}}\, {}_T\langle t| \int \mathrm{d}t'\, e^{-\mathrm{i}\omega t'}\, |t'\rangle_T = \frac{1}{\sqrt{2\pi}} \int \mathrm{d}t'\, e^{\mathrm{i}\omega t'} \delta(t-t') = \frac{1}{\sqrt{2\pi}} e^{\mathrm{i}\omega t} \,. \quad (4.8) $$

Note that, while it is $\langle\psi(t)|\psi(t)\rangle_S = 1\ \forall t \in \mathbb{R}$ (unitary evolution, as in standard quantum mechanics), one should not necessarily expect that $\left|\tilde{\psi}(\omega)\right\rangle_S$ has norm 1 for each real value of ω. In particular, if $\hbar\omega$ is not in the energy spectrum of the system, then $\left|\tilde{\psi}(\omega)\right\rangle_S = 0$, i.e. the vector does not contribute to the integral. Given that the energy spectrum is bounded, certainly there are values of ω for which this is the case. With these considerations, Eq. (4.7), with regards to the first integral, may also be reformulated as

$$ |\Psi\rangle\rangle = \int \mathrm{d}\omega\, \mu(\omega)\, |\omega\rangle_T \otimes |\phi(\omega)\rangle_S \,, \quad (4.9) $$

with $|\phi(\omega)\rangle_S$ normalized for any real value of ω, and $\mu(\omega)\,|\phi(\omega)\rangle_S = \left|\tilde{\psi}(\omega)\right\rangle_S$ — see also ibid., eq. (10). This notation will be useful in the example of Sec. 4.1.1.

Non-zero eigenvalues

Generalizing (4.2) and (4.1), let us consider the case when $|\Psi\rangle\rangle$ is an eigenvector of $\hat{\mathbb{J}}$ related to a general eigenvalue ϵ instead of zero. This brings to

$$ \epsilon\, |\Psi\rangle\rangle = \left(\hbar\hat{\Omega} \otimes \mathbb{1}_S + \mathbb{1}_T \otimes \hat{H}_S\right) |\Psi\rangle\rangle \,. \quad (4.10) $$

Partial scalar product by ${}_T\langle t|$ on the left yields

$$ \epsilon\, |\psi_{PW}(t)\rangle_S = -i\hbar \frac{\partial}{\partial t} |\psi_{PW}(t)\rangle_S + \hat{H}_S\, |\psi_{PW}(t)\rangle_S \,, \quad (4.11) $$

[3] In analogy with the well-known inner product of position and momentum eigenvectors in standard quantum mechanics: $\langle\mathbf{x}|\mathbf{p}\rangle = (2\pi\hbar)^{-3/2} e^{\mathrm{i}\mathbf{p}\cdot\mathbf{x}/\hbar}$ (or $\langle x|p\rangle = \frac{e^{\mathrm{i}px/\hbar}}{\sqrt{2\pi\hbar}}$ for one-dimensional systems). See, for example, Ballentine 1998, pp. 126–127.

where we have defined $\psi_{PW}(t) \coloneqq {}_T\langle t|\Psi\rangle\rangle$. Rearranging Eq. (4.11):

$$\left(\hat{H}_S - \epsilon \mathbb{1}_S\right) |\psi_{PW}(t)\rangle_S = i\hbar \frac{\partial}{\partial t} |\psi_{PW}(t)\rangle_S \,, \tag{4.12}$$

which is, formally, the Schrödinger equation for the state $|\psi_{PW}(t)\rangle_S$ with the Hamiltonian $\left(\hat{H}_S - \epsilon \mathbb{1}_S\right)$. With the initial condition $|\psi_{PW}(0)\rangle \coloneqq |\psi_0\rangle$, we have therefore:

$$|\psi_{PW}(t)\rangle_S = e^{-\frac{\mathrm{i}(\hat{H}_S - \epsilon)t}{\hbar}} |\psi_0\rangle_S = e^{\frac{\mathrm{i}\epsilon t}{\hbar}} e^{-\frac{\mathrm{i}\hat{H}_S t}{\hbar}} |\psi_0\rangle_S \,, \tag{4.13}$$

hence:

$$e^{-\frac{\mathrm{i}\hat{H}_S t}{\hbar}} |\psi_0\rangle_S = e^{-\frac{\mathrm{i}\epsilon t}{\hbar}} |\psi_{PW}(t)\rangle_S \,, \tag{4.14}$$

where we recognize $e^{-\frac{\mathrm{i}\hat{H}_S t}{\hbar}} |\psi_0\rangle_S$ as the time evolution from an initial state $|\psi_0\rangle_S$ at time $t = 0$, under the Hamiltonian $\hat{H}_S$, in standard quantum mechanics. If we define this evolved state as, simply, $|\psi(t)\rangle_S$, and recall the definition of $|\psi_{PW}(t)\rangle_S$, we have

$$|\psi(t)\rangle_S = e^{-\frac{\mathrm{i}\epsilon t}{\hbar}} {}_T\langle t|\Psi\rangle\rangle \,, \tag{4.15}$$

which, compared to Eq. (4.4), shows that the projection of the eigenstate $|\Psi\rangle\rangle$ of $\hat{\mathbb{J}}$ over an eigenbasis of time within the Page–Wootters model, namely ${}_T\langle t|\Psi\rangle\rangle$, is compatible with the prediction $|\psi(t)\rangle_S$ of standard quantum mechanics only *up to a corrective phase* $e^{-\frac{\mathrm{i}\epsilon t}{\hbar}}$. In other terms, with a non-zero eigenvalue ϵ of $\hat{\mathbb{J}}$, the model can still return the ordinary quantum mechanics evolution, but with an "energy shift" of value ϵ. See also Giovannetti et al. 2015, *"The Zero-eigenvalue"*.

4.1.1 Example: Hamiltonian eigenstate

An extreme case for the distribution $\mu(\omega)$ in (4.9) is, as an example, what in standard quantum mechanics would be the time evolution of an energy eigenstate (or an eigenstate of $\hat{H}_S$ in $\mathcal{H}_S$, within the Page–Wootters formalism). Let the eigenvalue be $E_0 \coloneqq \hbar\omega_0$; and let the initial state $|\psi_0(0)\rangle_S = |\psi_0^i\rangle_S$ a related eigenstate, such that $\hat{H}_S |\psi_0^i\rangle_S = E_0 |\psi_0^i\rangle_S$. Then the time evolution is

$$|\psi_0(t)\rangle_S = e^{-\frac{i}{\hbar}E_0 t} \left|\psi_0^i\right\rangle_S = e^{-i\omega_0 t} \left|\psi_0^i\right\rangle_S . \tag{4.16}$$

In Page–Wootters terms, the corresponding "history vector" is

$$|\Psi_0\rangle\rangle = \int \mathrm{d}t\, |t\rangle_T \otimes |\psi_0(t)\rangle_S\,, \tag{4.17}$$

where the integrand is the tensor product of an eigenvector of $\hat{T}$ in $\mathcal{H}_T$ and the time-evolved state vector in $\mathcal{H}_S$; but $|\Psi_0\rangle\rangle$ can also be expressed as

$$|\Psi_0\rangle\rangle = \int \mathrm{d}\omega\ |\omega\rangle_T \otimes \left|\tilde{\psi}_0(\omega)\right\rangle_S\,, \tag{4.18}$$

in terms of eigenvectors of the "Hamiltonians" $\hat{H}_T$ and $\hat{H}_S$ in the two spaces respectively —see also Eq. (4.7).

As $\left|\tilde{\psi}_0(\omega)\right\rangle_S$ is the Fourier transform of $|\psi_0(t)\rangle_S$, and using Eq. (4.16), it holds:

$$\left|\tilde{\psi}_0(\omega)\right\rangle_S = \frac{1}{\sqrt{2\pi}} \int \mathrm{d}t\, e^{-iwt} e^{-i\omega_0 t} \left|\psi_0^i\right\rangle_S = \delta(\omega+\omega_0) \left|\psi_0^i\right\rangle_S;$$

then, replacing into Eq. (4.18):

$$|\Psi_0\rangle\rangle = |-\omega_0\rangle_T \otimes \left|\tilde{\psi}_0(-\omega_0)\right\rangle_S\,, \tag{4.19}$$

showing that the frequency distribution in $\mathcal{H}_T$ is in fact concentrated at $\omega = -\omega_0$.[4]

4.1.2 Normalizable vectors of $\mathcal{H}_T \otimes \mathcal{H}_S$

A vector $|\Psi\rangle\rangle$ in $\mathcal{H}_T \otimes \mathcal{H}_S$, satisfying (4.2) and (4.1), encodes the whole (unitary) time evolution of a system.

$$|\Psi\rangle\rangle = \int \mathrm{d}t\, |t\rangle_T \otimes |\psi(t)\rangle_S = \int \mathrm{d}t\, \mathrm{d}^3\vec{r}\ \ \Psi(t;\vec{r})\ \ |t\rangle_T \otimes |\vec{r}\rangle_S\,, \tag{4.20}$$

with $|\vec{r}\rangle_S$ eigenstate of the position observable in $\mathcal{H}_S$, so that $\Psi(t;\vec{r})$ can be regarded as the wavefunction in position representation of the system at time t,

[4] The negative value should not be a surprise to the reader. The vector $|\Psi_0\rangle\rangle$ is an eigenstate of H_S (or, more correctly, of $\mathbb{1}_T \otimes \hat{H}_S$) in relation to the eigenvalue $\hbar\omega_0$. The same vector is also an eigenstate of $\hbar\hat{\Omega} \otimes \mathbb{1}_S$ for the eigenvalue $-\hbar\omega_0$. This guarantees the zero sum in (4.1) and (4.2).

in ordinary quantum mechanics terms. We know $\{|t\rangle_T \otimes |\vec{r}\rangle_S\}$ is an orthonormal basis of $\mathcal{H}_T \otimes \mathcal{H}_S$, therefore

$$\| |\Psi\rangle\rangle \|^2 = \int \mathrm{d}t\, \mathrm{d}^3\vec{r}\ |\Psi(t;\vec{r})|^2 = \int \mathrm{d}t \int \mathrm{d}^3\vec{r}\ |\Psi(t;\vec{r})|^2 = \int \mathrm{d}t\, 1 \to +\infty\,, \quad (4.21)$$

which means that such $|\Psi\rangle\rangle$ is an *improper* vector of $\mathcal{H}_T \otimes \mathcal{H}_S$.

Proper (i.e. normalizable) states are described in Giovannetti et al. 2015 as well, by replacing (or generalizing) the (4.20) with

$$|\Phi\rangle\rangle = \int \mathrm{d}t\, \phi(t)\, |t\rangle_T \otimes |\psi(t)\rangle_S\ . \quad (4.22)$$

If the function $\phi \in \mathscr{L}^2(\mathbb{R})$, then $|\Psi\rangle\rangle$ is a proper element of the product space, and $\| |\Psi\rangle\rangle \|^2 = \int \mathrm{d}t\, |\phi(t)|^2$.

The case of non-normalizable $|\Psi\rangle\rangle$ in (4.22), with normalized $|\psi(t)\rangle_S\ \forall t \in \mathbb{R}$, describes the unitary evolution, as seen throughout Chapter 4. As observed in Maccone 2018, "Quantum mechanics is formulated in terms of *systems*, typically limited in space but infinitely extended in time". If the state vector is *conditioned* at a particular time t, it holds $\|_T \langle t|\Psi\rangle\rangle\|_S = \||\psi(t)\rangle\|_S = 1$, meaning that, at each t, *the particle must certainly be in some (one) point in space.*

A normalized $|\Psi\rangle\rangle$ in the whole $\mathcal{H}_T \otimes \mathcal{H}_S$, instead, can be interpreted as a total probability of 1 in both space and time combined. It can be interpreted as describing an *event*, in that it must certainly be in some point in space *and* time (in terms of outcome of an idealized measurement). Such states have no correspondence to the full "history" of a system (and, therefore, to its unitary evolution according to standard quantum mechanics).

Such notion of *event* was formalized, recently, in Giovannetti et al. 2022. Apart from different notation, one can recognize, in Eq. 1 therein (by setting $\mu = \nu = 0$), the canonical commutation relations for the time operator $\hat{T}$ and its conjugate $\hat{H}_T$ (while $\mu = \nu = 1, 2, 3$ would bring to the well-known position–momentum relations). Moreover, Eq. 6 from ibid. can easily be recognized as a more compact form of Eq. (4.22) by rearranging its integration variables.

4.2 Uncertainty relations in $\mathcal{H}_T \otimes \mathcal{H}_S$

4.2.1 For unitary evolutions – general considerations

In a continuous time Page–Wootters universe —using the same symbols and definitions as in Sec. 4.1— one may observe that, in $\mathcal{H}_T$ and in the "time representation", it is $\hbar\hat{\Omega} \equiv -i\hbar\partial_t$.

Therefore, in analogy with $\hat{p} \equiv -i\hbar\partial_q$ in $\mathcal{H}_S$, a time–energy uncertainty relation can be derived with a proof that is formally identical to the well known position–momentum uncertainty relation.

Here by "energy" we mean the Hamiltonian in standard quantum mechanics which, in Page–Wootters notation, can be expressed as $\mathbb{1}_T \otimes \hat{H}_S$, which is also equal to $-\hbar\hat{\Omega} \otimes \mathbb{1}_S$, if applied to a solution of $\hat{\mathbb{J}}\,|\Psi\rangle\rangle = 0$ —Eqs. (4.1) and (4.2). The different sign does not change considerations related to the spread of statistical distributions. A formal proof will follow in Sec. 4.2.2.

However, unitary evolution means that a particle exists with certainty at all times, i.e. the packet is infinitely spread in time. Intuitively, one expects the standard deviation of the probability distribution of time observable to diverge i.e. $\sigma_T = \infty$.

The additional difficulty of dealing with infinities and improper state vectors motivates the study of *proper* (i.e. normalizable) states[5] of $\mathcal{H}_T \otimes \mathcal{H}_S$ instead, whose uncertainty relations for T and $\hbar\Omega$ will be discussed in Sec. 4.2.2.

4.2.2 For normalized elements of $\mathcal{H}_T \otimes \mathcal{H}_S$

A normalized element of $\mathcal{H}_T \otimes \mathcal{H}_S$ allows in principle for a finite value of the uncertainties σ_T and σ_Ω.

A physical state in $\mathcal{H}_T \otimes \mathcal{H}_S$ is not generally *separable*, thus the problem of time and energy relation cannot be immediately reduced to that of a pure state in $\mathcal{H}_T$.

[5] Introduced in Sec. 4.1.2.

Still, it is generally an entangled state in the product space $\mathcal{H}_T \otimes \mathcal{H}_S$. We can consider the operators $\hat{T} \otimes \mathbb{1}_S$ and $\hbar\hat{\Omega} \otimes \mathbb{1}_S$ defined therein.

We use the general Robertson–Schrödinger uncertainty relation which yields:

$$\begin{aligned}\sigma_T\sigma_E \coloneqq \sigma_{T\otimes\mathbb{1}_S}\sigma_{\hbar\Omega\otimes\mathbb{1}_S} &\geq \frac{1}{2}\left|\left\langle\left[\hat{T}\otimes\mathbb{1}_S, \hbar\hat{\Omega}\otimes\mathbb{1}_S\right]\right\rangle\right| \\ &= \frac{1}{2}\left|\left\langle\left(\hat{T}\otimes\mathbb{1}_S\right)\left(\hbar\hat{\Omega}\otimes\mathbb{1}_S\right) - \left(\hbar\hat{\Omega}\otimes\mathbb{1}_S\right)\left(\hat{T}\otimes\mathbb{1}_S\right)\right\rangle\right| \\ &= \frac{\hbar}{2}\left|\left\langle\hat{T}\hat{\Omega}\otimes\mathbb{1}_S - \hat{\Omega}\hat{T}\otimes\mathbb{1}_S\right\rangle\right| \\ &= \frac{\hbar}{2}\left|\left\langle\left[\hat{T},\hat{\Omega}\right]_T\otimes\mathbb{1}_S\right\rangle\right| = \frac{\hbar}{2}\left|\left\langle\left[\hat{T},\hat{\Omega}\right]\right\rangle_T\right| = \frac{\hbar}{2}\,, \end{aligned} \tag{4.23}$$

thus showing that $\sigma_T\sigma_E \geq \frac{\hbar}{2}$.

4.3 Finite-dimensional systems

> [...] discreteness in the world is simply the Fourier transform of compactness.
>
> *Physics and the Integers* (Tong 2011)

Finite-dimensional systems are of interest, phenomenologically, and in general easier to implement, both experimentally and numerically.

An experimental illustration of the Page–Wootters model will be discussed in Sec. 4.4. It is based on a clock (defined through the corresponding frequency operator) which has two discrete levels only.

However, finite-dimensional formulas present difficulties in identifying canonically conjugate pairs, and one cannot use the same explicit formalism that would be used for observables with a continuous spectrum. Moreover, operators satisfying a canonical commutation relation such as

$$[\hat{T},\hat{\Omega}] = i \tag{4.24}$$

cannot be both bounded, therefore they cannot exist in a finite-dimensional space (Weyl 1950).

This problem was studied in detail in Vourdas 2004. It was shown therein that satisfying the canonical commutation relation is not essential to build operators representing physical observables with the same role of position and momentum.[6]

Discrete, bounded, position-like and momentum-like operators can be obtained from each other via the *finite* or *discrete Fourier transform* (DFT). In our case, we are particularly interested in relating the time operator $\hat{T}$ and the "energy" operator $\hbar\hat{\Omega}$ in $\mathcal{H}_T$ —via the angular frequency operator $\hat{\Omega}$ which, in the continuous limit, would satisfy Eq. (4.24) exactly.

A benefit of finite-dimensional systems is the potential implementation on a finite array of qubits in a quantum computer. The use of Discrete Fourier Transform extends the overlap with technology and engineering to the domain of signal processing (Vourdas 2004). In *ordinary* quantum mechanics, the Fourier transform (discrete or continuous) is generally used to associate wavefunctions in position and momentum space (whereas time and frequency are *not* operators), while in communication engineering it is used to convert signals from the time to the frequency domain and vice versa. Thanks to the introduction of the Hilbert space $\mathcal{H}_T$, the interpretation in terms of time and frequency (or time and energy, up to a factor $\hbar$) is applicable to quantum theory as well, not only formally i.e. not in the sense of a mere operation among ("classical") parameters; but in the sense of conversion between representations of the same quantum state vector with respect to different eigenbasis, in full analogy with position and momentum in $\mathcal{H}_S$.

4.3.1 Discrete Fourier transform

We will add some more details to the analysis of Vourdas 2004 with additional emphasis on sign and scaling conventions which will affect our computation. Results will be interpreted in the context of the Page–Wootters model, in particular with regards to the temporal subspace $\mathcal{H}_T$.

[6] Or $\hat{T}$ and $\hbar\hat{\Omega}$ in $\mathcal{H}_T$ for a finite-dimensional Page and Wootters model.

Let us start with a continuous system where the Fourier transform $\phi \coloneqq \mathcal{F}\psi$ of an integrable function $\psi : \mathbb{R} \to \mathbb{C}$ is defined as

$$\phi(\omega) = (\mathcal{F}\psi)(\omega) = \frac{1}{\sqrt{2\pi}} \int \mathrm{d}t\, \psi(t) e^{-\mathrm{i}t\omega}, \tag{4.25}$$

and the well known *inversion* property

$$\psi(t) = \left(\mathcal{F}^{-1}\phi\right)(t) = \frac{1}{\sqrt{2\pi}} \int \mathrm{d}\omega\, \phi(\omega) e^{\mathrm{i}t\omega} \tag{4.26}$$

can be can be proven (see e.g. Folland 1992, Eq. 7.1).

Eq. (4.26) can be interpreted as a function of time expressed as a linear superposition of "pure frequencies" $e^{\mathrm{i}\omega t}$, with coefficients given by the Fourier transform $\phi(\omega)$.

In a discrete system of dimension N, a finite interval $(0, \Delta T)$ is considered, equally divided in N sub-intervals. If we set $\delta T = \frac{\Delta T}{N}$, N discrete points in time can be considered

$$t_n \in \{0, \ldots, (N-1)\delta T\}\,. \tag{4.27}$$

The corresponding frequencies are multiples of the *fundamental* frequency $\nu_1 = \frac{1}{\Delta T}$. The fundamental *angular* frequency is therefore $\omega_1 = \frac{2\pi}{\Delta T}$ and the N sample values are:

$$\omega_n \in \left\{0, \frac{2\pi}{\Delta T}, \ldots, \frac{2\pi(N-1)}{\Delta T}\right\}. \tag{4.28}$$

It is easily seen that:

$$\delta\Omega\delta T = \frac{2\pi}{N}\,; \quad \Delta\Omega\Delta T = 2\pi N\,. \tag{4.29}$$

Also:

$$\omega_n = \frac{2\pi}{N(\delta T)^2} t_n\,. \tag{4.30}$$

The discretization of (4.25) and (4.26) then reads[7]

$$\phi_n \coloneqq \phi(\omega_n) = \frac{1}{\sqrt{N}} \sum_{m=0}^{N-1} \psi_m e^{-\mathrm{i}nm2\pi/N} \tag{4.31}$$

and, respectively,

$$\psi_m \coloneqq \psi(t_m) = \frac{1}{\sqrt{N}} \sum_{n=0}^{N-1} \phi_n e^{\mathrm{i}nm2\pi/N}. \tag{4.32}$$

Eq. (4.31) is the definition of the *Discrete Fourier Transform* (DFT); Eq. (4.32) defines the *Inverse Discrete Fourier Transform* (IDFT). The factor $\frac{1}{\sqrt{N}}$ is chosen to guarantee *unitarity* of the transformation: $\sum_{n=0}^{N-1} |\psi_n|^2 = \sum_{n=0}^{N-1} |\phi_n|^2$.

From Eqs. (4.31) and (4.32) one can identify the *Discrete Fourier Matrix*, with elements F_{mn} (and its inverse, with elements $F^\dagger_{mn}$):

$$F_{mn} = \frac{1}{\sqrt{N}} e^{-\mathrm{i}nm2\pi/N} \; ; \qquad\qquad F^\dagger_{mn} = \frac{1}{\sqrt{N}} e^{\mathrm{i}nm2\pi/N}. \tag{4.33}$$

The (discrete) Fourier transform can be used to transform the time representation of a vector $|\psi\rangle_T \in \mathcal{H}_T$ into its angular frequency representation. Namely, the sequence[8] $\{\langle t_n|\psi\rangle\}_{n=0,\ldots,N-1}$ into $\{\langle \omega_m|\psi\rangle\}_{m=0,\ldots,N-1}$:

$$\langle \omega_m|\psi\rangle = \sum_n F_{mn} \langle t_n|\psi\rangle \,. \tag{4.34}$$

It is convenient to write down the "complex conjugate" of Eq. (4.34) as well:

$$\langle \psi|\omega_m\rangle = \sum_n F^\dagger_{mn} \langle \psi|t_n\rangle \tag{4.35}$$

(recalling that F is symmetric hence $F^*_{mn} = F^\dagger_{mn}$, $\forall m, n \in \{0, \ldots, N-1\}$).

As $|\psi\rangle$ (respectively: $\langle\psi|$) is a generic ket (or bra) in the Hilbert space, from

[7] See e.g. Oppenheim and Schafer 1989, 2014; Proakis and Manolakis 1996.

[8] We will omit the subscript "$_T$" from the following equations where there is no ambiguity that we are operating in the subspace $\mathcal{H}_T$ of the Page–Wootters model.

Eqs. (4.34) and (4.35) it follows:

$$\langle \omega_m| = \sum_n F_{mn} \langle t_n| \ , \tag{4.36}$$

$$|\omega_m\rangle = \sum_n F^\dagger_{mn} |t_n\rangle \ . \tag{4.37}$$

This shows that the Fourier matrix can be used, not only to transform the components of a vector from one eigenbasis to the canonically conjugate eigenbasis, but also to obtain the eigenvectors themselves (of the canonically conjugate operator).

Let us now introduce the *Fourier operator*:

$$\hat{F} \coloneqq \sum_{m,n=0}^{N-1} F_{mn} |t_m\rangle\langle t_n| \, . \tag{4.38}$$

Multiplying each element of the sum in Eq. (4.36) by $\langle t_m|t_m\rangle = 1$ we immediately get:

$$\langle \omega_m| = \langle t_m| \hat{F}. \tag{4.39}$$

Similarly, Eq. (4.37) can be expressed as

$$|\omega_m\rangle = \hat{F}^\dagger |t_m\rangle \, . \tag{4.40}$$

Finally, we use the spectral decomposition of $\hat{\Omega}$ (and $\hat{T}$), the results (4.39) and (4.40) above, and Eq. (4.30) to obtain:

$$\begin{aligned} \hat{\Omega} = \sum_m \omega_m |\omega_m\rangle\langle\omega_m| = \sum_m \omega_m \hat{F}^\dagger |t_m\rangle\langle t_m| \hat{F} \\ = \frac{2\pi}{N(\delta T)^2} \hat{F}^\dagger \left(\sum_m t_m |t_m\rangle\langle t_m| \right) \hat{F} = \frac{2\pi}{N(\delta T)^2} \hat{F}^\dagger \hat{T} \hat{F} \\ = \frac{2\pi N}{(\Delta T)^2} \hat{F}^\dagger \hat{T} \hat{F} \hat{F} = \frac{\delta\Omega}{\delta T} \hat{F}^\dagger \hat{T} \hat{F} \hat{F}. \end{aligned} \tag{4.41}$$

In conclusion:

$$\hat{\Omega} = \frac{2\pi}{N(\delta T)^2}\hat{F}^\dagger\hat{T}\hat{F} = \frac{2\pi N}{(\Delta T)^2}\hat{F}^\dagger\hat{T}\hat{F} = \hat{F}^\dagger\left(\delta\Omega\frac{\hat{T}}{\delta T}\right)\hat{F}\,; \tag{4.42}$$

$$\hat{T} = \frac{2\pi}{N(\delta\Omega)^2}\hat{F}\hat{\Omega}\hat{F}^\dagger = \frac{2\pi N}{(\Delta\Omega)^2}\hat{F}\hat{\Omega}\hat{F}^\dagger = \hat{F}\left(\delta T\frac{\hat{\Omega}}{\delta\Omega}\right)\hat{F}^\dagger\,; \tag{4.43}$$

where the operator $\frac{\hat{T}}{\delta T}$ in Eq. (4.42), in T representation, is diagonal with integer elements $\{0, \ldots, N-1\}$.

Conversely, Eq. (4.43) is obtained by taking the "conjugate" of all the computation from Eq. (4.34) to (4.41).

Note that Eqs. (4.42) and (4.43) differ from the results of Vourdas 2004. Besides the sign convention[9], this is due to the use of "natural" units therein, in the sense that both time and angular frequency have adimensional, integer eigenvalues: $t_n = \omega_n = 0, 1, \ldots, N-1$ (in fact, the paper defines "position" $\hat{X}$ and "momentum" $\hat{P}$, but in a similar fashion). In other words, in Vourdas 2004, the sampling interval and the fundamental harmonic angular frequency are set to $\delta T = \delta\Omega = 1$ (or their equivalent in terms of position and momentum).

4.3.2 Uncertainty in finite-dimensional systems

For canonical pairs of operators with a continuous, unbounded spectrum i.e. $\hat{q}$ and $\hat{p} \coloneqq -i\hbar\hat{\partial}_q$, it is in general straightforward to prove that

$$[\hat{q}, \hat{p}] = i\hbar \tag{4.44}$$

and therefore the Robertson form of the uncertainty relation

$$\Delta q \Delta p \geq \frac{1}{2}|\langle[\hat{q}, \hat{p}]\rangle| \tag{4.45}$$

[9] The paper, essentially, swaps the definition of Discrete Fourier Transform and its Inverse, while we follow e.g. Folland 1992, Sec. 7.6, which is more consistent to the definition of continuous Fourier transform found in most quantum mechanics textbooks, and used to convert position into momentum wavefunctions.

yields

$$\Delta q \Delta p \geq \frac{\hbar}{2}\,. \tag{4.46}$$

In finite d-dimensional Hilbert spaces, the commutator of canonically conjugate operators is not a constant —see Weyl 1950. Indeed, in an eigenbasis of $\hat{q}$, the latter is represented by a diagonal matrix Q, with diagonal elements $q_1, \ldots, q_d$. Let also P be the matrix representation of $\hat{p}$ in the same basis, and p_{mn} its elements, with $m, n = 1 \ldots d$. The left side of (4.44) is then represented as

$$\begin{aligned} QP - PQ &= \begin{pmatrix} q_1 & & \\ & \ddots & \\ & & q_d \end{pmatrix} \begin{pmatrix} p_{11} & \cdots & p_{1d} \\ \vdots & \ddots & \vdots \\ p_{d1} & \cdots & p_{dd} \end{pmatrix} - \begin{pmatrix} p_{11} & \cdots & p_{1d} \\ \vdots & \ddots & \vdots \\ p_{d1} & \cdots & p_{dd} \end{pmatrix} \begin{pmatrix} q_1 & & \\ & \ddots & \\ & & q_d \end{pmatrix} \\ &= \begin{pmatrix} q_1 p_{11} & \cdots & q_1 p_{1d} \\ \vdots & \ddots & \vdots \\ q_d p_{d1} & \cdots & q_d p_{dd} \end{pmatrix} - \begin{pmatrix} q_1 p_{11} & \cdots & q_d p_{1d} \\ \vdots & \ddots & \vdots \\ q_1 p_{d1} & \cdots & q_d p_{dd} \end{pmatrix} = \Big\{ (q_m - q_n) p_{mn} \Big\}_{m,n=1\,\ldots\,d} . \end{aligned} \tag{4.47}$$

All diagonal elements are thus zero, hence such matrix cannot represent a constant operator in any basis.

In other words, it is not possible to identify a pair of operators $\hat{q}$ and $\hat{p}$ satisfying Eq. (4.44) in a finite-dimensional Hilbert space. The value of $\frac{1}{2}|\langle[\hat{q},\hat{p}]\rangle| = \frac{1}{2}|\,\langle\psi|[\hat{q},\hat{p}]|\psi\rangle|$ would then depend on the particular state vector $|\psi\rangle \in \mathcal{H}_d$, and one should compute, explicitly, the value of $\min_{|\psi\rangle\in\mathcal{H}_d} \frac{1}{2}|\,\langle\psi|[\hat{q},\hat{p}]|\psi\rangle|$ to obtain a general lower bound.

Nonetheless, if the discrete system is meant as an approximation of a continuous one, it can still be of interest to compare the spread product $\Delta q \Delta p$ (of two discrete operators) with the lower limit predicted by the continuous theory.

4.4 Experimental illustration: review

The Page and Wootters model has been illustrated experimentally in recent years, with a very simple toy universe consisting of just two qubits —physically, the polarization states, vertical $|H\rangle$ or horizontal $|V\rangle$, of two photons (Moreva et al. 2014, 2015). A first qubit implements the clock, the second qubit acts as "the system" (or "the rest of the universe").

In another experiment by the same authors (Moreva et al. 2017), $\mathcal{H}_S$ is still implemented with polarization states $|H\rangle$ or $|V\rangle$ of a photon, but the clock states in $\mathcal{H}_T$ are given by the *position* of the same photon along the conventional x axis.

The latter is interesting because it implements a continuous time, which, among other things, allows identifying a canonically conjugate observable $\hat{\Omega}$. Or, conversely, a time operator $\hat{T}$, once $\hat{\Omega}$ is given (as shown in Sec. 4.3.2, it is impossible to satisfy (4.24) in a finite-dimension Hilbert space).

On the other hand, one problematic aspect of the experiment with continuous time is that it relies on *photon position* which is another still controversial topic (see, for example, Hawton and Dabierre 2015), similar, in that regards, to the quest for a quantum time operator that the experiment is trying to solve.

The first experiment, on the other hand (Moreva et al. 2014, 2015), uses (uncontroversial) two-level quantum systems for both the clock and the rest of the universe. While we cannot derive a $\hat{T}$ such that $[\hat{T}, \hat{\Omega}] = i$ because of the finite dimension of the space $\mathcal{H}_T$, both $\hat{\Omega}$ and $\hat{H}_S$ are given an explicit expression:

$$\hat{\Omega} = i\omega(|H\rangle\langle V| - |V\rangle\langle H|)_T \tag{4.48}$$

$$\hat{H}_S/\hbar = i\omega(|H\rangle\langle V| - |V\rangle\langle H|)_S\,, \tag{4.49}$$

as well as a zero-eigenstate of $\hat{\mathbb{J}}$ (as in eq. 4.2):

$$|\Psi\rangle\rangle = \frac{1}{\sqrt{2}}(|H\rangle_T\,|V\rangle_S - |V\rangle_T\,|H\rangle_S)\,. \tag{4.50}$$

It can be easily verified that the Wheeler-DeWitt condition (4.1) is satisfied.

In general, given a clock ($\hat{\Omega}$), the problem of finding a "rest of the universe" ($\hat{H}_S$) such that $\hbar\hat{\Omega}\otimes\mathbb{1}_S+\mathbb{1}_T\otimes\hat{H}_S=0$ (and vice versa) is not trivial (and particularly cumbersome in non-relativistic quantum mechanics where we cannot avail of negative energies etc.). Most literature focuses their examples on clocks only (Bryan and Medved 2017; Corbin and Cornish 2009; Prvanovic 2017), implicitly relying on the scale of a realistic universe in order to have the (4.1) satisfied (which was originally derived using General Relativity arguments).

4.5 Multi-Level Clock

4.5.1 Preliminaries

A clock that can measure only two times in one cycle of a periodic evolution is of limited interest —and limited falsifiability, as it can be easily interpolated by different models. The experiment described in Moreva et al. 2015 and related works attempts at addressing the issue:

> To obtain a more interesting clock, we perform the same conditional probability measurement introducing varying time delays to the clock photon, implemented through quartz plates of variable thickness.

However, it must be noted that such delay is in fact a classical external parameter. In what follows, instead, our approach to a more interesting clock will be based on simply increasing the number of levels of the clock, or in other words increasing the finite dimension of the Hilbert space $\mathcal{H}_T$. This is certainly feasible theoretically, possibly resorting to numerical computation.

4.5.2 Eigensystem in the product space and consistency with ordinary quantum theory

Appendix B.1 reports the details of symbolic and numeric computation for an $N=32$-level clock, "timing" a qubit subject to the same Hamiltonian of the experiment we have seen in Sec. 4.4.

In this case, for simplicity, we work in "natural units" $\hbar = \omega = 1$, where ω is the characteristic frequency in the same sense of the two-level clock experiment described in Section 4.4.

The clock is built as having a time operator which is diagonal in the chosen computational basis[10]:

$$\hat{T} \equiv \frac{2\pi}{N} \begin{pmatrix} 0 & & & \\ & 1 & & \\ & & \ddots & \\ & & & N-1 \end{pmatrix} .$$

With this choice, the clock spans the characteristic period of $\Delta T = 2\pi$.

The "spatial space" or "ordinary Hilbert space" $\mathcal{H}_S$ is still 2-dimensional, and the Hamiltonian in it is simply

$$\hat{H}_S \equiv i \begin{pmatrix} 0 & 1 \\ -1 & 0 \end{pmatrix} .$$

Frequency operator $\hat{\Omega}$ is derived, analytically, via Fourier transformation as seen in (4.42):

$$\hat{\Omega} = \frac{N}{2\pi} F_N^\dagger \hat{T} F_N \, .$$

With a large N, such derivation is extremely laborious. We do not resort to numeric FFT in this case, but we do benefit of computer-aided, yet exact symbolic computation.

Once $\hat{\Omega}$ is derived though, the eigenvalues and eigenvectors of $\hat{\mathbb{J}} = \hbar\hat{\Omega} \otimes \mathbb{1}_S + \mathbb{1}_T \otimes \hat{H}_S$ can only, realistically, be computed with numerical methods.

In order to illustrate interesting examples, not corresponding to the trivial

[10] Here there is no explicit reference to any particular physical implementation.

evolution of an eigenstate of H_S, but to some kind of Rabi oscillation or Larmor precession (Cohen-Tannoudji et al. 1977, c. IV), we pick, in *Mathematica*'s ordering, *just as an example*, an eigenvector $|\Phi_{41}\rangle\rangle$ of $\hat{\mathbb{J}}$ in $\mathcal{H}_T \otimes \mathcal{H}_T$, corresponding to eigenvalue $\epsilon_{41} = 11$.

Please note, *any* of the eigenvectors of $\hat{\mathbb{J}}$ could be chosen, even if related to a non-zero eigenvalue (with suitable phase correction term, as seen below and in Eq. (4.15), when comparing with standard quantum mechanics). However, one may consider an eigenstate of $\hat{\mathbb{J}}$ in $\mathcal{H}_T \otimes \mathcal{H}_S$, such as the above example, where ${}_T\langle t = 0|\Phi_{41}\rangle\rangle \in \mathcal{H}_S$ is *not* an eigenstate of the "ordinary" Hamiltonian $\hat{H}_S$, thus avoiding the "trivial" evolution of a Hamiltonian eigenstate, where the probabilities of the qubit being $|0\rangle_S$ or $|1\rangle_S$ would be simply constant.

Indeed, each eigenvector of $\hat{\mathbb{J}}$ encodes a whole possible discrete-time history of the qubit over a cycle.

So, for example, if components 1 and 2 of $|\Phi_{41}\rangle\rangle$ correspond to (the components of) an initial state of the qubit in $\mathcal{H}_S$ (i.e at "ordinary time" $t = 0$); components $2k+1$ and $2k+2$ correspond to $t = \frac{2\pi}{N}k := t_k$ of same, $\forall k \in \{0, \ldots, N-1\}$.

A comparison of Page–Wootters results with ordinary Schrödinger evolution is thus given by the comparisons

$$\langle\langle 2k+1|\Phi_{41}\rangle\rangle\, e^{-i\epsilon_{41}t_k} \sim \langle 0|\psi(t_k)\rangle_{\mathrm{S}} \tag{4.51}$$

$$\langle\langle 2k+2|\Phi_{41}\rangle\rangle\, e^{-i\epsilon_{41}t_k} \sim \langle 1|\psi(t_k)\rangle_{\mathrm{S}}\ , \tag{4.52}$$

where the phase $e^{-i\epsilon_{41}t_k}$ is motivated in Giovannetti et al. 2015, *"The Zero-eigenvalue"*, and inessential if one is merely interested in determining and comparing probabilities $|\langle 0, 1|\psi\rangle|^2$. Please note the double angle bracket notation for vectors and algebraic operations in the product space $\mathcal{H}_T \otimes \mathcal{H}_S$.

Figure 4.1 is the graphical representation of (the square modulus of) (4.51) and (4.52) i.e. the probability for the qubit in $\mathcal{H}_S$ to be $|0\rangle$ or $|1\rangle$.

The discrete graph, on top, plots the square modulus of components of $\hat{\mathbb{J}}$'s eigenvector $|\Psi_{41}\rangle\rangle$.

Odd-index $(2k+1)$ square-modulus components —occupying vertical *spaces*

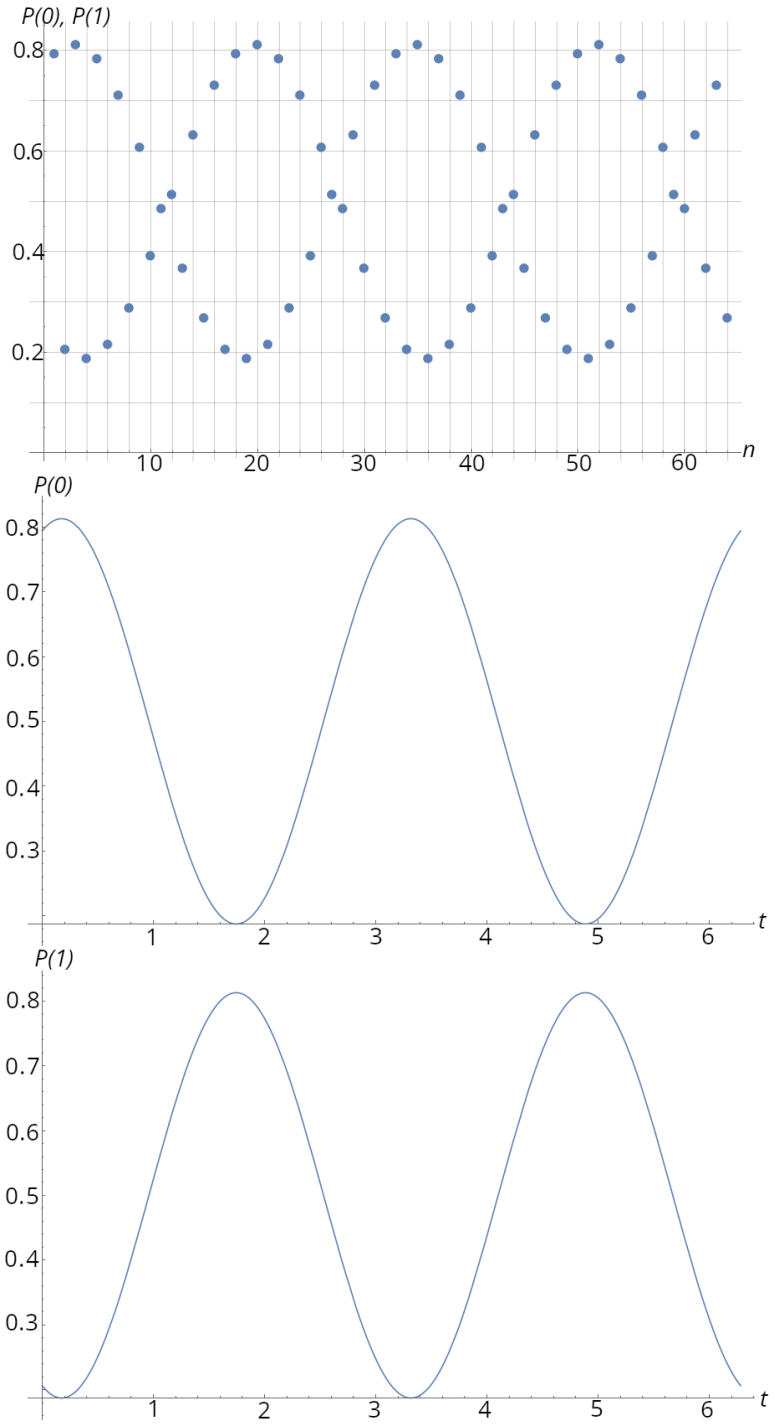

Figure 4.1: *Top*: probability of the qubit being measured $|0\rangle$ or $|1\rangle$ according to the discrete Page–Wootters model, computed as $P(0)|_{t=t_k} = |\langle\langle 2k+1|\Phi_{41}\rangle\rangle|^2$ and $P(1)|_{t=t_k} = |\langle\langle 2k+2|\Phi_{41}\rangle\rangle|^2$. *Centre, bottom*: same probabilities (in continuous time) according to ordinary quantum mechanics, $P(0)|_t = |\langle 0|\psi(t)\rangle_{\rm S}|^2$, $P(1)|_t = |\langle 1|\psi(t)\rangle_{\rm S}|^2$. See also Eqs. (4.51) and (4.52).

on the grid— are compared with the Schrödinger evolution of probability $|\langle 0|\psi\rangle|^2$ (first continuous plot, middle image).

Even-index $(2k+2)$ components —occupying vertical *lines* on the grid— are analogously compared with the Schrödinger evolution of probability $|\langle 1|\psi\rangle|^2$ (second continuous plot, bottom image).

Finally, Figure 4.2 compares the two sides of (4.51) and (4.52) in terms of *complex value* (therefore the term $e^{-i\epsilon t_k}$ is relevant, for eigenvalues $\epsilon \neq 0$ of $\hat{\mathbb{J}}$).

4.6 Page–Wootters and detector models for a two-level system

4.6.1 Detector models

As we have seen in the previous sections, proper elements of $\mathcal{H}_T \otimes \mathcal{H}_S$, localized in both space and time, can be interpreted as "events" (as opposed to full history vectors, which instead describe the unitary evolution of a quantum system *at all times*).

The arrival of a particle at a detector is a kind of event of particular interest from the perspective of time in quantum mechanics, for several reasons.

The first reason is the direct connection with experiments, "given the appalling evidence that time is also a random variable in the laboratories" (Muga et al. 2009, c. 4); and because, "[as] a matter of fact, a number of time observables are already routinely measured in laboratories, for example arrival times in time-of-flight experiments, but the theoretical foundation of these measurements is still being discussed" (Muga et al. 2007, Preface to the First Ed.).

The second reason is the existence of studies about detector models which also investigate time-of-arrival as a quantum observable, as we have seen in Section 3.4. None of those works are explicitly based on Page–Wootters relational model —of which, to our knowledge, there are no working examples of application to time-of-detection problems in the current literature. Section 4.6.2 and the remainder of

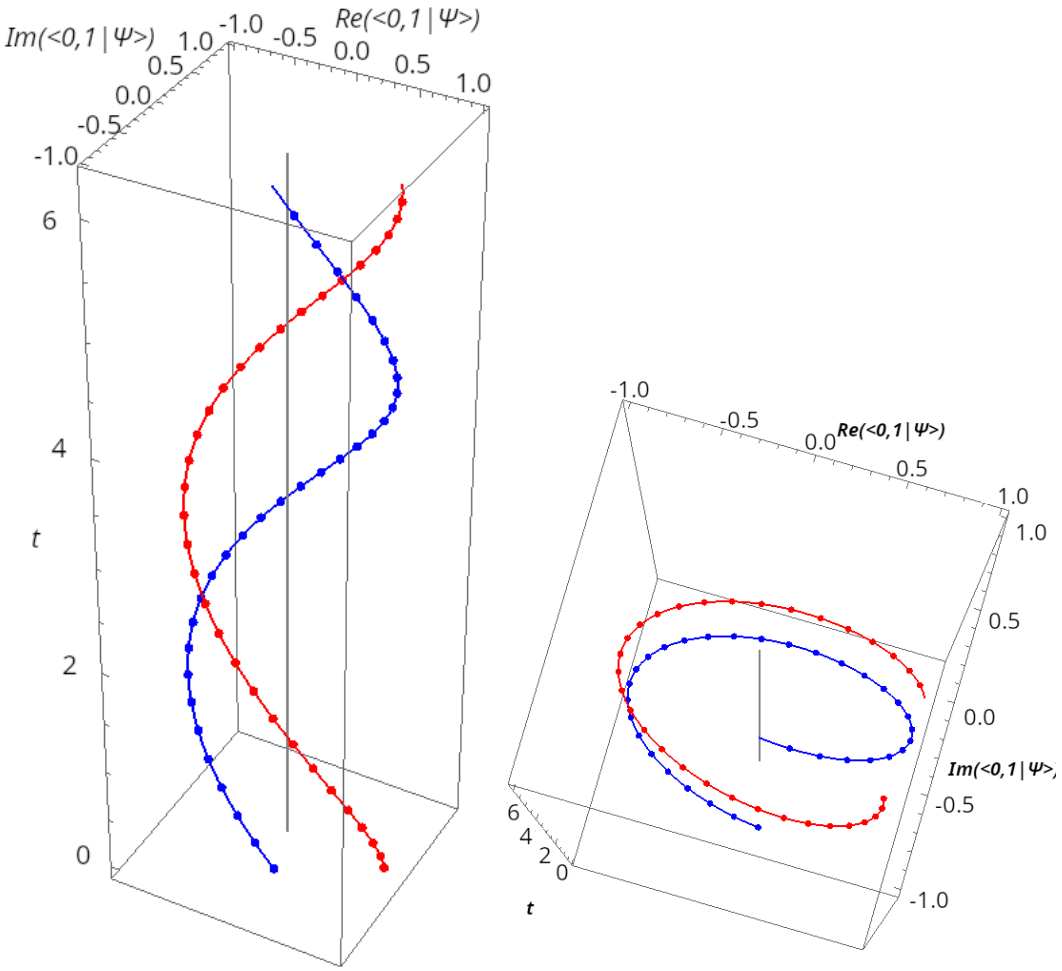

Figure 4.2: Page–Wootters discrete-time "evolution without evolution" (points) is interpolated by the (continuous lines) of standard quantum mechanics evolution. Horizontal axis are real and imaginary part of the wave function components. Vertical axis is time t. Red line plots $\langle 0|\psi(t)\rangle$. Blue line plots $\langle 1|\psi(t)\rangle$.

the chapter will be devoted to bridging such gap by implementing such application and comparing the results from the different models. Some emphasis will be given to *discrete* relational time using the techniques developed in Section 4.4.

One of the goals of this chapter is indeed combining PW and detector models.

Another route is POVM, see Chap. 2 and 3. Nonetheless, we know that a projective measurement on a bipartite system can be regarded as a POVM if we look at on one part only (e.g. Paris 2012), thus the clock space of the Page–Wootters mechanism, $\mathcal{H}_T$, can be regarded as a purification space (ibid.) for the "standard" Hilbert space where the time-of-arrival POVM is defined, and an interesting line of further research would be a more formal study of the logical connection between the two approaches, based on this principle. Both models respond to the issues raised by Pauli by giving up the pursuit of a *projective* measurement in the *standard* Hilbert space, and rather "opening" that Hilbert space in some sense.

4.6.2 Comparison with the Page and Wootters formalism

The detector absorption model in Kiukas et al. 2012 is not originally based on the notion of quantum relational time. It is "ordinary quantum mechanics" in the sense that states are in $\mathcal{H}_S$ with an external parameter time; but, contrary to quantum mechanics, the potential can be *complex*, causing the norm of the state vector to not be conserved (in fact, vanishing with time). In other terms, the evolution is not unitary, even for a pure state. Specifically, the Hamiltonian is corrected by an anti-hermitian term that models the detector.

One may wonder whether a proper, normalized Page–Wootters "position-time wavepacket" (as described in Section 4.1.2) can be used to describe *the event of being detected* (or being absorbed). It's expected to be peaked around the time when the absorption by the detector is maximum.

In the detector model of Kiukas et al. 2012, the detection by absorption corresponds to the *decrease* in norm of the wavefunction.

Therefore we expect the following relation to be true:

$$\langle\phi(t)|\phi(t)\rangle = -\frac{\mathrm{d}}{\mathrm{d}t}\|\psi_{\text{Kiukas}}(t)\|^2, \tag{4.53}$$

both sides of which indicate probability of arrival at time t. Here the function ϕ of time t has to be intended in the sense of (4.22).

Interestingly, the same paper provides a solution of (4.53). Despite not being based on the Page–Wootters model, eq. 9 in Kiukas et al. 2012 equates the squared norm of a "time representation" wavefunction to the opposite derivative of the squared norm of the "absorbed wavefunction". It reads:

> We will associate with any wave function $\psi \in \mathcal{H}$ another wave function $\hat{\psi}$, which is a function of time, so that $\left|\hat{\psi}(t)\right|^2$ is the arrival probability density. In other words, $\hat{\psi}$ is a wave function in a time representation. For each t, $\hat{\psi}(t)$ lies in the original Hilbert space H.

Therefore we "translate"

$$\hat{\psi}(t) \text{ into } |\phi(t)\rangle_S$$

and, consequently,

$$\left|\hat{\psi}(t)\right|^2 \text{ into } \langle\phi(t)|\phi(t)\rangle\,,$$

in the language of the Page–Wootters model and within the notation adopted.

Using eq. 8 in Kiukas et al. 2012 and translating into our notation we have:

$$\hat{\psi}(t) \coloneqq |\phi(t)\rangle_S = \begin{cases} \sqrt{\frac{2}{\hbar}}\hat{D}^{1/2}\,|\psi_{\text{Kiukas}}(t)\rangle_S & \text{if } t > 0 \\ 0 & \text{otherwise.} \end{cases} \tag{4.54}$$

Where at $t \leq 0$ the interaction with the detector is yet to come, but so it is, as a limit, for small values of $t > 0$, in other terms $\lim_{t\to 0^+} \left\|\hat{D}\,|\psi_{\text{Kiukas}}(t)\rangle\right\| = 0$, thus avoiding the apparent discontinuity.

The corresponding Page–Wootters (proper) vector of $\mathcal{H}_T \otimes \mathcal{H}_S$ is

$$|\Phi\rangle\rangle = \int \mathrm{d}t\,|t\rangle \otimes \hat{\psi}(t)\,, \tag{4.55}$$

to which the considerations of Section 4.2.2 and Section 4.2.2 in terms of time–frequency (or time–energy) uncertainty relation apply, with some analogy to what Kiukas et al. 2012 does within its own framework in relation to $\hat{\psi}$ and its Fourier transform.

In that regard, the (4.55) can be reformulated

$$|\Phi\rangle\rangle = \int \mathrm{d}\omega \, |\omega\rangle \otimes \mathcal{F}\hat{\psi}(\omega) \,, \tag{4.56}$$

where it is

$$\mathcal{F}\hat{\psi}(\omega) = -\frac{\sqrt[4]{2}i}{\sqrt{\pi}\left(-\omega^2 + \sqrt{2}i\omega + 1\right)} \, |1\rangle \tag{4.57}$$

—see notebook up to Eq. (A.3) for details.

(Non-unitary) evolution without evolution: plugging the complex potential in the *discrete* Page–Wootters model

Similarly to what seen in Section 4.5.2, we build the clock by defining —and representing in a convenient basis— the time operator and the corresponding frequency operator:

$$\hat{T} \equiv \frac{2\pi}{N} \begin{pmatrix} 0 & & & \\ & 1 & & \\ & & \ddots & \\ & & & N-1 \end{pmatrix} \qquad \hat{\Omega} = \frac{N}{2\pi} F_N^\dagger \hat{T} F_N \,, \tag{4.58}$$

where F is, again, the discrete Fourier operator of order N.

Next we define the Wheeler–DeWitt operator $\mathbb{J}$ as in (4.2), but $\hat{H}_S$ is replaced by the non-hermitian Hamiltonian of the detector model $K_S = \hat{H}_S - \mathrm{i}\hat{D}_S$ (Kiukas et al. 2012), where the subscript $_S$ has been added to stress that they would act

on the $\mathcal{H}_S$ part of the Page–Wootters' $\mathcal{H}_T \otimes \mathcal{H}_S$ "spacetime":

$$\mathbb{J} = \hbar\hat{\Omega} \otimes \mathbb{1}_S + \mathbb{1}_T \otimes \left(\hat{H}_S - \mathrm{i}\hat{D}_S\right). \tag{4.59}$$

$\hat{H}_S$ and $\hat{D}_S$ are the same as $\hat{H}$ and $\hat{D}$ respectively from the (3.21).

We then compute eigenvalues and eigenvectors of $\mathbb{J}$. Eigenvectors associated to the eigenvalue 0 will include the history of the qubit over a "period" (of what would have been a periodic evolution, without the absorptive detector).

Eigenvectors associated to non-zero eigenvalues will need a "phase correction", or energy shift[11] as seen, for example, in (4.51) and (4.52).

Linear combination of histories $\sum_n \alpha_n \left|n\right\rangle\rangle_{\text{hist.}}$ are also physically possible[12] and in fact we pick one that ensure that the initial state ${}_T\langle 0|\Psi\rangle\rangle$ is equal to $\left|0\right\rangle_S$ so to allow a comparison with the example in Kiukas et al. 2012. Such linear combination is not unique. For reasons of numerical stability, a linear combination with coefficients in the order of 1 would be ideal if it exists. In this particular problem, it does. We simply scan, as a first attempt, all possible values ${}_T\langle 0|n\rangle\rangle + {}_T\langle 0|m\rangle\rangle$ to find a combination that is equal to $\left|0\right\rangle_S$ – or maximizes the fidelity with that respect.[13]

All the above numerical computation is implemented with *NumPy* (T. E. Oliphant 2015), particularly in appendix A.1.1. The results are visualized in Fig. 4.3, and are *compatible* with the non-Page–Wootters solution previously shown in Fig. 3.1.

Detection probability amplitude, time of arrival distribution

In Kiukas et al. 2012 the probability of detection in time is given by how fast the norm decreases i.e. $-\frac{\mathrm{d}\|\psi\|^2}{\mathrm{d}t}$. A "wavefunction in time", whose squared modulus

[11] Again, see also ref. Giovannetti et al. 2015, *"The Zero-eigenvalue"*.

[12] As opposed to (linear combinations of) mere, uncorrected eigenstates of $\mathbb{J}$. Indeed, one may observe, at least in the case where $\mathbb{J}$ was hermitian, that $\{\left|n\right\rangle\rangle\}$ is a basis of $\mathcal{H}_T \otimes \mathcal{H}_S$ therefore $\sum_n \alpha_n \left|n\right\rangle\rangle$ would span *all elements* of $\mathcal{H}_T \otimes \mathcal{H}_S$ and the theory would not predict anything i.e. it would not discriminate unphysical histories.

[13] See the definition, and invocation, of the function `find_best()` in Appendix A.1.1.

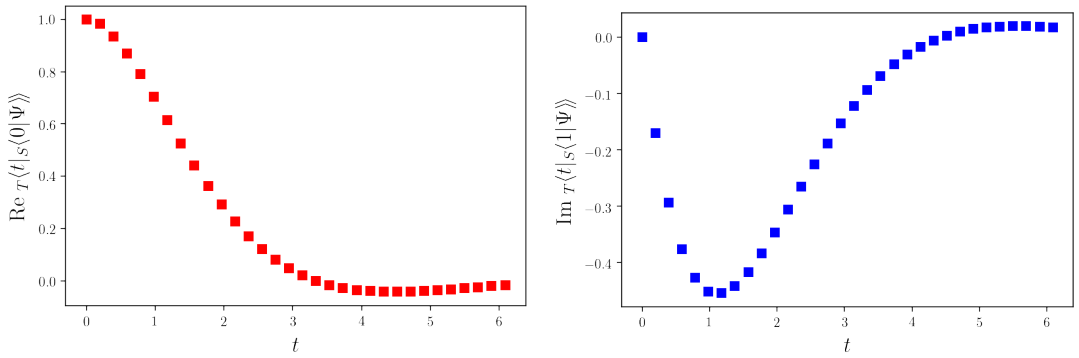

(a) (b)

Figure 4.3: Non-unitary "evolution without evolution" using the discrete Page–Wootters model, plugging in the complex potential of Kiukas et al. 2012. The result is compatible with the continuous "Schrödinger evolution" shown in Fig. 3.1. Note the different notation e.g. Re $_T\langle t|_S\langle 0|\Psi\rangle\rangle$ to fit within the framework of the P–W space-time $\mathcal{H}_T \otimes \mathcal{H}_S$.

equates the detection probability, is introduced in eq. (8) therein:[14]

$$\hat{\psi} = \theta(t)\sqrt{2/\hbar}\,\hat{D}^{1/2}\,\psi \tag{4.60}$$

In Page–Wootters terms, this translates into applying $\theta(\hat{T}) \otimes \sqrt{2/\hbar}\,\hat{D}_S^{1/2}$ to the each history vector $|n\rangle\rangle_{\text{hist.}}$ (and their linear combinations). The result is a detection-event *proper* element of $\mathcal{H}_T \otimes \mathcal{H}_S$ (that would be normalizable in a continuous, infinite-time model too):

$$|\Phi_n\rangle\rangle = \theta(\hat{T}) \otimes \sqrt{2/\hbar}\,\hat{D}_S^{1/2}\,|n\rangle\rangle_{\text{hist.}} = \theta(\hat{T})e^{-i\epsilon_n\hat{T}} \otimes \sqrt{2\hat{D}}\,|n\rangle\rangle\ . \tag{4.61}$$

Given we are considering, in our discrete model, only an interval of time within 0 and 2π, i.e. all non-negative times (or, more physically, only times when the detector is active), the Heaviside function θ (of operator) can be omitted, and simply replaced by the identity in time $\mathbb{1}_T$.

[14] Please note we are importing some notation from Kiukas et al. 2012 as per the symbol $\hat{\psi}$, at variance to what generally adhered to in this work, where the "hat" ($\hat{}$) denotes quantum observables and their corresponding operators.

Of course, for our problem, we take a linear combination

$$|\Phi\rangle\rangle = \sum_n \alpha_n \, |\Phi_n\rangle\rangle \tag{4.62}$$

where the coefficients α_n are the same that verified (not necessarily uniquely) the initial condition of the problem $|0\rangle_S = {}_T\langle 0|\Psi\rangle\rangle = \sum_n \alpha_n \, {}_T\langle 0|n\rangle\rangle_{\text{hist.}} = \sum_n \alpha_n \, {}_T\langle 0|n\rangle\rangle$.

The vector $|\Phi\rangle\rangle$, proper element of $\mathcal{H}_T \otimes \mathcal{H}_S$, is the Page–Wootters counterpart of the function "in time representation" $\hat{\psi}$, as described in Kiukas et al. 2012. In formulas:

$$\langle t|\Phi\rangle\rangle = \hat{\psi}(t)\,. \tag{4.63}$$

The "detection wavefunction" $|\Phi\rangle\rangle$ will always lie, *spatially*, in the space generated by $|1\rangle_S$, or in other terms:

$${}_T\langle t|\,{}_S\langle 0|\Phi\rangle\rangle = 0, \quad \forall t\,. \tag{4.64}$$

The linear space of $|1\rangle_S$ is the "detectable area" of the qubit in this problem, and $|\Phi\rangle\rangle$ is essentially the result of the action of the operator $\hat{D}$, that filters non-detectable components out from any vector of $\mathcal{H}_S$.

We derive the components of $|\Phi\rangle\rangle$ numerically in Section A.1.2, where they are encoded in the array `prob_detect_v`. We observe therein that the (4.64) is confirmed, and that ${}_T\langle t|_S\langle 1|\Phi\rangle\rangle$ is proportional to the $|1\rangle$-component of the evolution of the qubit (history $|\Psi\rangle\rangle$) at any time t (which is not surprising, being $\sqrt{2/\hbar}\hat{D}^{1/2}$ of the form $\begin{bmatrix} 0 & 0 \\ 0 & \kappa \end{bmatrix}$). In more formal terms:

$$\exists \kappa : \; {}_T\langle t|_S\langle 1|\Phi\rangle\rangle = \kappa \cdot {}_T\langle t|_S\langle 1|\Psi\rangle\rangle \;\; \forall t, \tag{4.65}$$

which, algebraically, is almost obvious, given the considerations above. However, it is worth noting that the expression on the right side (up to a factor κ) is, at each t, an ordinary quantum mechanical probability amplitude (probability amplitude of being $|1\rangle$ rather than $|0\rangle$); while the expression on the left side, as a function of

t, is a probability amplitude *in time*. Even when normalized (in the probabilistic sense), the two expressions are proportional but not equal (hence the factor κ). This is because the expression on the right must be normalized so that, at each t, $|{}_T\langle t|{}_S\langle 0|\Psi\rangle\rangle|^2 + |{}_T\langle t|{}_S\langle 1|\Psi\rangle\rangle|^2 = 1$ (or, actually, equal to $\langle\psi(t)|\psi(t)\rangle \leq 1$, the "lossy norm" due to absorption). Whereas the expression on the left must be normalized so that $\sum_t \|{}_T\langle t|\Phi\rangle\rangle\|_S^2 = P$, where P is the total probability that the detection/absorption happens at any time, and it's equal to 1 for an ideal detection.

The probability of detection in time is shown in Fig. 4.4a and is *consistent* with the result of the continuous and not explicitly Page–Wootters model of Kiukas et al. 2012 (see Fig. 3.2a).

Switching to the frequency (and, therefore, *energy*) domain, the discrete Fourier transform yields another proper vector $\left|\tilde{\Phi}\right\rangle\!\!\right\rangle$ of $\mathcal{H}_T \otimes \mathcal{H}_S$:

$$\left|\tilde{\Phi}\right\rangle\!\!\right\rangle = F \otimes \mathbb{1}_s \, |\Phi\rangle\!\rangle \ . \tag{4.66}$$

This vector numerical values, taken pairwise (or by groups of 3 for a qutrit etc.) are the components in the computational basis of the kets $\left|\tilde{\phi}(\omega)\right\rangle \in \mathcal{H}_S$ such that

$$|\Phi\rangle\!\rangle = \sum_n |t\rangle \, \langle t|\Phi\rangle\!\rangle = \sum_\omega |\omega\rangle \, \langle\omega|\Phi\rangle\!\rangle = \sum_\omega |\omega\rangle_T \otimes \left|\tilde{\phi}(\omega)\right\rangle_S \ . \tag{4.67}$$

As a numerical array, $\left|\tilde{\Phi}\right\rangle\!\!\right\rangle$ is the representation of $|\Phi\rangle\!\rangle$ under the basis $|\omega\rangle \otimes |0,1\rangle$ instead of $|t\rangle \otimes |0,1\rangle$, where the $|\omega\rangle$ constitute an eigenbasis of angular frequency $\hat{\Omega}$.

The squared norms $\left\langle\tilde{\phi}(\omega)\middle|\tilde{\phi}(\omega)\right\rangle_S = \|\langle\omega|\Phi\rangle\!\rangle\|_S^2$ give the probability of detection in the frequency domain, which is plotted in Fig. 4.4b and, again, consistent with Fig. 3.2b i.e. the result from the model of Kiukas et al. 2012.

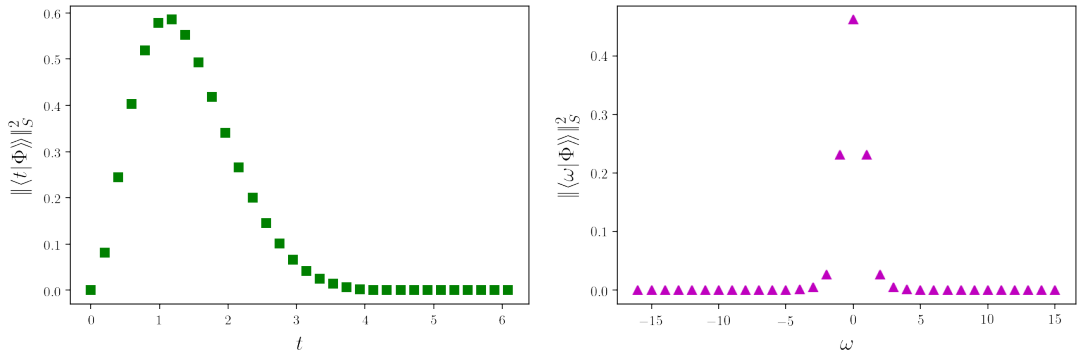

(a) (b)

Figure 4.4: Arrival at the detector, probability distribution: (a) in the time domain and (b) in the frequency domain.

Time–energy uncertainty relation

We compute numerically

$$\sigma_T \sigma_\Omega \approx 0.716\,, \tag{4.68}$$

while Kiukas et al. 2012 finds

$$\sigma_T \sigma_\Omega \approx 0.707\,. \tag{4.69}$$

The two models yield different predictions. A brief discussion follows.

Preliminarily, we should observe that the example in the paper sets the optimal parameters to minimize the time–energy uncertainty *within the given constraints* of the particular physical system, they do not necessarily achieve the theoretical Heisenberg minimum of $\frac{\hbar}{2}$ (or 0.5 in our numerical problem where $\hbar$ has been adimensionalized). More notably, parameters therein have been chosen so to minimize an alternative definition of time–energy uncertainty, $\langle T\rangle\, \sigma_E$, deemed more meaningful within the physics of the particular system.

Nonetheless, with minimal or not minimal uncertainty states (or "histories"), a comparison of such uncertainties between the discrete Page–Wootters model, implemented here, and the model in Kiukas et al. 2012, can be performed: the difference between the results in (4.68) and (4.69) may be large enough to be

not simply due to numerical approximation. A further line of investigation will involve increasing the resolution (number of levels) of the quantum clock. If the discrepancy persists, an experimental verification —as the one proposed in the paper itself— will then be of particular interest. The issue of discriminating different model of arrival time has been tackled recently by other authors as well (Roncallo et al. 2023).

4.7 Page–Wootters and detector models for a three-level system

A two-level system is the simplest non-trivial quantum system and, as seen in Sec. 4.6.2, it is sufficient to illustrate models of quantum time of arrival, such as those based on complex potentials, as well as relational models. Therein, numerical examples have been shown, where the two approaches —discrete Page–Wootters and the "non Hermitian" detector models— lead to compatible predictions.

A three-level atom (or a three-level quantum system in general) appears naturally as the next computational step; but far from being merely another exercise —just at a slightly higher level of complexity but otherwise showing, essentially, the same physics— it is in fact the *minimal* system *required* to realize a broad phenomenology that includes the *Stimulated Raman adiabatic passage* —STIRAP (Chen et al. 2010; Petiziol et al. 2020; Ruschhaupt et al. 2006; Torosov et al. 2014) and the *Electromagnetically induced transparency* —EIT (Fleischhauer et al. 2005).

As usual, we are going to set $\hbar = 1$ in the following numerical computation, based, once again, on the *NumPy* framework (T. E. Oliphant 2015), within a *Jupyter notebook* (Kluyver et al. 2016). Details can be consulted in the Appendix A.1.3. Full source code is available from the repository at ref. De Rosa 2022.

4.7.1 Hermitian evolution

In our numerical example, the following Hamiltonian is considered:

$$H \equiv \frac{1}{96}\begin{pmatrix} -2 & 0 & 32 \\ 0 & 2 & 8 \\ 32 & 8 & 3 \end{pmatrix}, \tag{4.70}$$

with respect to the basis $\{|0\rangle, |1\rangle, |2\rangle\}$. Let also the initial state be $|\psi(0)\rangle = |0\rangle \equiv \begin{pmatrix} 1 \\ 0 \\ 0 \end{pmatrix}$.

The system will evolve *unitarily*, according to $|\psi(t)\rangle = e^{-\mathrm{i}Ht}|\psi(0)\rangle$, which is computed numerically:

```
import numpy as np
from scipy.linalg import expm, norm

H = np.array([
  [-2,     0,      32],
  [0,      2,       8],
  [32,     8,       3]
], np.complex_) / 96

psi_0 = np.array([1, 0, 0], np.complex_)

def U(t):
    return expm(-1j*H*t)

def unitary_psi(t):
    return U(t) @ psi_0
```

We are interested in the probability of the system to be in $|0\rangle$, $|1\rangle$, or $|2\rangle$, which is given by $|\langle 0,1,2|\psi(t)\rangle|^2$:

```
def prob(t):
  probabilities = [0, 0, 0]
  for i in 0, 1, 2:
```

```
    probabilities[i] = norm(unitary_psi(t)[i])**2
    return probabilities
```

Such probabilities over time are shown in Figure 4.5.

We are also interested in probability *amplitudes*: complex values of $\langle 0|\psi(t)\rangle$, $\langle 1|\psi(t)\rangle$, and $\langle 2|\psi(t)\rangle$ are represented in the three-dimensional plot in Fig. 4.6. Once again, the two horizontal axes are used for the real and imaginary part of $\langle 0,1,2|\psi(t)\rangle$, while the independent variable t (time) is represented on the vertical axis.

A note on graphical representation

Other than visualizing complex-valued functions with three-dimensional plots, another visualization technique, utilized in various plots in this Section, consists of leveraging the fact that the system has exactly 3 levels, thus allowing three primary colors, red, green and blue, to be combined in proportion to the probabilities $|\langle i|\psi(t)\rangle|$ respectively for $i = 0, 1, 2$. This allows an immediate visualization of which level, $|0\rangle$, $|2\rangle$ or $|2\rangle$, predominates statistically, if any. To better clarify this with an example, a snippet of the implementation of Fig. 4.5 follows.

```
# [...]
import matplotlib
import matplotlib.pyplot as plt

# [...]
for i in 0, 1, 2:
  probs[i] = np.fromiter((prob(t)[i] for t in times), np.float)

# [...]
rgbs = []
for i in range(NPLOTPOINTS):
    rgbs.append(
        (
            probs[0][i],
            probs[1][i],
            probs[2][i]
        )
    )

# [...]
fig, ax = plt.subplots(figsize=(12,6))
```

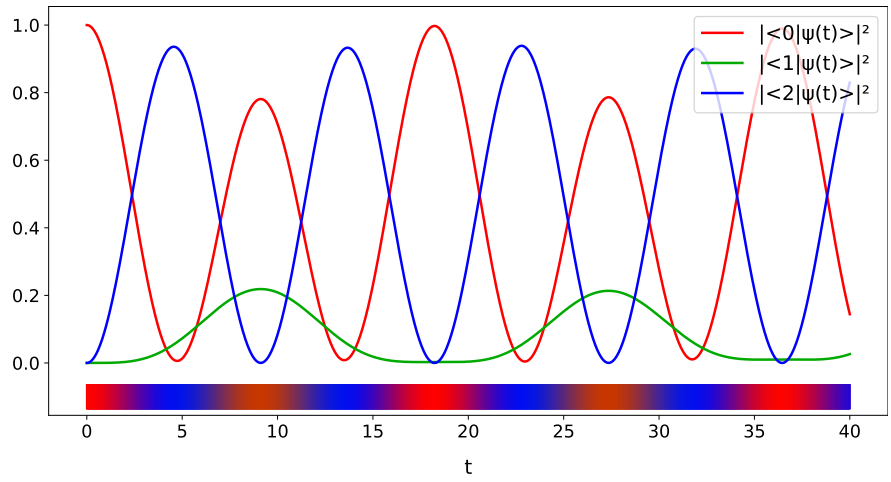

(a) Probabilities for the three-level system (see legend on top-right). *Note*: a three-level system allows a graphical representation where primary colors can be combined (see the bar at the bottom) to immediately visualize which probability dominates.

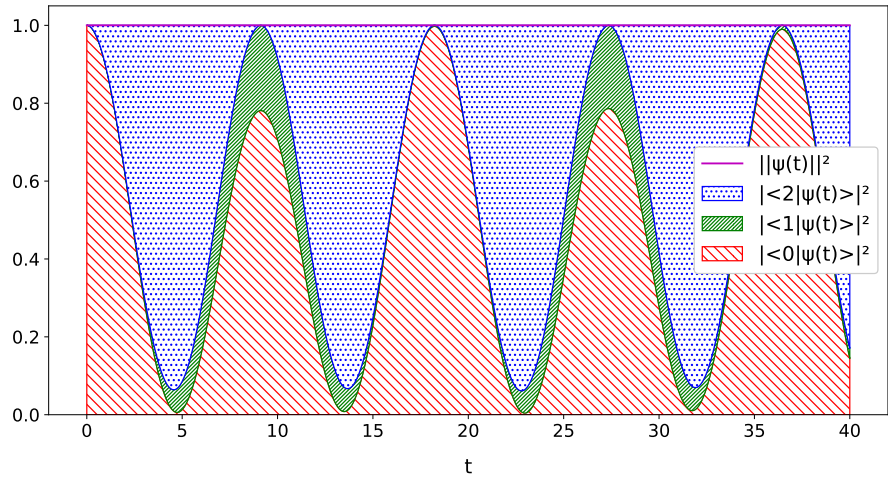

(b) *Stacked* probability chart shows that the sum $\sum_{i=0}^{2} |\langle i|\psi(t)\rangle|^2$ is equal to 1 at any time t. That is equal to the norm $\|\psi(t)\|^2$, which is indeed conserved as the system evolves *unitarily*. It can be compared with Fig. 4.7a where the norm is not conserved and the evolution is non-unitary.

Figure 4.5: *Unitary* time evolution of a three-level system, showing the probabilities $|\langle i|\psi(t)\rangle|^2$ for the system to be in state $|i\rangle$, $\forall\, i \in \{0, 1, 2\}$.

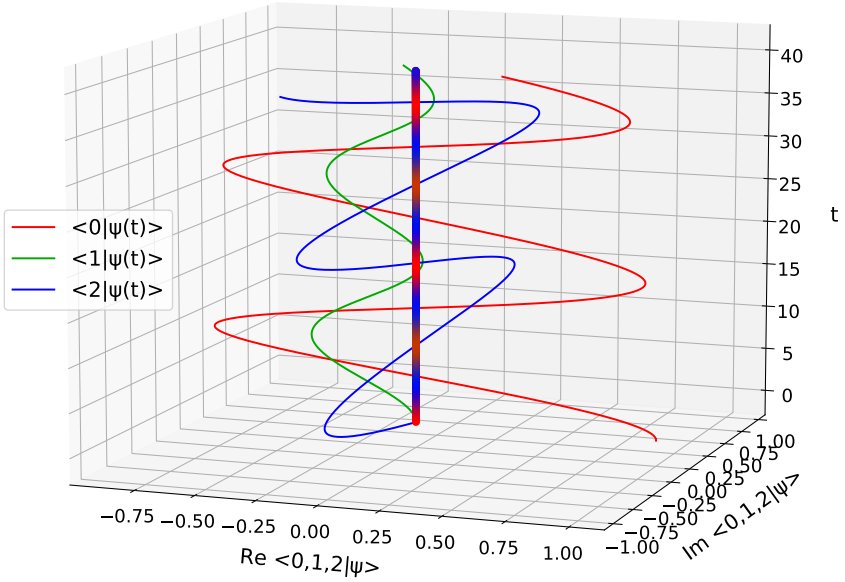

(a) "Side" view.

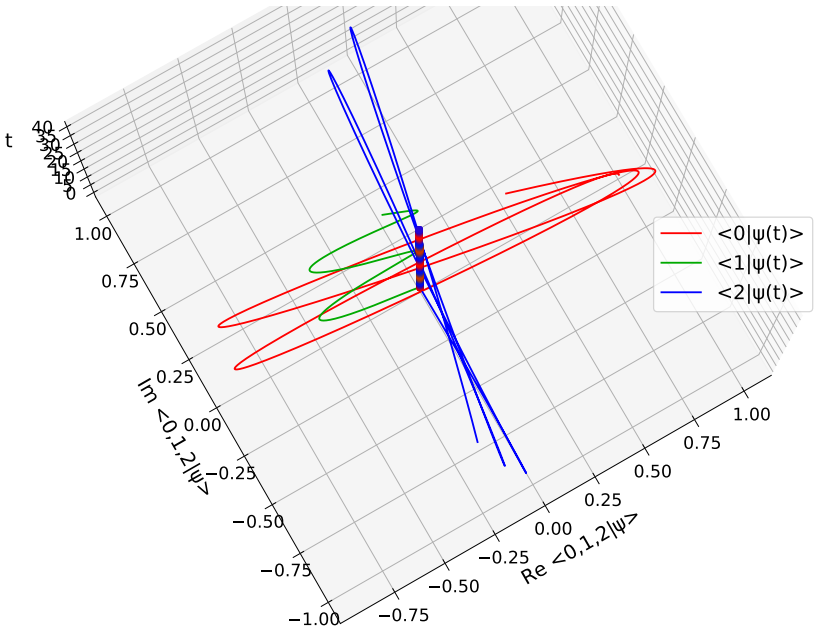

(b) "Top" view.

Figure 4.6: *3-D plot* showing the complex values of the probability *amplitudes* $\langle 0,1,2|\psi(t)\rangle$. Real and imaginary parts of those values are represented on the first two axes, while the independent variable (time, t) is represented on the third axis. – Additionally, the vertical axis is colored to encode *probabilities* (absolute values) in a similar fashion to Fig. 4.5a.

```
ax.set_xlabel('t')
ax.scatter(times, np.zeros(NPLOTPOINTS)-0.1, c=rgbs, marker='|', s=400)
```

4.7.2 Complex potential – non-Hermitian evolution

In a similar fashion to what seen in Section 3.4, the Hermitian Hamiltonian $\hat{H}$, from Eq. (4.70), is replaced by

$$K \coloneqq \hat{H} - \mathrm{i}\hat{D}, \tag{4.71}$$

where

$$\hat{D} \equiv \begin{pmatrix} 0 & 0 & 0 \\ 0 & 0 & 0 \\ 0 & 0 & \gamma \end{pmatrix}. \tag{4.72}$$

This models the absorptive detection of the "arrival" of the system at state $|2\rangle$. A numeric value of $\gamma = 0.1$ is chosen for the current simulation. Repeating the calculation for the time-evolution brings to probabilities, and probability amplitudes, that are graphically visualized in Fig. 4.7a, and 4.8, and can be compared with the Hermitian (i.e. unitary) case, Figs. 4.5b and 4.6 respectively. It appears clearly, in Fig. 4.7a, that the norm of the state vector is not conserved, but decreases monotonically.

According to the absorptive detector model, the loss of normalization $-\frac{\mathrm{d}\|\psi\|^2}{\mathrm{d}t}$ indicates the probability of detection with respect to time, in other words: the time-of-arrival probability distribution. It is plotted in Fig. 4.7b.

The same results about probabilities and normalization loss are plotted over a longer time interval in Fig. 4.9. By comparing the latter, back with Fig. 4.5b, it is apparent that in the unitary case the system periodically oscillates between $|0\rangle$ and $|2\rangle$ —transitioning through the intermediate level $|1\rangle$, but with a small value of $|\langle 1|\psi(t)\rangle|^2$. Instead, within the non-unitary evolution, and with the chosen parameters, the system is "driven" from $|0\rangle$ to $|1\rangle$ and, after a transient

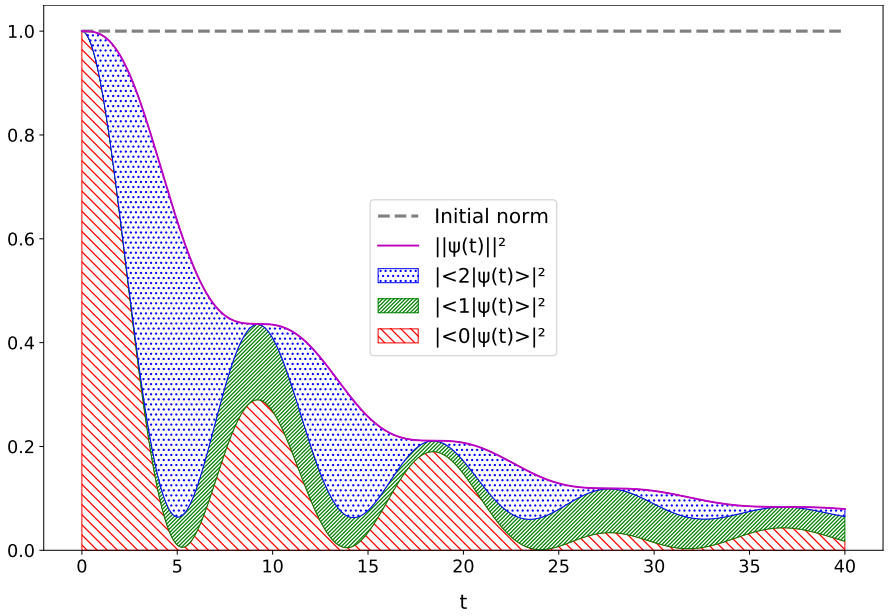

(a) *Stacked* probability chart for the non-Hermitian case (absorption model), showing that the norm $\|\psi(t)\|^2 = \sum_{i=0}^{2} |\langle i|\psi(t)\rangle|^2$ is not constant and is, in fact, monotonically decreasing. The actual probability of the system to be in state $|0\rangle$, $|1\rangle$ or $|2\rangle$ will need to be renormalized due to the loss of normalization. Namely, $P_i = |\langle i|\psi(t)\rangle|^2 / \|\psi(t)\|^2$, $\forall\, i \in \{0, 1, 2\}$.

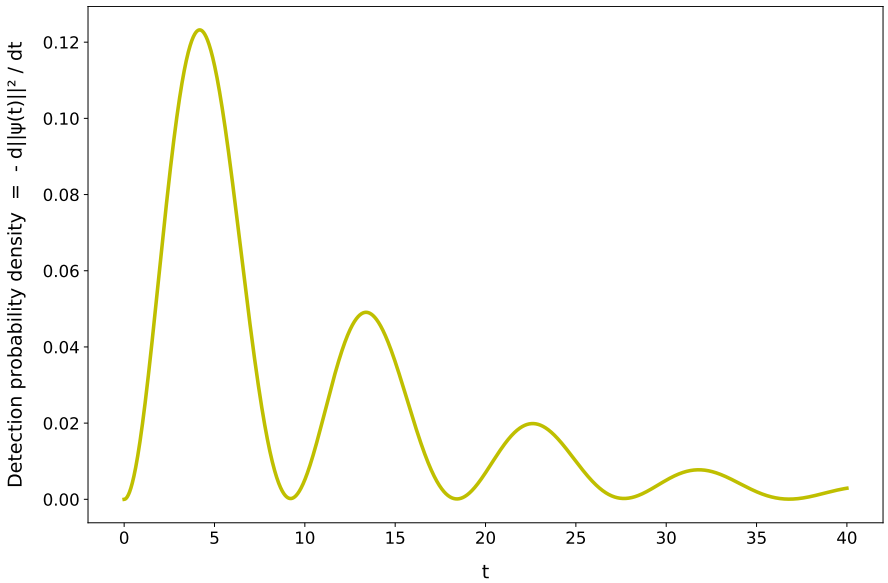

(b) According to the absorptive detection model, the probability distribution of the time-of-arrival (at the "absorbing" state $|2\rangle$) is given by the normalization loss rate $-\frac{\mathrm{d}\|\psi\|^2}{\mathrm{d}t}$, shown in the plot.

Figure 4.7: Absorptive detector model: norm loss and state probabilities.

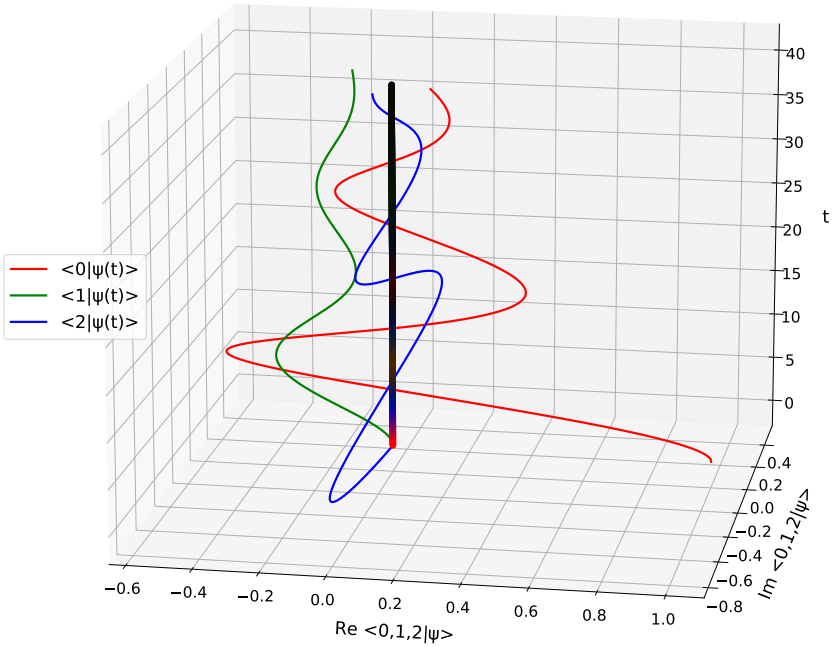

(a) "Side" view.

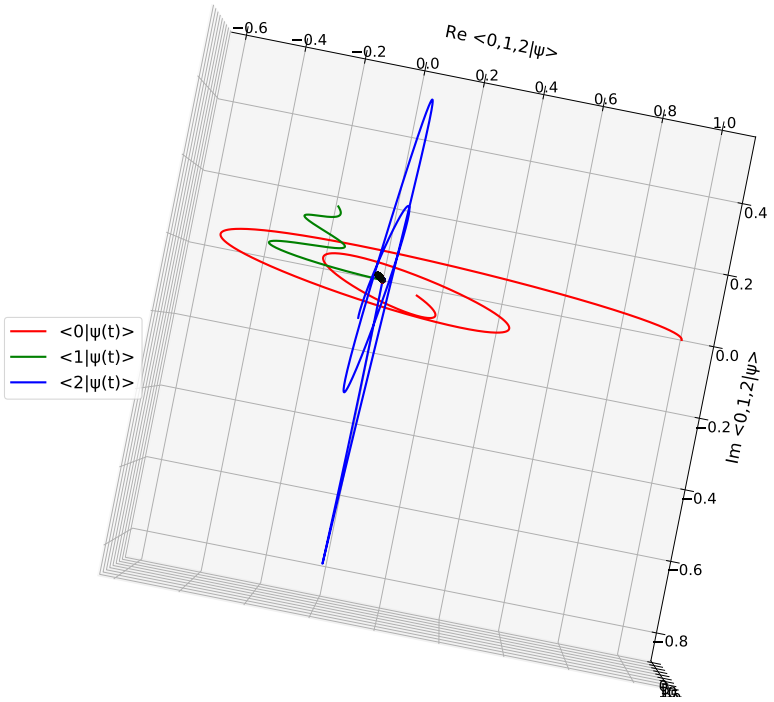

(b) "Top" view.

Figure 4.8: Non-Hermitian evolution: 3-D complex plot: probability amplitudes, with "lossy" norm (visually, lines get closer to the time axis as t increases).

oscillation between the three levels, shows an asymptotic behavior. The fidelity with respect to $|1\rangle$, $\frac{|\langle 1|\psi(t)\rangle|^2}{\|\psi(t)\|^2}$, evaluated numerically at $t = 150$ is given by

```
# Pick the last value of time
times_extended[-1]
```

```
150.0
```

```
# Fidelity
(np.abs(evolution_extended[1])**2)[-1] / norms_extended[-1]**2
```

The result is about 94%.

```
0.9414855990054901
```

It is also worth noting that the norm does not fully vanish with $t \to +\infty$, meaning there is a finite probability that detection (or "absorption", or spontaneous decay) never happens:

$$P_{\text{nd}} = \lim_{t \to +\infty} 1 - \|\psi(t)\|^2.$$

At the "large" value of $t = 150$ of our numerical computation, this yields

```
norms_extended[-1]**2
```

```
0.05684539507975811
```

i.e. roughly 6% of non-absorption probability.

4.7.3 Discrete Page–Wootters

Let us consider a Page–Wootters *discrete* clock, with N_T levels, i.e. the clock Hilbert space has finite dimension N_T, where we choose $N_T = 60$ (somehow resembling the 60 ticks indicating minutes or seconds in a conventional clock[15]).

Let also N_S indicate the Hilbert space dimension of the of "the rest of the

[15]For an intuitive, and suggestive, depiction, the reader may want to look at Smith and Ahmadi 2019, Fig. 1, where the quantum levels of the clock are $N_T = 12$ —please note, however, that the paper allows for the clock and the remaining system to *interact*, whereas, in the original formulation of the Page–Wootters mechanism, they are only *entangled*.

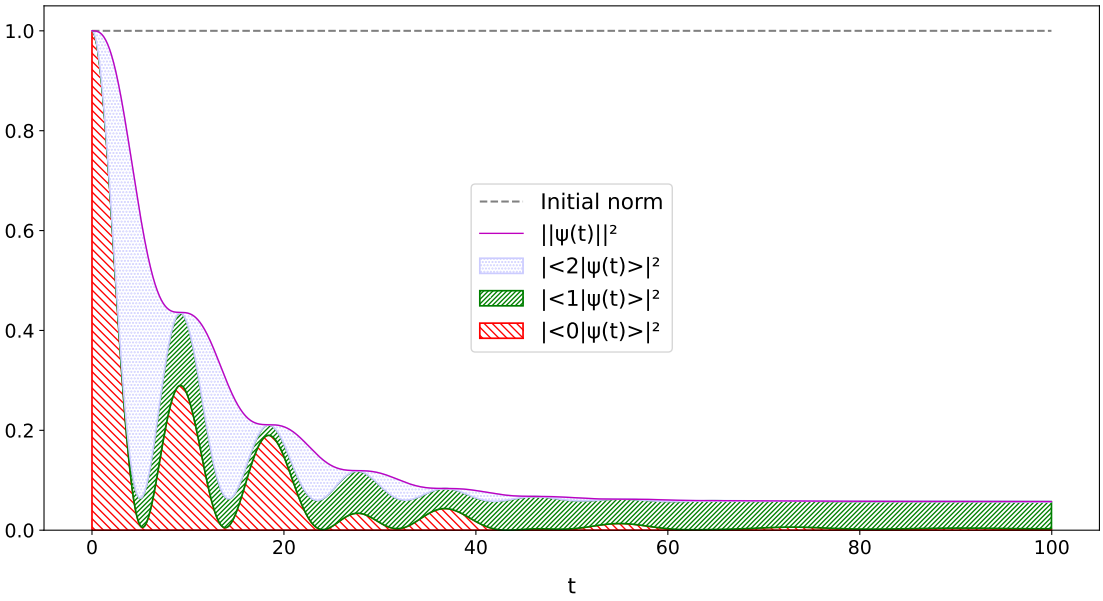

(a) Probabilities and normalization loss.

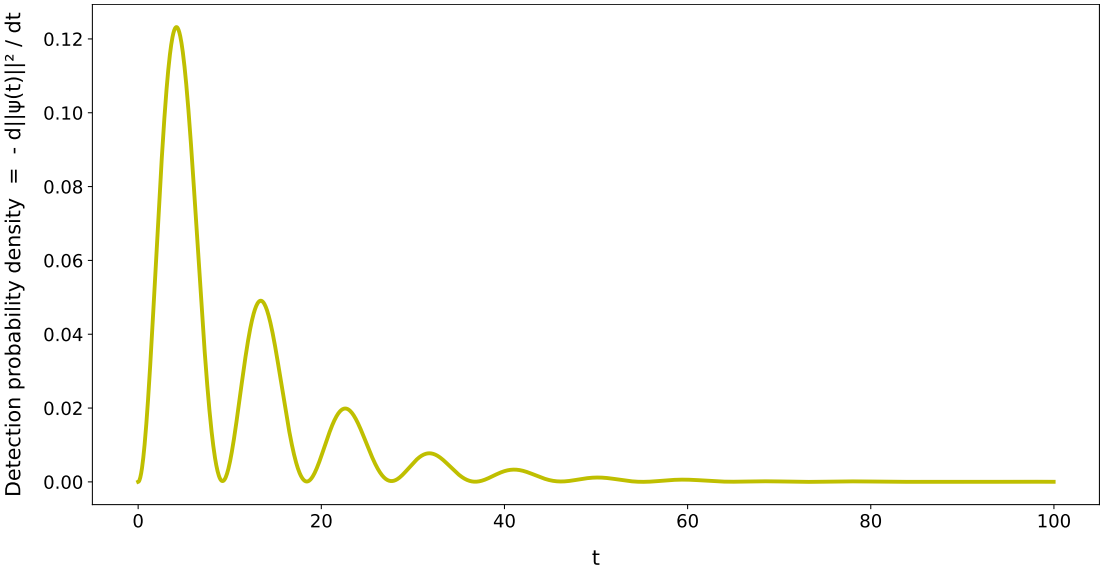

(b) Normalization loss rate, or time-of-arrival probability distribution.

Figure 4.9: Absorptive detector model: same results as in Fig. 4.7, over a longer time interval.

universe" $\mathcal{H}_S$ (in the sense of Marletto and Vedral 2017, among others). In the current example it is $N_S = 3$.

A basis of $\mathcal{H}_T$ is chosen where the time operator $\hat{T}$ is diagonal:

$$\hat{T} \equiv \frac{\Delta T}{N_T} \begin{pmatrix} 0 & 0 & \dots & 0 \\ 0 & 1 & \dots & 0 \\ \vdots & \vdots & \ddots & \vdots \\ 0 & 0 & \dots & N_T - 1 \end{pmatrix}, \tag{4.73}$$

where ΔT if the time interval under study. And the frequency operator $\hat{\Omega}$ is computed via *Discrete Fourier Transform (DFT)*:

$$\hat{\Omega} = \frac{2\pi N_T}{\Delta T^2} F^\dagger \hat{T} F. \tag{4.74}$$

It is worth noting that, from a numerical computation perspective, different library implementations use different conventions and definitions for the discrete Fourier matrix. Therefore, appropriate factors in the relation between $\hat{T}$ and $\hat{\Omega}$ may be required. In our code:

```
# [...]
TMIN, TMAX = 0, 40
TMIN_N, TMAX_N = float(TMIN), float(TMAX)

# [...]
from scipy.linalg import dft, norm, expm, det, inv

# [...]
# Number of levels of the clock aka dimension of Time Hilbert space
NT = 60

# Time interval under study
DT = TMAX_N  # assume we start with time 0

# Time operator
T = DT * np.diag(np.arange(NT)) / NT

# Discrete Fourier
F = dft(NT, scale='sqrtn')
```

```
F_dagger = F.conj().T

# Frequency operator
Omega = F_dagger @ T @ F * 2*np.pi * NT / DT**2
```

Then the "Hamiltonian" $\mathbb{J}$, acting on $\mathcal{H}_T \otimes \mathcal{H}_S$, and defined in Eq. (4.59) is derived, with eigenvalues and eigenvectors::

```
J = np.kron(Omega, np.eye(3)) + np.kron(np.eye(NT), K())

eigenvalues, eigenvectors = np.linalg.eig(J)
eigenvectors = eigenvectors.T
```

where the Python function `K()` is the non-Hermitian operator K of Eq. (4.71).

Eigenvectors need to be "initially normalized in $\mathcal{H}_S$" in the sense of a state vector $|\psi(t)\rangle$ satisfying $\||\psi(0)\|^2 = 1$ or, in Page–Wootters terms, a vector $|\Psi\rangle\rangle$, in $\mathcal{H}_T \otimes \mathcal{H}_S$, satisfying $\langle\langle\Psi|0\rangle_T\langle 0|\Psi\rangle\rangle = 1$.

```
eigenvectors_normalized_in_S = np.empty((NT*NS, NT*NS), dtype=complex)
for i in range(NT*NS):
    eigenvectors_normalized_in_S[i] = eigenvectors[i] / norm(eigenvectors[i
        ][:3])
```

A "phase correction" may be needed in order to allow a comparison with the time evolution predicted with "standard" quantum mechanics (although, still, with a non-Hermitian Hamiltonian, or *complex potential*). Namely, corrections related to non-zero eigenvalues are required —see Eq. (4.13). It is worth recalling that, as the Wheeler-DeWitt equation reads $\mathbb{J}\,|\Psi\rangle\rangle = 0$, eigenvectors of $\mathbb{J}$ related to eigenvalues —say, ϵ_i— which are not zero, need to be corrected by "rigidly shifting the spectrum of H_S by $[\epsilon_i]$" (once again, Giovannetti et al. 2015, "*The Zero-eigenvalue*"):

$$|\epsilon_i\rangle\rangle \;\longrightarrow\; |\Phi_i\rangle\rangle := e^{-\mathrm{i}\hat{T}\epsilon_i \otimes \mathbb{1}_S}\,|\epsilon_i\rangle\rangle\,, \tag{4.75}$$

where it has been set $\hbar = 1$. This translates in code as follows:[16]

```
histories = np.empty((NT*NS, NT*NS), dtype=complex)
```

[16] In the Python code, `i` is an iteration index and `1j` is the imaginary unit (the latter is a convention of the language). In eq.(4.75), i is a summation index and i (upright typeface) is the imaginary unit. The context may also help in interpreting the notation correctly.

```
for i in range(NT*NS):
    histories[i] = \
        expm(np.kron( -1j*T*eigenvalues[i], np.eye(NS) )) @ \
        eigenvectors_normalized_in_S[i]
```

With a slightly different notation, the `histories[i]` correspond to the $|\Phi_i\rangle\rangle$ in Eq. (4.75). They are named `histories` because each of them (and any linear combination, per quantum superposition principle) encodes a possible evolution (although with discrete time resolution) of the system along the whole time interval $[0, \Delta T]$.

A comparison can be made, in principle, between the quantities

$$\begin{aligned} \langle t_n | \Psi \rangle\rangle \sim |\psi(t_n)\rangle \,, \\ \forall n = 0, \ldots, N_T - 1 \end{aligned} \tag{4.76}$$

where

$$t_n = \frac{n \Delta T}{N_T}$$

and $|\Psi\rangle\rangle$ is one of the $|\Phi_{i=0,\ldots,N_T N_S - 1}\rangle\rangle$, or a linear combination of them, so that

$${}_T\langle 0 | \Psi \rangle\rangle = |\psi_0\rangle_S \,. \tag{4.77}$$

Initial value problem

As there is no individual $|\Phi_i\rangle\rangle$, in our numeric example, satisfying the (4.77), a suitable linear combination $|\Psi\rangle\rangle \coloneqq \sum_{i=0}^{N_T N_S - 1} c_i \, |\Phi_i\rangle\rangle$ needs to be found. Algebraically, the problem consists in N_S linear equations in $N_T N_S$ variables, therefore there is certainly more than one solution —a solution space of dimension $(N_T - 1) N_S$ indeed.

The following algorithm, among infinite possibilities, and merely for reasons of numerical stability, picks N_S vectors, say,

$$|\Phi_i\rangle\rangle \,, |\Phi_j\rangle\rangle \,, |\Phi_k\rangle\rangle$$

(for $N_S = 3$), so that, *to the best approximation*,

$$ {}_T\langle 0|\Phi_i\rangle\rangle,\ {}_T\langle 0|\Phi_j\rangle\rangle,\ {}_T\langle 0|\Phi_k\rangle\rangle $$

form an orthonormal basis in $\mathcal{H}_S$.[17] Then, with some elementary linear algebra, one can obtain the N_S coefficients —say a, b and c— so that

$$ a \cdot {}_T\langle 0|\Phi_i\rangle\rangle + b \cdot {}_T\langle 0|\Phi_j\rangle\rangle + c \cdot {}_T\langle 0|\Phi_k\rangle\rangle = |\psi_0\rangle\,. \tag{4.78} $$

With these coefficients, it will be

$$ |\Psi\rangle\rangle = a \cdot |\Phi_i\rangle\rangle + b \cdot |\Phi_j\rangle\rangle + c \cdot |\Phi_k\rangle\rangle \tag{4.79} $$

the (Page–Wootters) "history vector" to be plugged in (4.76) for comparison with standard quantum mechanics.

Full implementation code is available at Appendix A.1.5, function `find_linear_independent_initial()` returns:

```
def find_linear_independent_initial(eigenvectors=eigenvectors_normalized_in_S):

  # [...]
  return best_i, best_j, best_k, best_det
```

Then it is invoked:

```
best_i, best_j, best_k, best_det = find_linear_independent_initial()
```

and (the coefficients of) the linear combination is (are) derived. The following resolves (4.78):

```
states = np.array([
    histories[best_i][:NS],
    histories[best_j][:NS],
```

[17] "Best approximation" (of an orthonormal base in $\mathcal{H}_S$) in the sense of finding three (or in general N_S) different $i, j, k \in \{0, \ldots, N_S - 1\}$ that minimize $\left| 1 - \det \begin{pmatrix} {}_S\langle 0|\,{}_T\langle 0|\Phi_i\rangle\rangle & {}_S\langle 1|\,{}_T\langle 0|\Phi_i\rangle\rangle & {}_S\langle 2|\,{}_T\langle 0|\Phi_i\rangle\rangle \\ {}_S\langle 0|\,{}_T\langle 0|\Phi_j\rangle\rangle & {}_S\langle 1|\,{}_T\langle 0|\Phi_j\rangle\rangle & {}_S\langle 2|\,{}_T\langle 0|\Phi_j\rangle\rangle \\ {}_S\langle 0|\,{}_T\langle 0|\Phi_k\rangle\rangle & {}_S\langle 1|\,{}_T\langle 0|\Phi_k\rangle\rangle & {}_S\langle 2|\,{}_T\langle 0|\Phi_k\rangle\rangle \end{pmatrix} \right|$.

```
    histories[best_k][:NS]
])

# Find what linear combination would bring to the desired initial state psi_0_n
coeffs = inv(states.T) @ psi_0
```

and

```
history = coeffs.dot(np.array([
    histories[best_i],
    histories[best_j],
    histories[best_k]
]))
```

implements (4.79).

Comparison

The following code (with notation slightly changed compared to Appendix A.1.5, for clarity)

```
pwpsi = history.reshape((-1,NS)).T
```

rearranges the `history` array in such a way that

```
pwpsi[m][n]
```

is

$$ {}_S\langle m|\,{}_T\langle t_n|\Psi\rangle\rangle $$

and can be compared with

$$ \langle m|\psi(t_n)\rangle $$

from "ordinary" quantum mechanics, $\forall\ m \in \{0,\ldots,N_S{-}1\}$ and $n \in \{0,\ldots,N_T{-}1\}$.

Such comparison is visualized in Fig. 4.11, showing excellent agreement between the discrete Page–Wootters model (square points) and "standard" quantum evolution (continuous line). Page–Wootters "history vector" components are also shown on their own in Fig. 4.10.

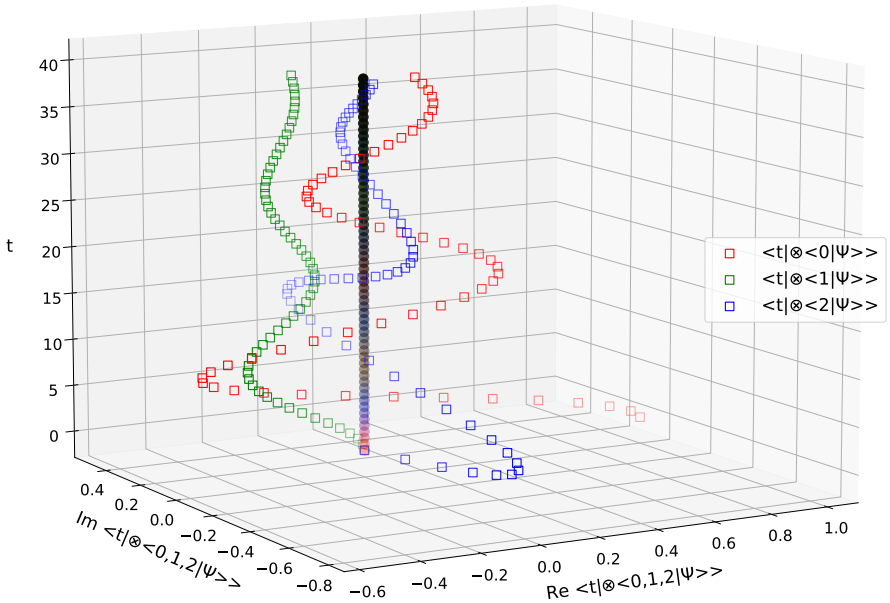

(a) 3-D plot: side view.

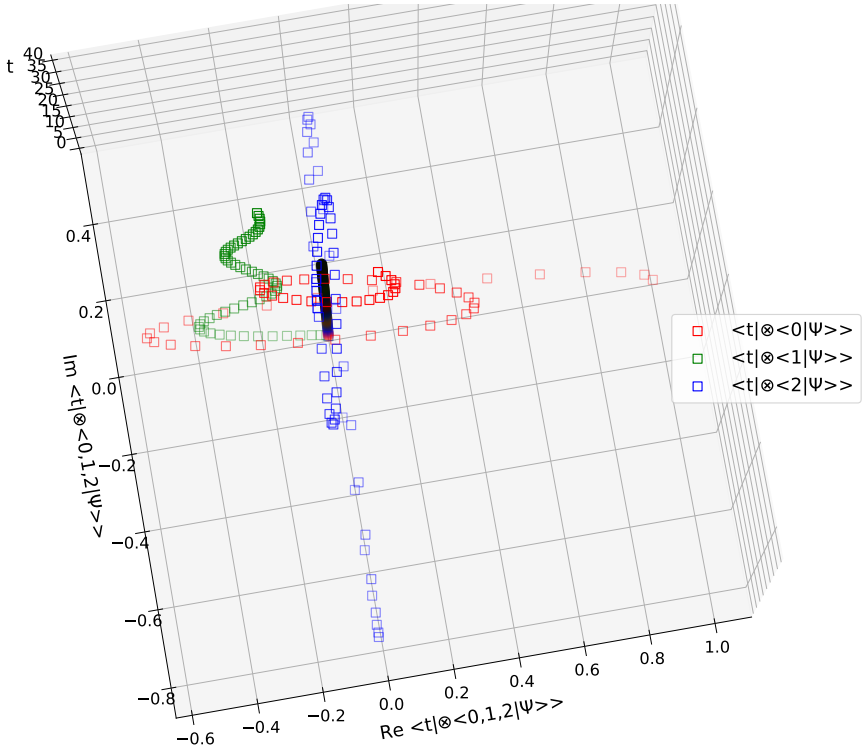

(b) 3-D plot: top view.

Figure 4.10: Components (complex values) of the discrete-Page–Wootters vector $|\Psi\rangle\rangle \in \mathcal{H}_T \otimes \mathcal{H}_S$ ("evolution without evolution"). Can be compared with Fig. 4.8.

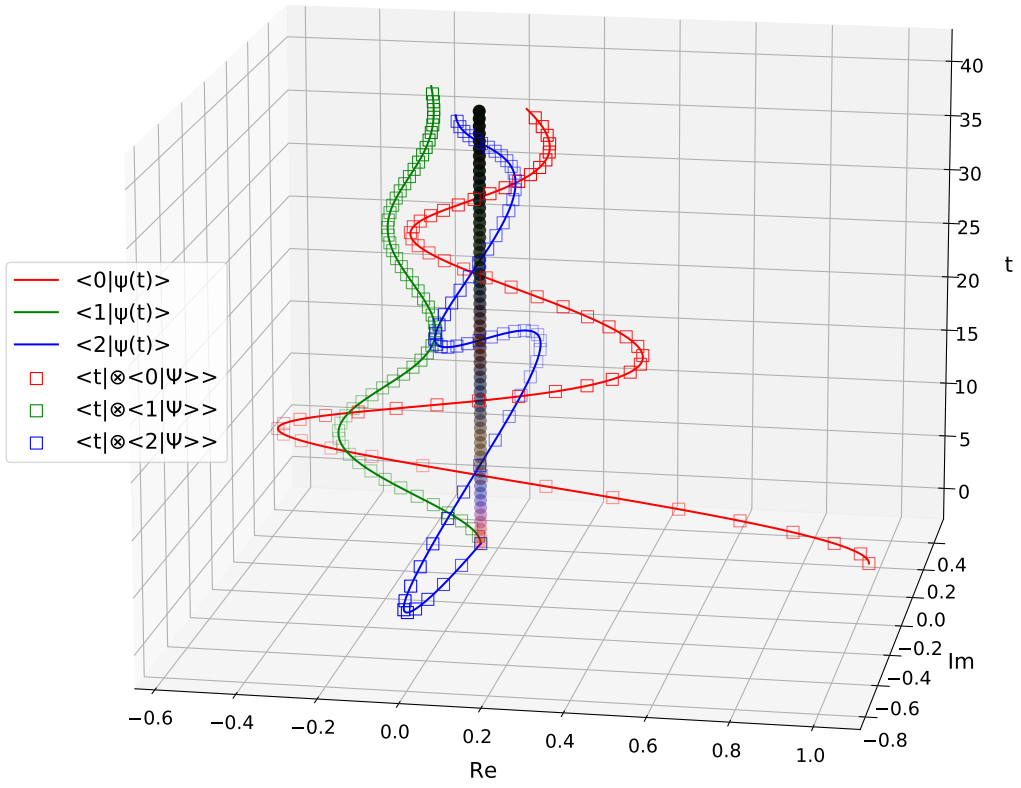

(a) 3-D plot: side view

Figure 4.11: Discrete Page–Wootters results (points) compared to continuous Schrödinger evolution (continuous lines).

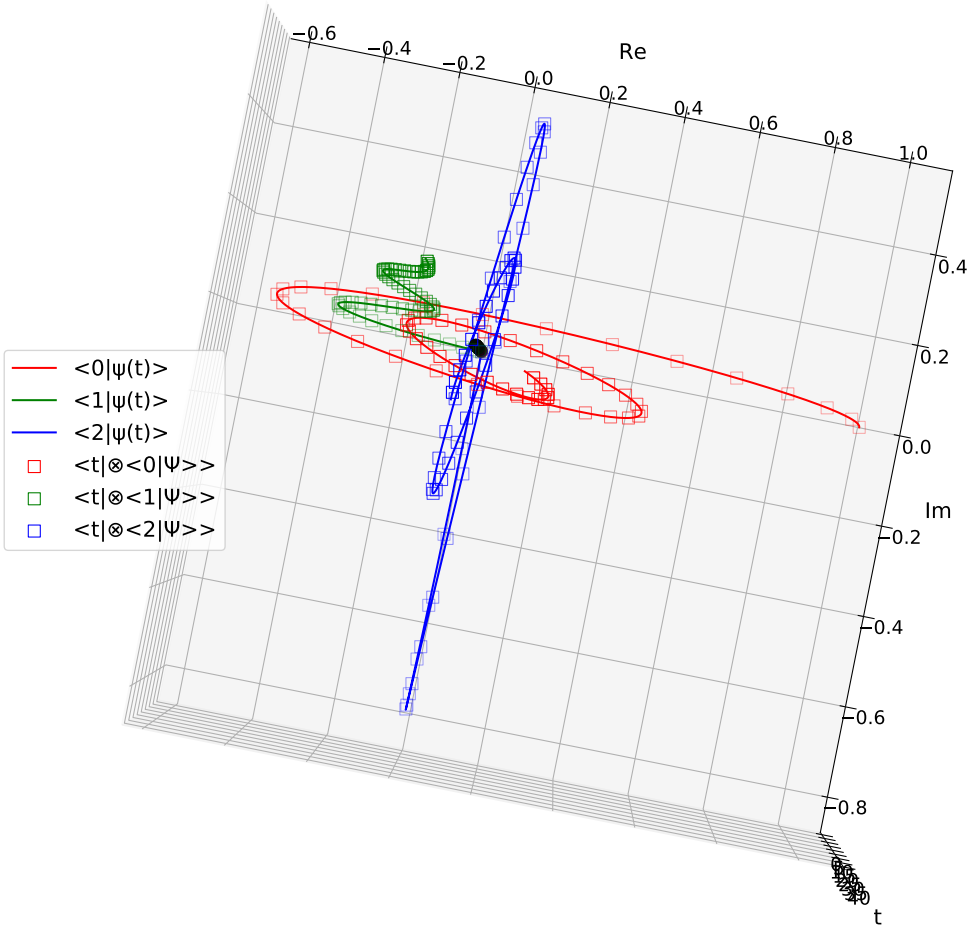

(b) 3-D plot: top view

Figure 4.11: *Continued from Fig. 4.11a.* Discrete Page–Wootters results (points) compared to continuous Schrödinger evolution (continuous lines).

4.7.4 Time-of-arrival (conditional) probability

From Maccone and Sacha 2020, a time-of-arrival probability distribution can be derived for the three-level system at hand, within the Page–Wootters formalism. In a finite-dimensional Hilbert space there is no notion of position or "region of space", but, as stated in the same paper,

> [...] the whole discussion can be easily extended to the "time at which any event happens". For example, if one considers a spin instead of a particle on a line, one can define the "time at which the spin is up".
>
> [...] the notion of "event" in quantum mechanics [can be] defined as "something that happens to a quantum system", where "something" means "a system observable property taking some value [...]".

Rather than spin up or down, in the present example, the arrival time at level $|2\rangle$ can be derived:

$$P^{PW}(t_n|2) \coloneqq P^{PW}\Big(t_n\Big|2,[0,\Delta T]\Big) = \frac{\big|\langle t_n|\otimes\langle 2|\cdot|\Psi\rangle\rangle\big|^2}{\sum_{n'=0}^{N_T-1}\big|\langle t_{n'}|\otimes\langle 2|\cdot|\Psi\rangle\rangle\big|^2}\,, \qquad \text{where } t_{n'} = n'\delta T = \frac{n'\Delta T}{N_T}; \quad (4.80)$$

which gives the (conditional, *Bayesian*) probability that, given that a detection of $|2\rangle$ happens within $t\in[0,\Delta T]$, it happens at time t_n (or, more correctly, between t_n and t_{n+1}).

On the other hand, and outside the Page–Wootters formalism, within the absorptive detector model (see e.g. Sec. 4.7.2 or Fig. 4.7b) the detection probability density reads $p(t) = -\frac{\mathrm{d}\|\psi\|^2}{\mathrm{d}t}$.

Thus, the *conditional* probability density that —*provided* a detection[18] of the system at $|2\rangle$ happens within $t\in[0,\Delta T]$— it does happen at a particular time t is

$$p(t|2) \coloneqq p(t\mid 2,[0,\Delta T]) = \frac{-\frac{\mathrm{d}\|\psi\|^2}{\mathrm{d}t}}{\int_0^{\Delta T}-\frac{\mathrm{d}\|\psi\|^2}{\mathrm{d}t'}\,\mathrm{d}t'} = \frac{-\frac{\mathrm{d}\|\psi\|^2}{\mathrm{d}t}}{\|\psi(0)\|^2-\|\psi(\Delta T)\|^2}\,. \quad (4.81)$$

[18] Or measurement of related observable eigenvalue, or spontaneous decay from $|2\rangle$ as in Sec. 3.4.1.

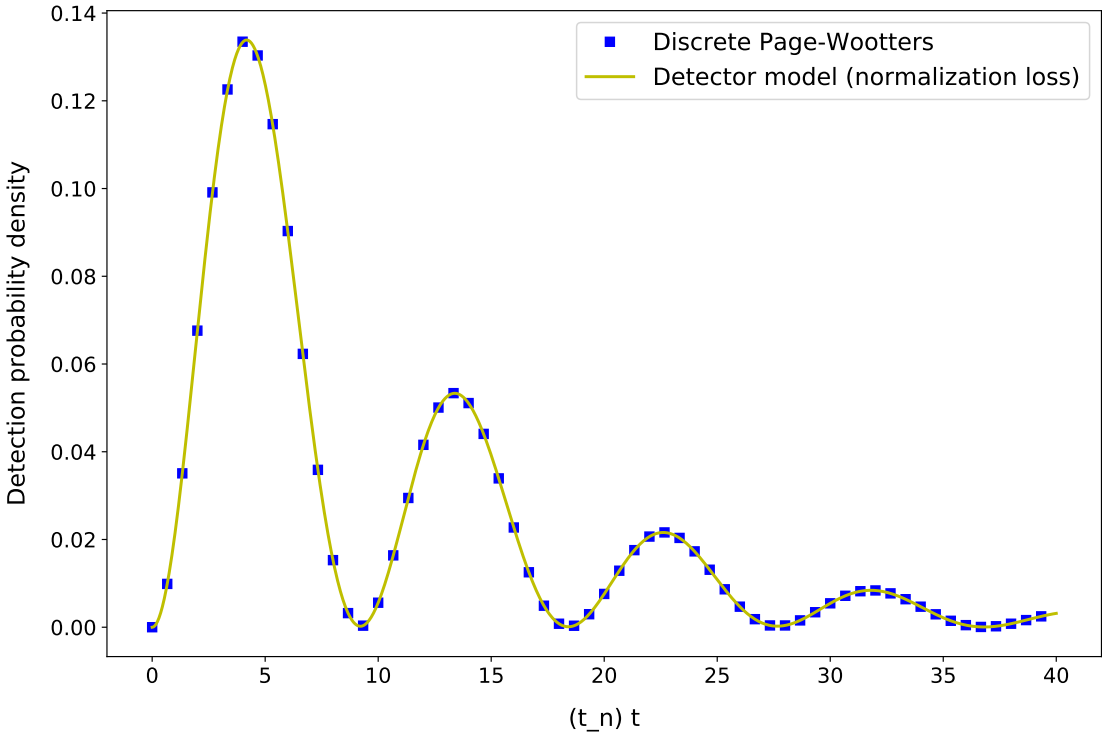

Figure 4.12: Conditional probability density for time of arrival at state $|2\rangle$. Discrete points: $P^{PW}(t_n|2)/\delta T$ (Page–Wootters). Continuous line: $p(t|2)$ (detector model).

The "state of arrival" in (4.81) is $|2\rangle$ because the operator in (4.72) is essentially $\hat{D} = \gamma\,|2\rangle\langle 2|$. The same state has been chosen in (4.80) to allow a comparison. However, $P^{PW}(t_n|2)$ is a probability, while $p(t|2)$ is a probability *density*. Therefore, the (4.80) should be divided by δT, i.e. the duration of the time interval the probability refers to, before being plotted in Fig 4.12, where the two models show indeed fully compatible results.

NumPy code

Relevant portion of code to compute the (4.80) follows. Values of probability density $\frac{1}{\delta T}P^{PW}(t_n|2)$ are stored in the array `Y`:

```
# [...]
def tn_ox_arrived(n):
  # tensor product
```

```
  return np.kron(t_eigenstate(n), arrived_state)

history_normalized = history / norm(history)  ## normalized in H_T \otimes H_S

def joint_prob(n):
  return np.abs(tn_ox_arrived(n) @ history_normalized)**2

X = np.arange(NT)
iterable = (joint_prob(n) for n in X)
Y = np.fromiter(iterable, float)
dT  = DT / (NT)

# A "time bin"
X = X * dT # real time
Y = Y / dT # probability _density_

bayes_denominator = np.sum(Y * dT)
Y = Y / bayes_denominator
```

The (4.81) is partly implemented directly in the plotting code:

```
ax.plot(times, -np.gradient(norms**2, times) / bayesian_denominator_nonpw,
c='y', linewidth=2, label='Detector␣model␣(normalization␣loss)')
```

particularly with the expression `-np.gradient(norms**2, times)/ bayesian_denominator_nonpw`. The array `norms` was previously assigned values of $\|\psi(t)\|$ while computing the non-unitary evolution for the problem in Sec. 4.7.2. Here, explicitly:

```
# [...]
def B(_t, _gamma=GAMMA):
  return expm(-1j*K(_gamma)*_t)

def non_unitary_psi(_t, _gamma=GAMMA):
  return B(_t, _gamma) @ psi_0

# [...]
_iter_norm = (norm(non_unitary_psi(_t)) for _t in times)
norms = np.fromiter(_iter_norm, np.float)
```

where, again, the function `K()` returns the matrix in (4.71). As per the "Bayesian denominator":

```
# loss of normalization, or integral of antiderivative...
bayesian_denominator_nonpw = 1 - norm(evolution.T[NPLOTPOINTS-1])**2
```

Full code for this Section can be consulted at Appendix A.1.6.

Chapter 5

Conclusions and Outlook

5.1 Discussion

The initial draft title for this work was: *It's* $|1\rangle$ *o'clock – Relational Time and Applications*. May time have eigenvectors and eigenvalues? We have illustrated, mainly through numerical examples at various degrees of complexity, and developing from existing theoretical work, how time can be treated as a quantum observable (described by a self-adjoint operator with its eigenvalues —and eigenvectors).

The Pauli objection (presented in Section 3.1) can be overcome if the time operator $\hat{T}$ is defined in a different Hilbert space (that we name $\mathcal{H}_T$), distinct from the space, say $\mathcal{H}_S$, where the Hamiltonian is defined, as set out by the Page and Wootters model (Giovannetti et al. 2015; Leon and Maccone 2017; Maccone and Sacha 2020; Marletto and Vedral 2017; Page and Wootters 1983).

One can introduce an extra Hilbert space, to that of ordinary quantum mechanics, in which the time operator is defined. Or, more "realistically", identify, in a closed system, a subsystem acting as a clock for the rest of it. Requirements are non-interaction and full entanglement.

In terms of potential further development, Section 5.2 introduces the possibility of a special-relativistic extension by formulating the Klein–Gordon equation

in Page–Wootters terms. More themes of further research are mentioned in Section 5.3.

5.2 Relativistic formulation: Klein-Gordon

The Klein-Gordon equation is the relativistic extension of the (*square of*) a wave equation for a free spinless particle. Indeed, both sides have the dimension of the square of an energy, and finding their square root (in the operator sense) is non trivial task which was only resolved with the Dirac equation, from which the intrinsic *spin* (particularly spin $\hbar/2$) logically emerges, rather then being artificially introduced in the theory to comply with the phenomenology (Greiner 2000, Sakurai and Napolitano 2011, c. 8, Thaller 1992, Webber 2006, handout 2).

Both equations did not have much fortune as first-quantized equations, for conceptual difficulties and historical reasons, including the rise of Quantum Field Theory and second quantization. They do have a fundamental role though as field equations (before quantization methods are enacted). (Peskin and Schroeder 1995).

The purpose of the present work is, in a sense, promoting time to a quantum observable, or formally to a linear, self-adjoint operator in some Hilbert space. The passage from quantum mechanics to field theory does not represent any progress towards such goal, in that not only it does not "promote" time to an operator $\hat{t}$, but it also "demotes" the three position operators $\hat{x}$, $\hat{y}$ and $\hat{z}$ to mere (classical) *parameters*. However, consistently to relativistic covariance, time and space coordinates are treated on equal footing. The Page and Wootters model offers the opportunity to do the same, but both time and position are operators!

5.2.1 Page and Wootters squared

From the (4.2) and (4.1):

$$-\hbar\hat{\Omega}\otimes\mathbb{1}_S\,|\Psi\rangle\rangle = \mathbb{1}_T\otimes\hat{H}_S\,|\Psi\rangle\rangle\ . \tag{5.1}$$

Squaring the operators on both sides, we have:

$$\hbar^2\hat{\Omega}^2\otimes\mathbb{1}_S\ \ |\Psi\rangle\rangle = \mathbb{1}_T\otimes\hat{H}_S^2\ \ |\Psi\rangle\rangle = \mathbb{1}_T\otimes\left(\hat{p}^2c^2+m_0^2c^4\right)|\Psi\rangle\rangle\ , \tag{5.2}$$

where the last equality is due to the "quantization" of the relation $E^2 = p^2c^2 + m_0^2c^4$ into $\hat{H}_S^2 = \hat{p}^2c^2 + m_0^2c^4$.

We know from previous sections that in the $\{|t\rangle\}_T$ basis $\hat{\Omega}$ is represented as $-i\hbar\frac{\partial}{\partial t}$. We know from standard quantum mechanics that in the $\{|x\rangle\,|y\rangle\,|z\rangle\}_S$ basis is $\hat{p}\equiv-i\hbar\nabla$. Therefore in the product basis the (5.2) yields:

$$-\hbar^2\frac{\partial^2}{\partial t^2}\Psi = \left(-\hbar^2c^2\nabla^2+m_0^2c^4\right)\Psi \tag{5.3}$$

which, up to some elementary algebra, is the well known *Klein-Gordon equation*.

In standard quantum mechanics (first quantization, relativistic or not)

$$|\psi(t)\rangle = \int \mathrm{d}x\,\mathrm{d}y\,\mathrm{d}z\,\Psi(x,y,z;t)\,|x\rangle\otimes|y\rangle\otimes|z\rangle\ . \tag{5.4}$$

In this formulation

$$|\Psi\rangle\rangle = \int \mathrm{d}x\,\mathrm{d}y\,\mathrm{d}z\,\mathrm{d}t\,\Psi(x,y,z,t)\,|x\rangle\otimes|y\rangle\otimes|z\rangle\otimes|t\rangle\ , \tag{5.5}$$

and t is no longer a classical parameter, but an eigenvalue of the time operator, or a label for time basis elements. Please note that, as a function of four variables, Ψ is not normalizable i.e. it is not a proper element of $\mathscr{L}^2(\mathbb{R}^4)$ (normalization issues are tackled in Giovannetti et al. 2015, eq. 23 and following).

5.2.2 Covariant notation

The (5.3) can be rearranged and expressed in explicitly covariant form:

$$\left[\partial_\mu \partial^\mu + \left(\frac{mc}{\hbar}\right)^2\right]\Psi = 0 \tag{5.6}$$

with standard relativistic notation.

Similarly —at operator level, in the tensor product space— the (5.2) can be rearranged:

$$\left[-\hat{\mathrm{P}}_\mu \hat{\mathrm{P}}^\mu + \left(\frac{mc}{\hbar}\right)^2\right]|\Psi\rangle\rangle = 0 \tag{5.7}$$

with

$$\begin{aligned}
\hat{\mathrm{P}}_0 &= \frac{\hbar\hat{\Omega}}{c} \otimes \mathbb{1}_x \otimes \mathbb{1}_y \otimes \mathbb{1}_z \\
\hat{\mathrm{P}}_1 &= \mathbb{1}_T \otimes \hat{p}_x \otimes \mathbb{1}_y \otimes \mathbb{1}_z \\
\hat{\mathrm{P}}_2 &= \mathbb{1}_T \otimes \mathbb{1}_x \otimes \hat{p}_y \otimes \mathbb{1}_z \\
\hat{\mathrm{P}}_3 &= \mathbb{1}_T \otimes \mathbb{1}_x \otimes \mathbb{1}_y \otimes \hat{p}_z
\end{aligned} \tag{5.8}$$

and the usual relation between contravariant and covariant 4-vectors:

$$a_\mu = \eta^\mu_\nu a^\nu; \quad \eta = \mathrm{diag}(+1, -1, -1, -1). \tag{5.9}$$

It is tempting to name the (5.7) and (5.8) the *Page–Wootters-Klein-Gordon* equation.[1]

Looking back at Table 4.1, it can thus be extended as:

[1] Or *Klein-Gordon-Wheeler-DeWitt-Page–Wootters-Giovannetti-Lloyd-Maccone* equation, thus giving credits to all authors, particularly if we consider that the idea of an extra Hilbert space was conceived originally in Giovannetti et al. 2015.

	$\mathcal{H}_T$	$\mathcal{H}_S$	Mass term
Space–time "positions"	$\hat{t}$	$\hat{x}$	
Canonically conjugate	$\hat{P}_0 = \frac{\hbar\hat{\Omega}}{c} \equiv -i\partial_0$	$\hat{P}_{1,2,3} \equiv -i\nabla$	
Dynamics (terms in the Wheeler-DeWitt equation)	$\hat{P}_0\hat{P}^0 \equiv -\hbar^2\partial_0\partial^0$	$\hat{P}_j\hat{P}^j \equiv -\hbar^2\partial_j\partial^j$	$\left(\frac{mc}{\hbar}\right)^2$

Table 5.1: Operators in the space-time Hilbert spaces.

5.3 Other topics

5.3.1 Computation methods and decomposition

In Sec. 4.3, it was noted that "a benefit of finite-dimensional systems is the potential implementation on a finite array of qubits in a quantum computer". Indeed, experimentally, besides looking for a suitable N-level system to act as a clock, we may want to "encode" 2^n levels into the combined state of n qubits and decompose $\mathbb{J}$ (or, actually, $e^{-i\mathbb{J}\tau/\hbar}$) into simpler Hamiltonians (respectively: evolutions) acting on individual qubits (*gates*), therefore allowing the experiment to be run on a quantum processor. A decomposition method that can be considered for the purpose is the Trotter-Suzuki scheme (Bederián and Dente 2011; Wiebe et al. 2010).

5.3.2 Additional themes

Further studies would be required to explore the potential to model —in terms of relational time— other quantum systems and processes such as: *time crystals* (Nakatsugawa et al. 2017; Syrwid et al. 2017; Wilczek 2012); *atomic clocks* (Muga et al. 2009); *irreversibility* and "arrow of time" (Josset 2017); *spontaneous emission* (Melo e Souza et al. 2016); as well as *reference frames* and transformations (Adlam 2022).

Appendix A

Jupyter Notebooks[1]

Technical note

Original files available at the code repository, ref. De Rosa 2022.

Printable and embeddable TEX files have been generated with

- "Download as Markdown" from Jupyter user interface
- Installing and running `pandoc`[2] on the generated `.md` file[3]

```
pandoc --listings -f markdown -t latex myfile.md -o myfile.tex
```

- Tweaking generated `\label`'s and other references as needed to avoid inconsistencies and overlaps

A.1 Detector model: Kiukas, Ruschhaupt, Schmidt, Werner

[1] For a reference on the software tools utilized: Jones et al. 2001; Meurer et al. 2017; Kluyver et al. 2016; Hunter 2007; T. E. Oliphant 2015.

[2] http://pandoc.org/

[3] See also https://tex.stackexchange.com/a/314785.

```
from sympy import *
#from sympy.physics.matrices import mdft
from sympy.physics.quantum import TensorProduct
from sympy.functions.special.delta_functions import Heaviside
from sympy.physics.quantum.dagger import Dagger

from sympy.stats import ContinuousRV, variance, std

from sympy.plotting import plot, plot3d_parametric_line

import numpy as np
import matplotlib
import matplotlib.pyplot as plt

matplotlib.rcParams['text.usetex'] = True
#matplotlib.rcParams['text.latex.preamble'] = r'''
#    \usepackage{DejaVuSans}
#    \usepackage{xparse}
#    \usepackage{amsmath}
#    \usepackage{physics}
#'''
#matplotlib.rcParams['mathtext.fontset'] = 'dejavusans'
#matplotlib.rcParams['mathtext.default'] = 'sf'
matplotlib.rcParams['figure.dpi'] = 140
# matplotlib.rcParams['figure.figsize'] = (8,8/sqrt(2))
matplotlib.rcParams['axes.labelsize'] = 16

# https://matplotlib.org/gallery/mplot3d/lines3d.html?highlight=parametric
# This import registers the 3D projection, but is otherwise unused.
from mpl_toolkits.mplot3d import Axes3D  # noqa: F401 unused import
```

```
gamma = Symbol('gamma', real=True)
t = Symbol('t', real=True)
tprime = Symbol('t\'', real=True)
omega = Symbol('omega', real=True)
nu = Symbol('nu', real=True)
```

```
def D(_gamma):
    return Rational(1, 2) * Matrix([
        [0, 0],
        [0, _gamma]
    ])
```

```
H = Matrix ([
[0, 1] ,
[1, 0]
])
```

```
init_printing ()
```

```
H
```

$$\begin{bmatrix} 0 & 1 \\ 1 & 0 \end{bmatrix}$$

```
H.eigenvects()
```

$$\left[\left(-1, \quad 1, \quad \left[\begin{bmatrix} -1 \\ 1 \end{bmatrix}\right]\right), \quad \left(1, \quad 1, \quad \left[\begin{bmatrix} 1 \\ 1 \end{bmatrix}\right]\right)\right]$$

It's manually seen that $\langle H \rangle = 0$ and $\langle H^2 \rangle = 1$, therefore $\sigma_H = 1$.

```
def K(_gamma):
    return H - I*D(_gamma)
```

```
K(2*sqrt(2))
```

$$\begin{bmatrix} 0 & 1 \\ 1 & -\sqrt{2}i \end{bmatrix}$$

```
K(2*sqrt(2)).eigenvects()
```

$$\left[\left(-\frac{\sqrt{2}}{2} - \frac{\sqrt{2}i}{2}, \quad 1, \quad \left[\begin{bmatrix} -\frac{1}{\frac{\sqrt{2}}{2} + \frac{\sqrt{2}i}{2}} \\ 1 \end{bmatrix}\right]\right), \quad \left(\frac{\sqrt{2}}{2} - \frac{\sqrt{2}i}{2}, \quad 1, \quad \left[\begin{bmatrix} -\frac{1}{-\frac{\sqrt{2}}{2} + \frac{\sqrt{2}i}{2}} \\ 1 \end{bmatrix}\right]\right)\right]$$

```
def B(_gamma):
    return lambda t: exp(-I*K(_gamma)*t)
```

```
def U():
    return lambda t: exp(-I*H*t)
```

```
def non_unitary_psi(_t):
    return B(2*sqrt(2))(_t) * Matrix([1,0])
```

```
def unitary_psi(_t):
    return U()(_t) * Matrix([1,0])
```

```
non_unitary_psi(t)
```

$$\begin{bmatrix} \frac{\sqrt{2}ite^{-\frac{\sqrt{2}t}{2}-\frac{\sqrt{2}it}{2}}}{2\left(\frac{\sqrt{2}t}{2}+\frac{\sqrt{2}it}{2}\right)} - \frac{\sqrt{2}ite^{-\frac{\sqrt{2}t}{2}+\frac{\sqrt{2}it}{2}}}{2\left(\frac{\sqrt{2}t}{2}-\frac{\sqrt{2}it}{2}\right)} \\ \frac{\sqrt{2}e^{-\frac{\sqrt{2}t}{2}-\frac{\sqrt{2}it}{2}}}{2} - \frac{\sqrt{2}e^{-\frac{\sqrt{2}t}{2}+\frac{\sqrt{2}it}{2}}}{2} \end{bmatrix} \tag{A.1}$$

New period

```
2*pi / (sqrt(2)/2)
```

$$2\sqrt{2}\pi$$

Components are either pure real or pure imaginary:

```
plot(re(non_unitary_psi(t)[0]), (t, 0, 10),
     line_color='r', xlabel=r'$t$', ylabel=r'$\mathrm{Re}\left\langle␣0␣|␣\psi␣\
         right\rangle␣$')
```

```
<sympy.plotting.plot.Plot at 0x7fe25ffc9898>
```

```
plot(im(non_unitary_psi(t)[1]), (t, 0, 10),
     line_color='b', xlabel=r'$t$', ylabel=r'$\mathrm{Im}\left\langle␣1␣|␣\psi␣\
         right\rangle␣$')
```

```
<sympy.plotting.plot.Plot at 0x7fe25fec1780>
```

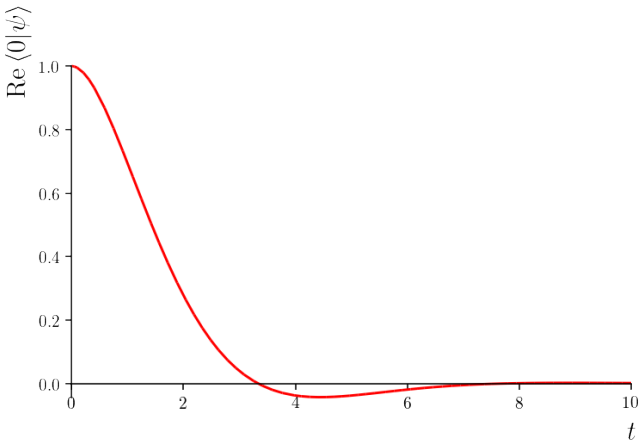

Figure A.1: png

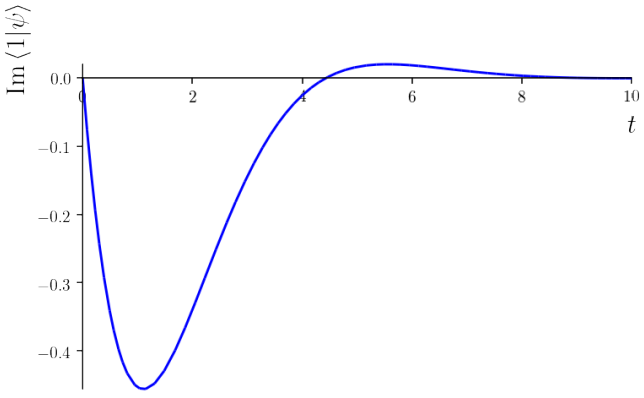

Figure A.2: png

```
# verify that our manual simplification is correct
#plot(-sqrt(2)*exp(-t*sqrt(2)/2)*sin(t*sqrt(2)/2), (t, 0, 10) )
```

```
def lossy_norm(_t):
    psi = B(2*sqrt(2))(_t) * Matrix([1,0])
    return (abs(psi[0]**2) + abs(psi[1]**2))
```

```
lossy_norm(t)
```

$$\left|\left(\frac{\sqrt{2}e^{-\frac{\sqrt{2}t}{2}-\frac{\sqrt{2}it}{2}}}{2}-\frac{\sqrt{2}e^{-\frac{\sqrt{2}t}{2}+\frac{\sqrt{2}it}{2}}}{2}\right)^2\right|+\left|\left(\frac{\sqrt{2}ite^{-\frac{\sqrt{2}t}{2}-\frac{\sqrt{2}it}{2}}}{2\left(\frac{\sqrt{2}t}{2}+\frac{\sqrt{2}it}{2}\right)}-\frac{\sqrt{2}ite^{-\frac{\sqrt{2}t}{2}+\frac{\sqrt{2}it}{2}}}{2\left(\frac{\sqrt{2}t}{2}-\frac{\sqrt{2}it}{2}\right)}\right)^2\right|$$

```
non_unitary_psi_n = lambdify(t, non_unitary_psi(t), "numpy")
```

```
_lossy_norm_n = lambdify(t, lossy_norm(t), "numpy")
def lossy_norm_n(__t):
    # prevent a warning, even if we know it's real
    return np.real(_lossy_norm_n(__t))
```

```
lossy_norm_n
```

```
<function __main__.lossy_norm_n(__t)>
```

```
def non_unitary_psi_renorm_n(_t):
    return non_unitary_psi_n(_t) / np.sqrt(lossy_norm_n(_t))
```

```
T = np.linspace(1e-16, 2*np.pi, 2000)
```

```
fig = plt.figure(figsize=(8,8))
#fig = plt.figure()


ax = fig.gca(projection='3d')
ax.view_init(10,-45) # rotate 3d point of view

ax.plot(
    np.real(non_unitary_psi_n(T)[0][0]), np.imag(non_unitary_psi_n(T)[1][0]), T,
    linewidth=1.25
```

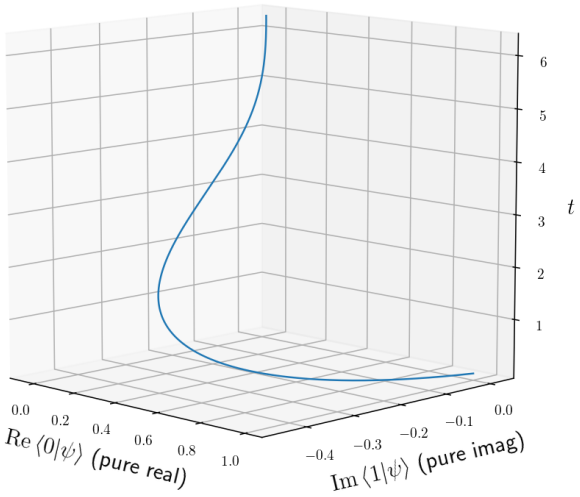

Figure A.3: png

```
)

##ax.legend()

plt.xlabel(r'$\mathrm{Re}\left\langle␣0␣|␣\psi␣\right\rangle$␣(pure␣real)',
    labelpad=8)
plt.ylabel(r'$\mathrm{Im}\left\langle␣1␣|␣\psi␣\right\rangle$␣(pure␣imag)',
    labelpad=10)
ax.set_zlabel(r'$t$')
```

```
Text(0.5, 0, '$t$')
```

```
plot(lossy_norm(t),(t, 0, 2*pi), line_color='g',
     ylabel=r'$\left|\psi\right|^2$', xlabel=r'$t$')
```

```
<sympy.plotting.plot.Plot at 0x7fe25fe6a6a0>
```

```
def prob_0_detect(t):
    return abs(non_unitary_psi(t)[0]**2) / lossy_norm(t)
```

```
def prob_1_detect(t):
    return abs(non_unitary_psi(t)[1]**2) / lossy_norm(t)
```

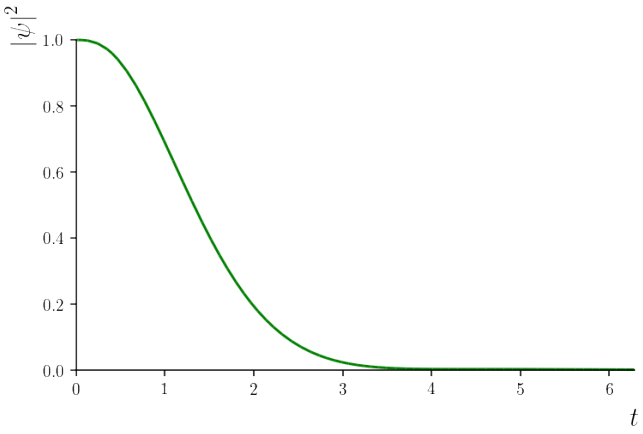

Figure A.4: png

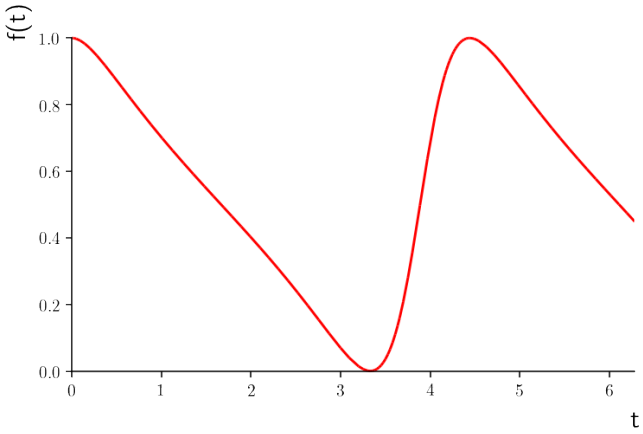

Figure A.5: png

```
plot(prob_0_detect(t),(t, 0, 2*pi), line_color='r')
```

```
<sympy.plotting.plot.Plot at 0x7fe25fddca20>
```

```
plot(prob_1_detect(t),(t, -0, 2*pi), line_color='b')
```

```
<sympy.plotting.plot.Plot at 0x7fe25fd87ac8>
```

```
plot(re(non_unitary_psi(t)[0])/sqrt(lossy_norm(t)), (t, 0, 2 * 2*sqrt(2)*pi),
    line_color='r')
```

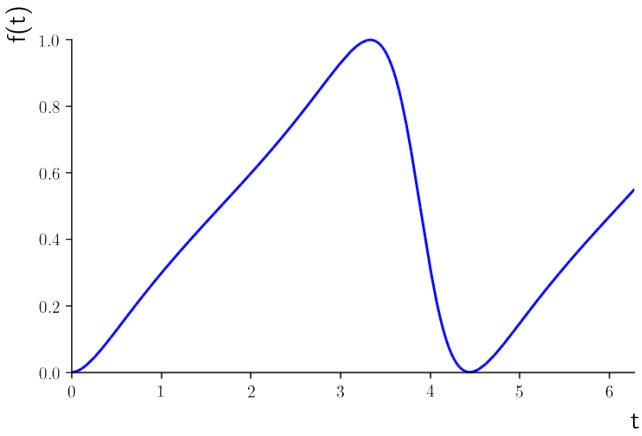

Figure A.6: png

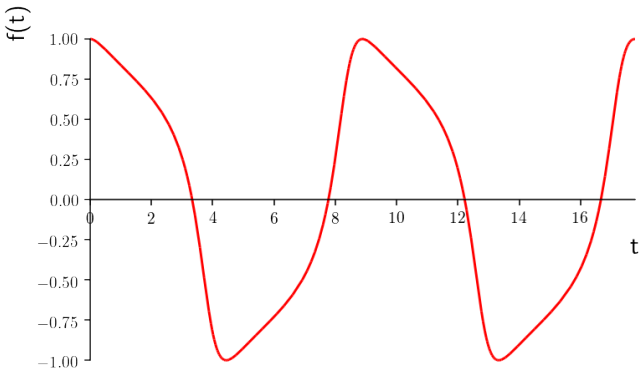

Figure A.7: png

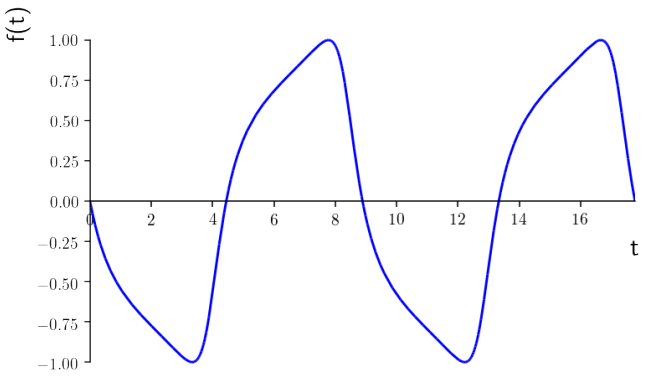

Figure A.8: png

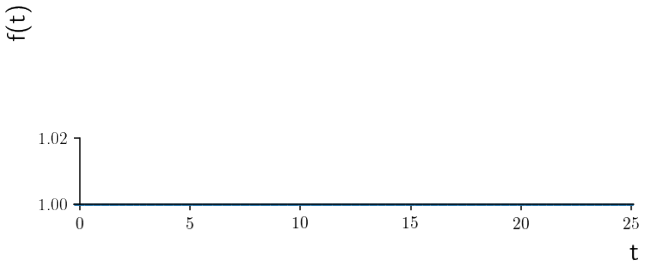

Figure A.9: png

```
<sympy.plotting.plot.Plot at 0x7fe25fd03128>
```

```
plot(im(non_unitary_psi(t)[1])/sqrt(lossy_norm(t)), (t, 0, 2 * 2*sqrt(2)*pi),
    line_color='b')
```

```
<sympy.plotting.plot.Plot at 0x7fe25f98eeb8>
```

```
plot(prob_0_detect(t) + prob_1_detect(t),(t, -0.25, 8*pi))
```

```
<sympy.plotting.plot.Plot at 0x7fe261980c50>
```

```
def prob_0_unitary(t):
    return abs(unitary_psi(t)[0]**2)
```

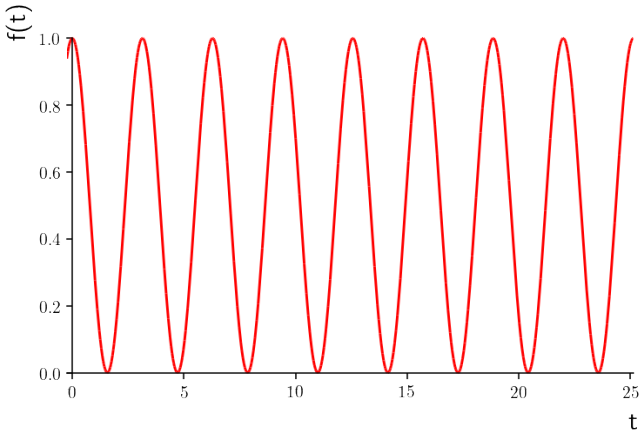

Figure A.10: png

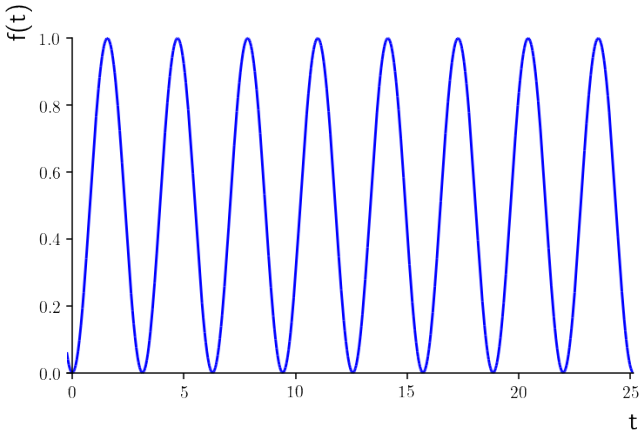

Figure A.11: png

```
def prob_1_unitary(t):
    return abs(unitary_psi(t)[1]**2)
```

```
plot(prob_0_unitary(t),(t, -0.25, 8*pi), line_color='r')
```

```
<sympy.plotting.plot.Plot at 0x7fe261a495c0>
```

```
plot(prob_1_unitary(t),(t, -0.25, 8*pi), line_color='b')
```

```
<sympy.plotting.plot.Plot at 0x7fe25ff64710>
```

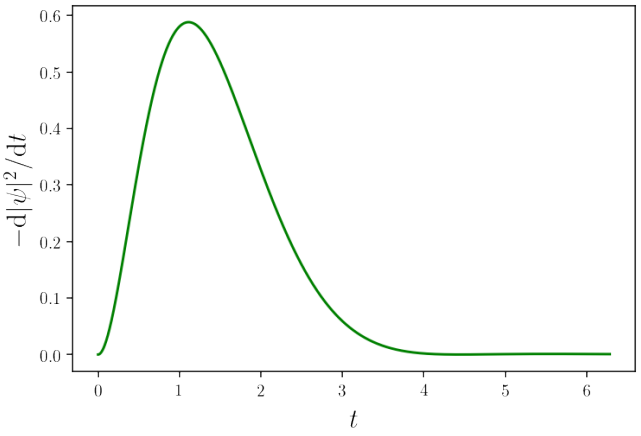

Figure A.12: png

```
lossy_norm_n(2)
```

0.19265133139031912

```
X = np.linspace(1e-6, 2*np.pi, 1000)  # avoid singularity in t=0
```

```
Y = lossy_norm_n(X)
```

```
plt.xlabel('$t$')
plt.ylabel(r'$\,-\,\mathrm{d}|\psi|^2\,/\,\mathrm{d}t\,$')
plt.plot(X, -np.gradient(Y, X), 'g')
```

```
[<matplotlib.lines.Line2D at 0x7fe25f7ddba8>]
```

```
# we have set gamma = 2*sqrt(2)
def hatpsi(_t):
    return \
        Heaviside(_t) * \
        2**(Rational(3,4)) * \
        Matrix([
            [0, 0],
            [0, 1]
        ]) * \
        non_unitary_psi(_t)
```

```
def hatpsi_n(_t):
    return \
        np.heaviside(_t, 0) * \
        2**(3/4) * \
        np.array([
            [0, 0],
            [0, 1]
        ]) * \
        non_unitary_psi_n(_t)
```

```
hatpsi(t)
```

$$\begin{bmatrix} 0 \\ 2^{\frac{3}{4}} \left(\frac{\sqrt{2} e^{-\frac{\sqrt{2} t}{2} - \frac{\sqrt{2} i t}{2}}}{2} - \frac{\sqrt{2} e^{-\frac{\sqrt{2} t}{2} + \frac{\sqrt{2} i t}{2}}}{2} \right) \theta\left(t\right) \end{bmatrix} \tag{A.2}$$

```
def hatpsisquarednorm(_t):
    return abs(hatpsi(_t)[0]**2) + abs(hatpsi(_t)[1]**2)

def hatpsisquarednorm_n(_t):
    return abs(hatpsi_n(_t)[0]**2) + abs(hatpsi_n(_t)[1]**2)
```

```
hatpsisquarednorm(-1)
```

$$0$$

```
plot(hatpsisquarednorm(t), (t, -1, 2*pi), line_color='g',
     ylabel=r'$\left|\hspace{-.15em}\left|\hat{\psi}\right|\hspace{-.15em}\
         right|^2$=$-\mathrm{d}\left|\hspace{-0.15em}\left|\psi\right|\
         hspace{-0.15em}\right|^2/\mathrm{d}t$',
     xlabel=r'$t$'
    )
```

```
<sympy.plotting.plot.Plot at 0x7fe25f7b05f8>
```

```
#plot(prob_1_detect(t), hatpsisquarednorm(t), (t, -0.25, 8*pi))
```

```
def prob_0_hatpsi(_t):
    return abs(hatpsi(_t)[0]**2) / (abs(hatpsi(_t)[0]**2) + abs(hatpsi(_t)
        [1]**2))
```

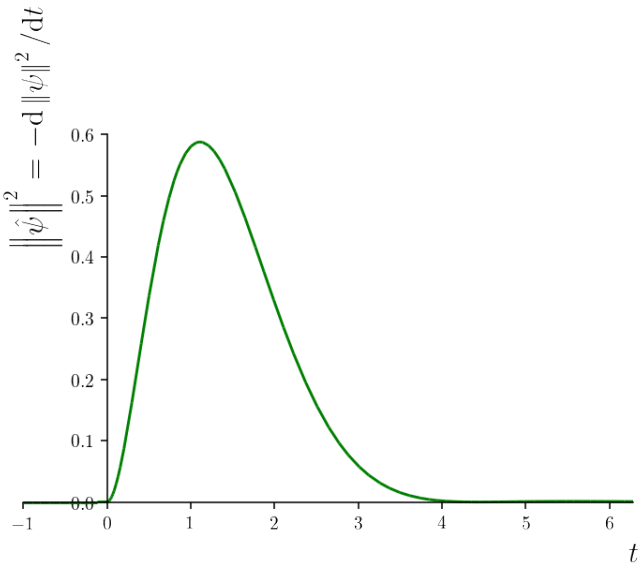

Figure A.13: png

```
def prob_1_hatpsi(_t):
    return abs(hatpsi(_t)[1]**2) / (abs(hatpsi(_t)[0]**2) + abs(hatpsi(_t)
        [1]**2))
```

```
plot( abs(hatpsi(t)[1]**2), (t, -2, 2*pi), line_color='b')
```

```
<sympy.plotting.plot.Plot at 0x7fe25f7797f0>
```

```
def fhatpsi1(_nu):
    return fourier_transform(hatpsi(t)[1], t, _nu)
```

```
simplify(fhatpsi1(nu))
```

$$-\frac{2^{\frac{3}{4}}i}{-4\pi^2\nu^2 + 2\sqrt{2}i\pi\nu + 1}$$

```
plot(abs(fhatpsi1(nu))**2, (nu, -1, 1), line_color='#bbbbbb')
```

```
<sympy.plotting.plot.Plot at 0x7fe25f63ac18>
```

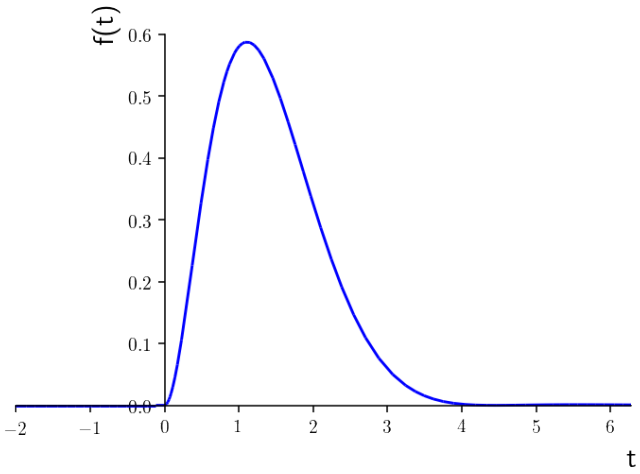

Figure A.14: png

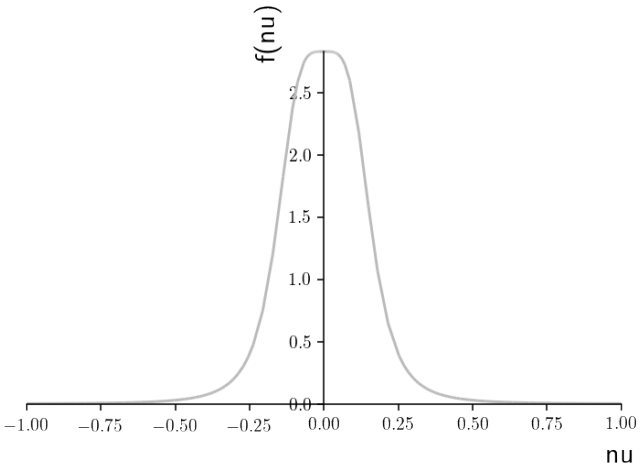

Figure A.15: png

The above Fourier transform is defined in frequency (ν) not angular frequency (ω), therefore needs rescaling.

```
def fhatpsiomega(_omega):
    return fhatpsi1(_omega/(2*pi)) / sqrt((2*pi))
```

```
fhatpsiomega(omega)
```

$$-\frac{\sqrt[4]{2}i}{\sqrt{\pi}\left(-\omega^2+\sqrt{2}i\omega+1\right)} \tag{A.3}$$

```
abs(fhatpsiomega(omega))**2
```

$$-\frac{\sqrt{2}}{\pi\left(-\omega^4-1\right)}$$

```
integrate(abs(fhatpsiomega(omega))**2, (omega, -oo, +oo))
```

$$1$$

```
plot(abs(fhatpsiomega(omega))**2, (omega, -2*pi, 2*pi), line_color='magenta',
     xlabel=r'$\omega$', ylabel=r'$P(\omega)$')
```

```
<sympy.plotting.plot.Plot at 0x7fe25dad3860>
```

```
# graphical comparison with a normalized Gaussian
sigma = 1.0
plot((1/(sqrt(2*pi)*sigma)) * exp(-omega**2/(2*(sigma)**2)), (omega, -2*pi, 2*pi
    ), line_color='magenta')
```

```
<sympy.plotting.plot.Plot at 0x7fe25dae10f0>
```

A.1.1 (Discrete) Page-Wootters model

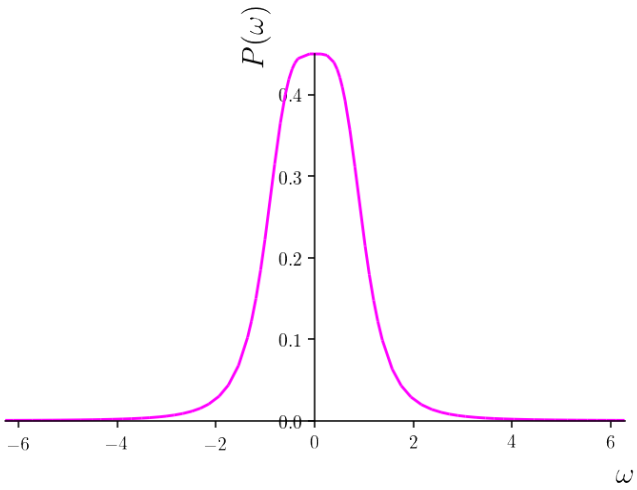

Figure A.16: png

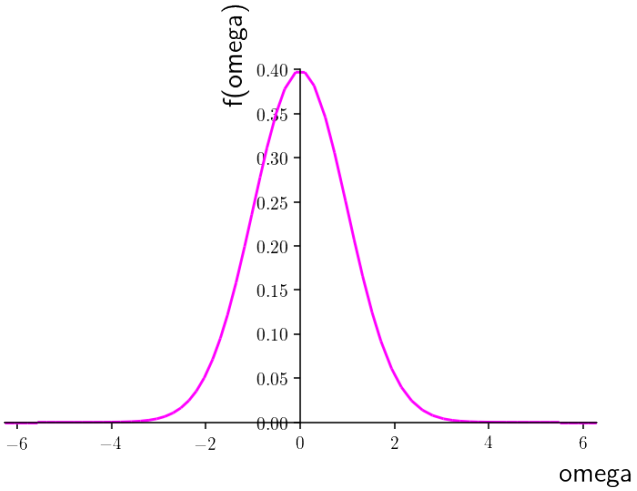

Figure A.17: png

```
from scipy.linalg import dft, norm, expm
from scipy import stats
```

```
T = np.diag(np.arange(0,32)) * np.pi / 16
```

```
# The NumPy Fourier matrix is the conjugate of Mathematica's one,
# hence the trailing .conj()
F = dft(32, scale='sqrtn')
```

```
F_dagger = F.conj().T
```

```
Omega = F_dagger @ T @ F * 16 / np.pi
```

```
oeigenvalues, oeigenvectors = np.linalg.eig(Omega)
```

```
np.round(oeigenvalues)
```

```
array([-0.+0.j, 31.+0.j,  1.+0.j, 30.+0.j,  2.+0.j, 29.-0.j,  3.+0.j,
       28.-0.j,  4.-0.j, 27.-0.j,  5.-0.j, 26.+0.j,  6.-0.j, 25.+0.j,
        7.-0.j,  8.+0.j, 24.+0.j,  9.-0.j, 23.+0.j, 10.+0.j, 22.+0.j,
       11.+0.j, 21.-0.j, 12.+0.j, 13.-0.j, 20.-0.j, 14.-0.j, 15.-0.j,
       19.+0.j, 16.-0.j, 17.+0.j, 18.-0.j])
```

```
H = np.array([
    [0, 1],
    [1, 0]
])
```

```
D = np.array([
    [0, 0],
    [0, np.sqrt(2)]
])
```

```
K = H - 1j*D
```

```
K
```

```
array([[0.+0.j        , 1.+0.j        ],
       [1.+0.j        , 0.-1.41421356j]])
```

```
J = np.kron(Omega, np.eye(2)) + np.kron(np.eye(32), K)
```

```
eigenvalues, eigenvectors = np.linalg.eig(J)
```

```
EnergyCorrectionMatrices = np.zeros((64, 64, 64), np.complex)
for n in range(64):
    #EnergyCorrectionMatrices[n] = np.kron(
    #    expm(-1j*eigenvalues[n]*T),
    #    np.eye(2)
    #)
    EnergyCorrectionMatrices[n] = expm(-1j*eigenvalues[n]*np.kron(T, np.eye(2)))
# TODO: DRY
EnergyCorrectionMatricesT = np.zeros((64, 32, 32), np.complex)
for n in range(64):
    EnergyCorrectionMatricesT[n] = expm(-1j*eigenvalues[n]*T)
```

```
def history_vector(eigenindex):
    # Needs matrix transposition ".T" (different convention as opposed to
        Mathematica)
    eigenvector = eigenvectors.T[eigenindex]
    return EnergyCorrectionMatrices[eigenindex] @ eigenvector

# "unflatten" the history_vector v into a a sequence of qubit component pairs
def reshape(v):
    return np.reshape(v, (-1,2))

# also make the first component real
def normalize_initial(v):
    vout = np.zeros(64, np.complex)
    # A phase factor to make it real
    vout = v * np.exp(-1j * np.angle(v[0]))
    # And a factor to normalize the initial state
    vout = vout / sqrt(
        np.abs(vout[0]**2) + np.abs(vout[1]**2)
    )
    return vout
```

```
# Find the best linear combination to obtain |0> as initial state
def find_best():
    max_prob0 = 0
    max_prob0_i = 0
    max_prob0_j = 0
    for i in range(32):
        for j in range(32):
            qbi = reshape(history_vector(i))
            qbj = reshape(history_vector(j))
            qbit_hist = qbi + qbj
            prob0 = np.abs(qbit_hist[0][0]**2) / (
```

```
                np.abs(qbit_hist[0][0]**2) + np.abs(qbit_hist[0][1]**2)
            )
            if prob0 > max_prob0:
                max_prob0 = prob0
                max_prob0_i = i
                max_prob0_j = j
    print (max_prob0_i, max_prob0_j, max_prob0)
    return (max_prob0_i, max_prob0_j)
```

```
# start with |0> as close as possible
i, j = find_best()
qbhistvec = normalize_initial(history_vector(i) + history_vector(j))
qbhist = reshape(qbhistvec)
```

```
1 21 1.0
```

```
qbhist = qbhist.astype(complex)
```

Consistently with "ordinary QM" findings, the component along |0> stays purely real, and the component along |1> stays purely imaginary.

```
# Fill data for plotting
times = np.arange(0, 2*np.pi, np.pi/16)
norms = np.zeros(32)
probs0 = np.zeros(32)
probs1 = np.zeros(32)
# Components 0 are pure real, components 1 are pure imag
real_parts0 = np.real(qbhist.T[0])
imag_parts1 = np.imag(qbhist.T[1])

for i in range(0, 32):
    norms[i] = (np.abs(qbhist[i][0]**2) + np.abs(qbhist[i][1]**2))
    probs0[i] = np.abs(qbhist[i][0]**2) / (
        np.abs(qbhist[i][0]**2) + np.abs(qbhist[i][1]**2) )
    probs1[i] = np.abs(qbhist[i][1]**2) / (
        np.abs(qbhist[i][0]**2) + np.abs(qbhist[i][1]**2) )
```

```
plt.ylabel(r'$\mathrm{Re}{\;}_{T}\hspace{-.2em}\left\langle␣t␣|␣{}_{S}\hspace
    {-.2em}\left\langle␣0␣|␣\Psi␣\right\rangle\hspace{-.17em}\right\rangle␣$')
plt.xlabel(r'$t$')
plt.plot(times, real_parts0/norms[0], 'rs')
```

```
[<matplotlib.lines.Line2D at 0x7fe25d36e438>]
```

```
plt.ylabel(r'$\mathrm{Im}{\;}_{T}\hspace{-.2em}\left\langle␣t␣|␣{}_{S}\hspace
```

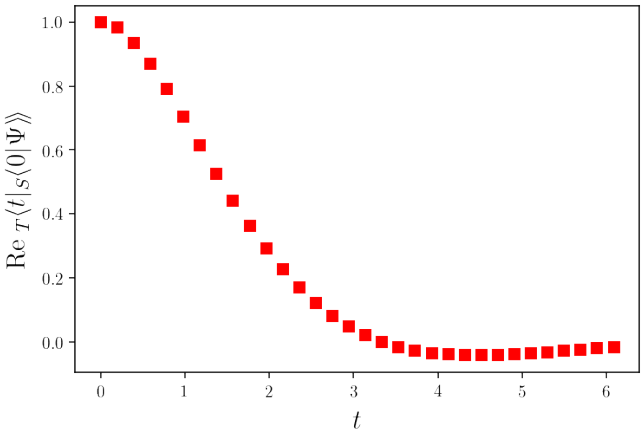

Figure A.18: png

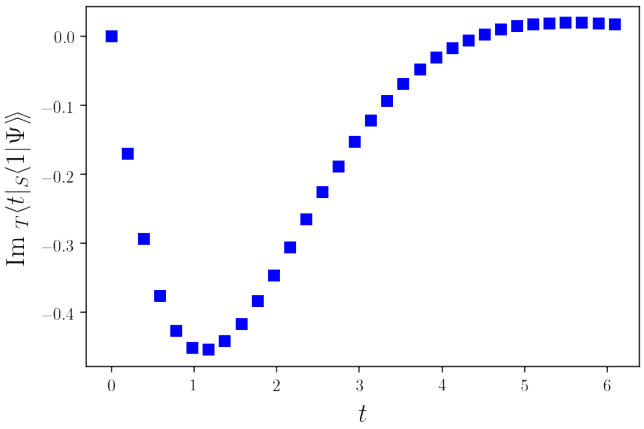

Figure A.19: png

```
    {-.2em}\left\langle␣1␣|␣\Psi␣\right\rangle\hspace{-.17em}\right\rangle␣$')
plt.xlabel(r'$t$')
plt.plot(times, imag_parts1/norms[0], 'bs')
```

```
[<matplotlib.lines.Line2D at 0x7fe25d27da90>]
```

```
plt.plot(times, norms/norms[0], 'g^')
```

```
[<matplotlib.lines.Line2D at 0x7ff538fd94e0>]
```

```
plt.plot(times, probs0, 'rs')
```

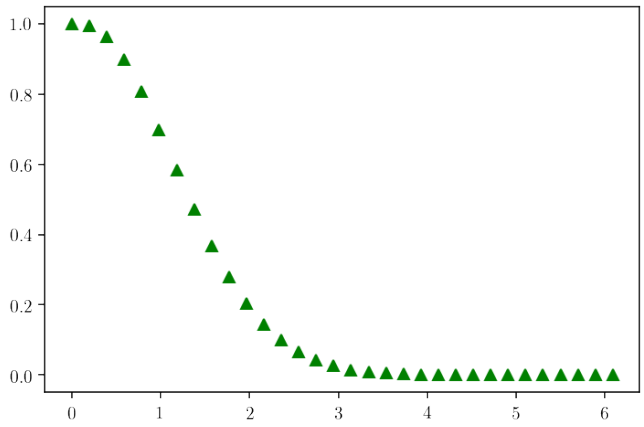

Figure A.20: png

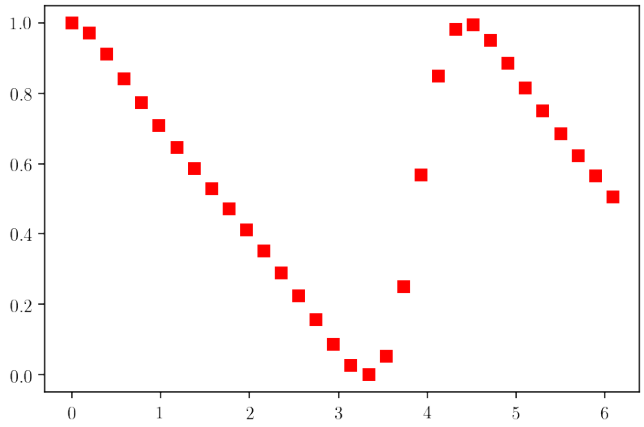

Figure A.21: png

```
[<matplotlib.lines.Line2D at 0x7ff538f341d0>]
```

```
plt.plot(times, probs1, 'bs')
```

```
[<matplotlib.lines.Line2D at 0x7ff538f05f60>]
```

```
fig = plt.figure(figsize=(7,7))

#ax = fig.gca(projection='3d')
ax = fig.add_subplot(111, projection='3d')
ax.view_init(10,-45) # rotate 3d point of view
```

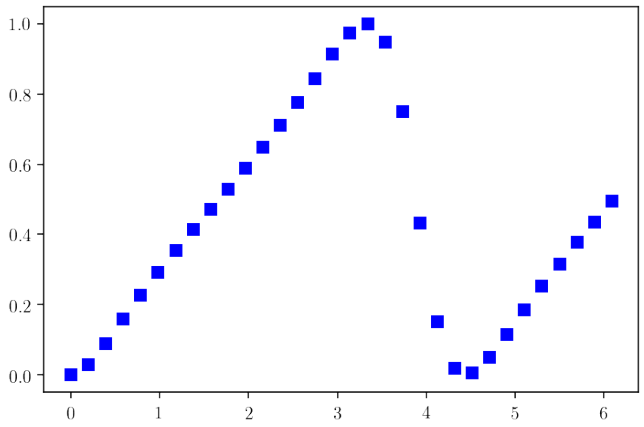

Figure A.22: png

```
ax.scatter(
    real_parts0, imag_parts1, times
)

##ax.legend()

plt.xlabel(r'$\mathrm{Re}\left\langle␣0␣|␣\psi␣\right\rangle$␣(pure␣real)')
plt.ylabel(r'$\mathrm{Im}\left\langle␣1␣|␣\psi␣\right\rangle$␣(pure␣imag)')
ax.set_zlabel('t')
```

```
Text(0.5, 0, 't')
```

A.1.2 Detection event

```
sqr2D = np.array([
    [0, 0],
    [0, 2**(3/4)]
])
```

```
qbhistvec = qbhistvec.astype(np.complex)
```

```
sqr2D = sqr2D.astype(np.complex)
```

```
i, j = find_best()
```

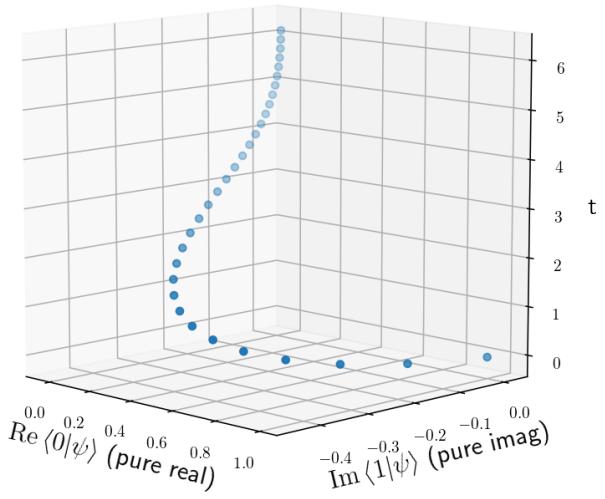

Figure A.23: png

```
    1 21 1.0
```

```
prob_detect_v = \
    (np.kron(EnergyCorrectionMatricesT[i], sqr2D) @ eigenvectors.T[i]) + \
    (np.kron(EnergyCorrectionMatricesT[j], sqr2D) @ eigenvectors.T[j])

# normalize
prob_detect_v = prob_detect_v / norm(prob_detect_v)
```

```
prob_detect_v
```

```
    array([ 0.00000000e+00+0.00000000e+00j,  4.05729696e-14-3.29580328e-14j,
    0.00000000e+00+0.00000000e+00j,  3.36832200e-14+1.26984798e-01j,
    0.00000000e+00+0.00000000e+00j,  3.06907025e-14+2.18919713e-01j,
    0.00000000e+00+0.00000000e+00j,  2.41489201e-14+2.81218057e-01j,
    0.00000000e+00+0.00000000e+00j,  1.80594950e-14+3.18975095e-01j,
    0.00000000e+00+0.00000000e+00j,  1.20048666e-14+3.36874181e-01j,
    0.00000000e+00+0.00000000e+00j,  9.72568181e-15+3.39129482e-01j,
    0.00000000e+00+0.00000000e+00j,  4.71495487e-15+3.29458326e-01j,
    0.00000000e+00+0.00000000e+00j,  7.30731013e-16+3.11076934e-01j,
    0.00000000e+00+0.00000000e+00j, -2.33137990e-15+2.86713992e-01j,
    0.00000000e+00+0.00000000e+00j, -5.20645847e-15+2.58637303e-01j,
    0.00000000e+00+0.00000000e+00j, -4.44962992e-15+2.28689430e-01j,
    0.00000000e+00+0.00000000e+00j, -6.18946566e-15+1.98328975e-01j,
    0.00000000e+00+0.00000000e+00j, -6.10682346e-15+1.68674732e-01j,
    0.00000000e+00+0.00000000e+00j, -4.03206934e-15+1.40550532e-01j,
    0.00000000e+00+0.00000000e+00j, -2.53146101e-15+1.14529119e-01j,
    0.00000000e+00+0.00000000e+00j, -2.58800567e-15+9.09738099e-02j,
```

```
    0.00000000e+00+0.00000000e+00j, -1.97906316e-15+7.00770781e-02j,
    0.00000000e+00+0.00000000e+00j, -1.23528338e-15+5.18955215e-02j,
    0.00000000e+00+0.00000000e+00j, -6.26340868e-16+3.63809059e-02j,
    0.00000000e+00+0.00000000e+00j,  2.17479468e-17+2.34072020e-02j,
    0.00000000e+00+0.00000000e+00j, -1.78333164e-16+1.27936759e-02j,
    0.00000000e+00+0.00000000e+00j,  6.08942511e-17+4.32421818e-03j,
    0.00000000e+00+0.00000000e+00j,  2.30528236e-16-2.23682783e-03j,
    0.00000000e+00+0.00000000e+00j,  6.95934298e-16-7.13201872e-03j,
    0.00000000e+00+0.00000000e+00j,  1.04607624e-15-1.06009991e-02j,
    0.00000000e+00+0.00000000e+00j,  1.52453107e-15-1.28731662e-02j,
    0.00000000e+00+0.00000000e+00j,  1.32662476e-15-1.41624569e-02j,
    0.00000000e+00+0.00000000e+00j,  1.11675707e-15-1.46639178e-02j,
    0.00000000e+00+0.00000000e+00j,  1.08196035e-15-1.45517399e-02j,
    0.00000000e+00+0.00000000e+00j,  7.51391562e-16-1.39784710e-02j,
    0.00000000e+00+0.00000000e+00j,  5.59465932e-16-1.30751439e-02j])
```

```
imag_prob_ampl_detect = np.imag( prob_detect_v.reshape(-1, 2).transpose()[1] )
```

We compare the detection probability amplitude (component along $|1\rangle$, imaginary part) with the same component of the evolution. In other words, we compare a probability amplitude over time with a probability amplitude over space (i.e. being $|1\rangle$ rather than $|0\rangle$).

```
imag_parts1 / imag_prob_ampl_detect
```

```
array([-1.34148089, -1.34148089, -1.34148089, -1.34148089, -1.34148089,
    -1.34148089, -1.34148089, -1.34148089, -1.34148089, -1.34148089,
    -1.34148089, -1.34148089, -1.34148089, -1.34148089, -1.34148089,
    -1.34148089, -1.34148089, -1.34148089, -1.34148089, -1.34148089,
    -1.34148089, -1.34148089, -1.34148089, -1.34148089, -1.34148089,
    -1.34148089, -1.34148089, -1.34148089, -1.34148089, -1.34148089,
    -1.34148089, -1.34148089])
```

which shows that the two vectors are essentially the same, up to a renormalization and change of sign. Of course, probability over time and over space require a different normalization. The two would be conceptually incomparable, but an explanation is in Maccone and Sacha 2020, eq. 6.

```
prob_detect = np.zeros(32)
for t_idx in range(32):
    prob_detect[t_idx] = \
        np.abs(prob_detect_v[2*t_idx])**2 + np.abs(prob_detect_v[2*t_idx+1])**2
```

```
plt.plot(times, prob_detect * 16 / np.pi, 'bs')
```

```
[<matplotlib.lines.Line2D at 0x7ff538e5b550>]
```

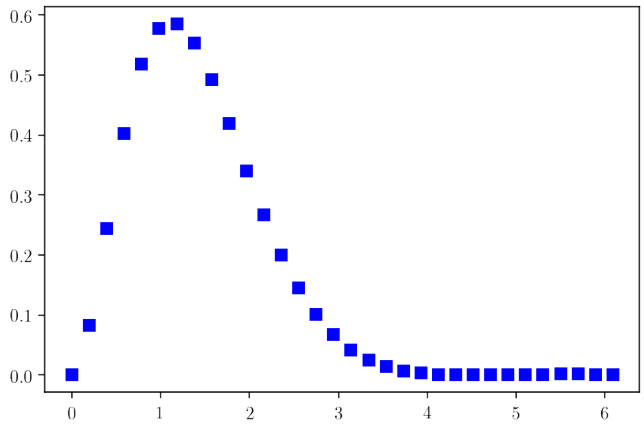

Figure A.24: png

```
detect_fft = \
    np.kron(F, np.eye(2)) @ prob_detect_v
detect_fft = detect_fft / norm(detect_fft)
```

```
prob_detect_fft = np.zeros(32)
for o in range(32):
    prob_detect_fft[o] = \
        np.abs(detect_fft[2*o]**2) + \
        np.abs(detect_fft[2*o + 1]**2)
```

```
# Arrays are "rolled" because the second half
# of the spectrum is identified with
# negative frequencies.
plt.plot(range(-16, 16), np.roll(prob_detect_fft, -16), 'y^')
```

```
[<matplotlib.lines.Line2D at 0x7ff538db5ac8>]
```

Use Scipy routines to compute sigmas

```
xk = range(-16,16)
pk = np.roll(prob_detect_fft, -16)
detect_fft_pdist = stats.rv_discrete(name='prob_detect_fft_minus16', values=(xk,
     pk))
```

```
sigma_omega = detect_fft_pdist.std()
```

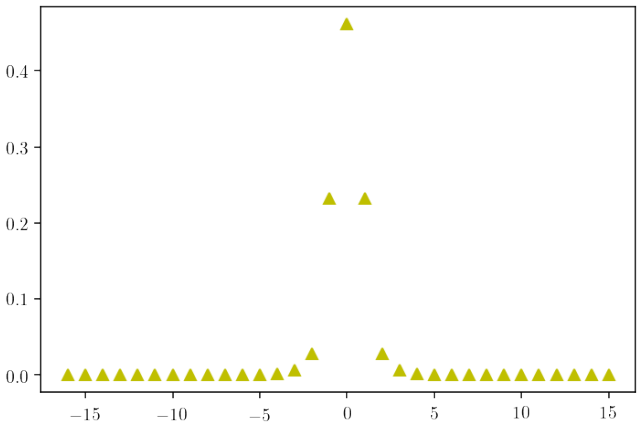

Figure A.25: png

```
xk = times
pk = prob_detect
detect_pdist = stats.rv_discrete(name='prob_detect', values=(xk, pk))
```

```
sigma_t = detect_pdist.std()
```

```
sigma_t * sigma_omega
```

0.7159703170687718

It's still quite a bit more than 0.5, i.e. the minimum uncertainty...

But this is in fact consistent with the paper.

A.1.3 Detector model: 3-level system

Three-level "Λ" system, of interest for * detector models (decay into a metastable state), * STIRAP * EIT

```
import numpy as np

import matplotlib
import matplotlib.pyplot as plt
```

```
from scipy.linalg import expm, norm

# matplotlib.rcParams['text.usetex'] = False

# https://matplotlib.org/gallery/mplot3d/lines3d.html?highlight=parametric
# This import registers the 3D projection, but is otherwise unused.
from mpl_toolkits.mplot3d import Axes3D  # noqa: F401 unused import
```

```
matplotlib.rcParams['font.size'] = 14
matplotlib.rcParams['axes.labelsize'] = 16
matplotlib.rcParams['legend.fontsize'] = 16
matplotlib.rcParams['axes.labelpad']  = 14
```

```
#matplotlib.rcParams
```

```
from IPython.display import display, Latex #, Math
```

```
%%javascript
    // do not generate scroll areas, expand figures instead
    IPython.OutputArea.auto_scroll_threshold = 9999
```

```
<IPython.core.display.Javascript object>
```

```
H = np.array([
    [-2,     0,      32],
    [0,      2,       8],
    [32,     8,       3]
], np.complex_) / 96
```

```
def U(t):
    return expm(-1j*H*t)
```

```
psi_0 = np.array([1, 0, 0], np.complex_)
```

```
def unitary_psi(t):
    return U(t) @ psi_0
```

```
def prob(t):
    probabilities = [0, 0, 0]
    for i in 0, 1, 2:
        probabilities[i] = norm(unitary_psi(t)[i])**2
    return probabilities
```

```
TMIN, TMAX, TMAX_EXTENDED = 0, 40, 150
TMIN_N, TMAX_N = float(TMIN), float(TMAX)
```

```
NPLOTPOINTS = 3200
```

```
times = np.linspace(TMIN_N, TMAX_N, num=NPLOTPOINTS)
times_extended = np.linspace(TMIN_N, TMAX_EXTENDED, num=NPLOTPOINTS)
```

```
probs = [None, None, None]
for i in 0, 1, 2:
    probs[i] = np.fromiter((prob(t)[i] for t in times), np.float)
#     fig, ax = plt.subplots(figsize=(12, 6*np.max(probs[i])))
#     ax.plot(times, probs[i])
#     plt.show()
```

```
# Avoid *tiny* negative numbers, just out of numeric approximation, which will
    cause problems later,
# when their value is in fact just zero.
probs = np.round(probs, decimals=12)
```

```
UNISYM = {
    'psi': u'\u03C8',
    '^2' : u'\u00B2'
}
PROB_LABELS        = ['', '', '']
PROB_AMP_LABELS    = ['', '', '']
PROB_AMP_LABELS_PW = ['', '', '']

for i in 0, 1, 2:
    PROB_AMP_LABELS[i] = '<' + str(i) + '|' + UNISYM['psi'] + '(t)' + '>'
    PROB_LABELS[i]     = '|' + PROB_AMP_LABELS[i] + '|' + UNISYM['^2']

    PROB_AMP_LABELS_PW[i] = '<t|\u2297<%d|\u03A8>>' % i
```

https://matplotlib.org/gallery/lines_bars_and_markers/stackplot_demo.html#sphx-glr-gallery-lines-bars-and-markers-stackplot-demo-py

```
prob_stack = np.vstack(probs)
```

```
colors  =  ['#d44', '#4d4', '#44d']
colors  =  ['r', 'g', 'b']
hatches =  ['\\\\\\', '/////////', '...']

linewidths =  [1, 1, 1]
```

```
labels      =  PROB_LABELS

fig, ax = plt.subplots(figsize=(12, 6))

stacks = ax.stackplot(times, (probs[0], probs[1], probs[2]))
ax.set_xlabel('t')

for stack, hatch, color, label, linewidth in zip(stacks, hatches, colors, labels
    , linewidths):
    stack.set_facecolor('w')
    stack.set_edgecolor(color)
    stack.set_label(label)
    stack.set_hatch(hatch)
    stack.set_linewidth(linewidth)

ax.plot(times, probs[0] + probs[1] + probs[2], c='m', label='||\u03C8(t)||\u00B2
    ', linewidth=1.5)

desired_order    = [0, 3, 2, 1]
_handles, _labels = ax.get_legend_handles_labels()
handles          = [ _handles[i] for i in desired_order ]
labels           = [ _labels[i]  for i in desired_order ]
ax.legend(handles, labels, loc='center␣right', framealpha=1)

plt.savefig('_img/detect3.021/hermitian3color.pdf', bbox_inches='tight',
    pad_inches=0)
plt.show()
```

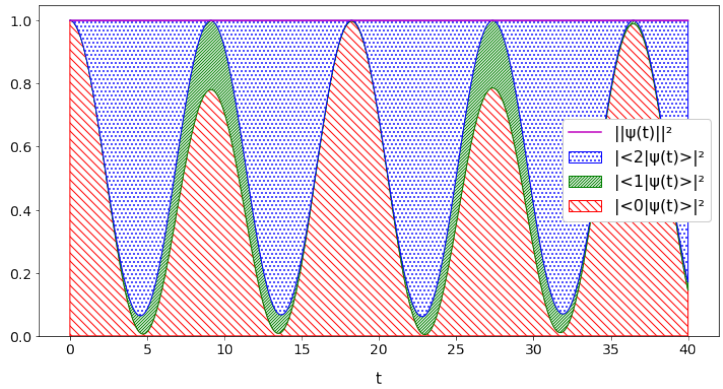


```
rgbs = []
for i in range(NPLOTPOINTS):
    rgbs.append(
        (
            probs[0][i],
            probs[1][i],
            probs[2][i]
```

```
        )
    )
```

```
fig, ax = plt.subplots(figsize=(12,6))
ax.set_xlabel('t')
ax.scatter(times, np.zeros(NPLOTPOINTS)-0.1,
            c=rgbs, marker='|', s=400)

# "virtual", don't really want to show, only for legend
_c = ['r', '#0a0', 'b']
for i in 0, 1, 2:
    ax.plot(
        times, probs[i],
        c=_c[i],
        linewidth=2,
    )

ax.legend(
    PROB_LABELS,
    loc='upper right'
)

plt.savefig('_img/detect3.021/hermitian3lines.pdf', bbox_inches='tight',
    pad_inches=0)
```

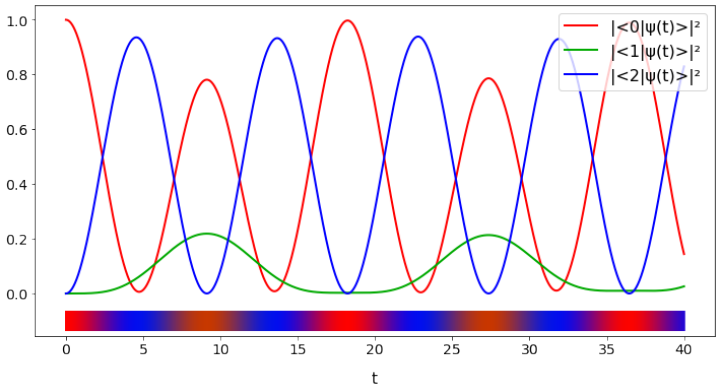


```
unitary_psis = [np.zeros(NPLOTPOINTS)] * 3
for i in 0, 1, 2:
    unitary_psis[i] = np.fromiter( (unitary_psi(t)[i] for t in times), np.
        complex )
```

```
# 3D parametric plot
for (vertical_angle,horizontal_angle,height,width,lloc,view) in (10,-70,12,12,'
    center left','side'), (80,-120,12,12,'right','top'):
    # fig = plt.figure(figsize=(w5dth, height), dpi=250)2
```

```
    fig = plt.figure(figsize=(width, height))

    ax = fig.gca(projection='3d')

    ax.view_init(vertical_angle, horizontal_angle) # rotate 3d point of view

    ax.set_xlabel('Re␣<0,1,2|\u03C8>')
    ax.set_ylabel('Im␣<0,1,2|\u03C8>')
    ax.set_zlabel('t')

    ax.scatter(
        np.zeros(NPLOTPOINTS, dtype=np.float),
        np.zeros(NPLOTPOINTS, dtype=np.float),
        times,
        c = rgbs,
        s = 24
    )
    for i in 0, 1, 2:
        ax.plot(
            np.real(unitary_psis[i]),
            np.imag(unitary_psis[i]),
            times,
            label = PROB_AMP_LABELS[i],
            #depthshade=False,
            c = _c[i]
        )
        ax.legend(loc=lloc)
    plt.savefig('_img/detect3.021/hermitianSpaceTime_%s.pdf' % view, bbox_inches
        =0, pad_inches=0)
```

A.1.4 Complex potential (detection by absorption)

```
H_n = H
```

```
GAMMA = 0.1
```

```
def D(_gamma=GAMMA):
    # no 1/2 factor, absorbed in the _gamma in the matrix here
    return np.array([
        [0, 0,      0],
        [0, 0,      0],
        [0, 0, _gamma]
    ], dtype=np.complex)
```

```
D()
```

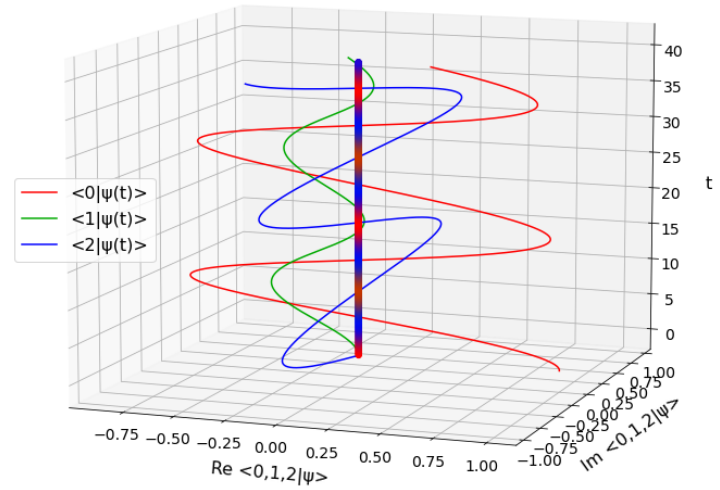

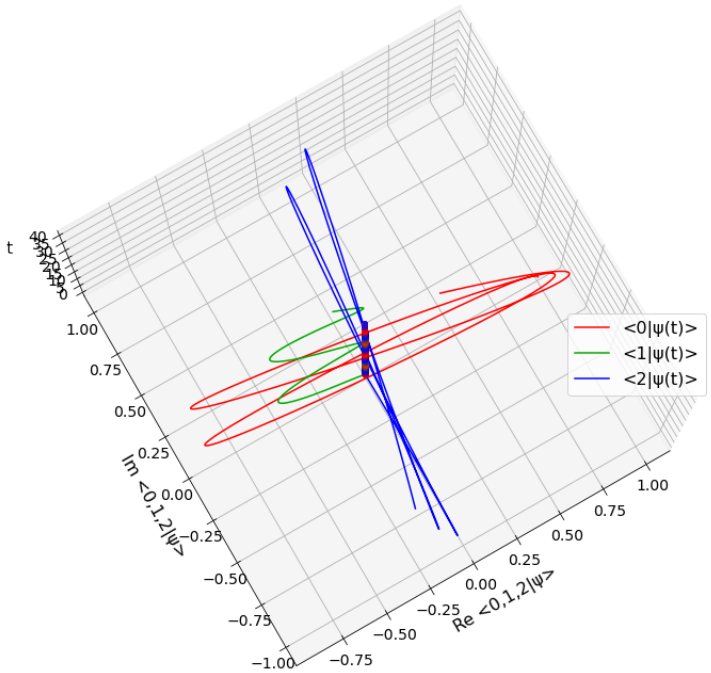


```
array([[0. +0.j, 0. +0.j, 0. +0.j],
```

```
       [0. +0.j, 0. +0.j, 0. +0.j],
       [0. +0.j, 0. +0.j, 0.1+0.j]])
```

```
def K(_gamma=GAMMA):
    return H_n - 1j*D(_gamma)
```

```
K()
```

```
array([[-0.02083333+0.j ,  0.        +0.j ,  0.33333333+0.j ],
       [ 0.        +0.j ,  0.02083333+0.j ,  0.08333333+0.j ],
       [ 0.33333333+0.j ,  0.08333333+0.j ,  0.03125   -0.1j]])
```

```
def B(_t, _gamma=GAMMA):
    return expm(-1j*K(_gamma)*_t)
```

```
B(0)
```

```
array([[1.+0.j, 0.+0.j, 0.+0.j],
       [0.+0.j, 1.+0.j, 0.+0.j],
       [0.+0.j, 0.+0.j, 1.+0.j]])
```

```
def non_unitary_psi(_t, _gamma=GAMMA):
    return B(_t, _gamma) @ psi_0
```

```
evolution = np.zeros((3, NPLOTPOINTS), dtype=np.complex)
evolution_extended = np.zeros((3, NPLOTPOINTS), dtype=np.complex)

for i in 0, 1, 2:
    _iter = (non_unitary_psi(_t)[i] for _t in times)
    _iter_extended = (non_unitary_psi(_t)[i] for _t in times_extended)

    evolution[i] = np.fromiter(_iter, np.complex)
    evolution_extended[i] = np.fromiter(_iter_extended, np.complex)

_iter_norm = (norm(non_unitary_psi(_t)) for _t in times)
norms = np.fromiter(_iter_norm, np.float)

_iter_norm_extended = (norm(non_unitary_psi(_t)) for _t in times_extended)
norms_extended = np.fromiter(_iter_norm_extended, np.float)
```

```
colors  =  ['#f66', '#6d6', '#88f']
colors  =  ['r', 'g', 'b']
hatches =  ['\\\\\\', '////////', '...']
labels     =  PROB_LABELS
```

```
fig, ax = plt.subplots(figsize=(12, 8))

ax.plot(times, np.ones(NPLOTPOINTS), c='grey', linestyle='dashed', label='
    Initial␣norm', linewidth=2.5)

ax.plot(times, norms**2, c='m', linewidth=1.5, label='||\u03C8(t)||\u00B2')

stacks = ax.stackplot(times, (
    np.abs(evolution[0])**2,
    np.abs(evolution[1])**2,
    np.abs(evolution[2])**2
))

ax.set_xlabel('t')

for stack, hatch, color, label in zip(stacks, hatches, colors, labels):
    stack.set_linewidth(.5)
    stack.set_facecolor('w')
    stack.set_edgecolor(color)
    stack.set_label(label)
    stack.set_hatch(hatch)

handles, labels = ax.get_legend_handles_labels()
desired_order = [0, 1, 4, 3, 2]
handles = [ handles[i] for i in desired_order ]
labels  = [  labels[i] for i in desired_order ]
ax.legend(handles, labels, loc='center')

plt.savefig('_img/detect3.021/loss3color.pdf', bbox_inches='tight', pad_inches
    =0)
plt.show()
```

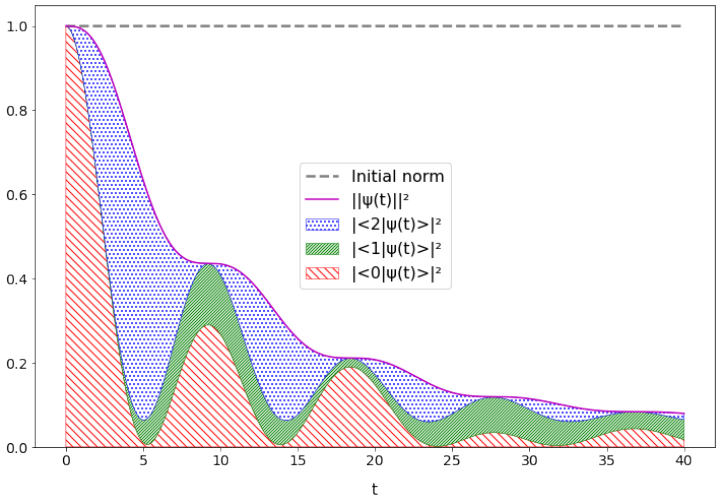

```
# loss of normalization, or integral of antiderivative...
bayesian_denominator_nonpw = 1 - norm(evolution.T[NPLOTPOINTS-1])**2  # TODO!
    explain/replace
```

```
fig, ax = plt.subplots(figsize=(12, 8))
ax.set_xlabel('t')
ax.set_ylabel('Detection␣probability␣density␣␣=␣␣-␣d||\u03C8(t)||\u00B2␣/␣dt')
ax.plot(times, -np.gradient(norms**2, times), c='y', linewidth=3)
plt.savefig('_img/detect3.021/loss.pdf', bbox_inches='tight', pad_inches=0)
```

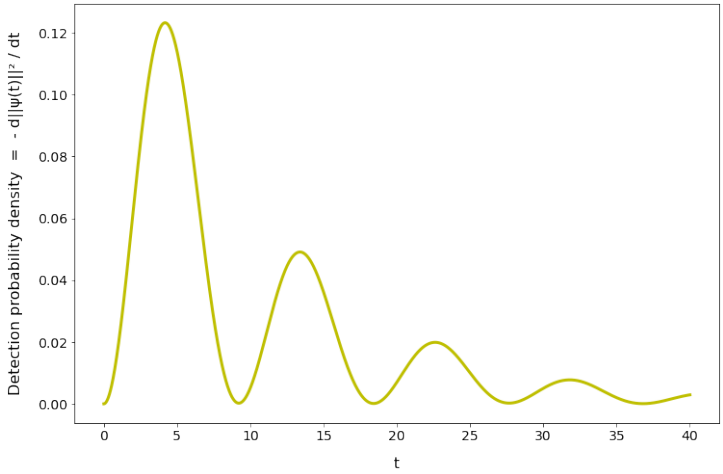


```
labels = PROB_LABELS

colors  =  ['r', 'g', '#ccf']
hatches =  ['\\\\\\\\', '////////', '.....']

fig, ax = plt.subplots(figsize=(14, 7))

ax.set_xlabel('t')

ax.plot(times_extended, np.ones(NPLOTPOINTS), c='grey', linestyle='dashed',
    label='Initial␣norm')

ax.plot(times_extended, norms_extended**2, c='m', linewidth=1, label='||\u03C8(t
    )||\u00B2')

stacks = ax.stackplot(times_extended, (
    np.abs(evolution_extended[0])**2,
    np.abs(evolution_extended[1])**2,
    np.abs(evolution_extended[2])**2
))

for stack, hatch, color, label in zip(stacks, hatches, colors, labels):
```

```
    stack.set_linewidth(1.25)
    stack.set_facecolor('w')
    stack.set_edgecolor(color)
    stack.set_label(label)
    stack.set_hatch(hatch)

handles, labels = ax.get_legend_handles_labels()
desired_order = [0, 1, 4, 3, 2]
handles = [ handles[i] for i in desired_order ]
labels  = [  labels[i] for i in desired_order ]
ax.legend(handles, labels, loc='center')

plt.savefig('_img/detect3.021/loss3color_ext.pdf', bbox_inches='tight',
    pad_inches=0)
plt.show()
```

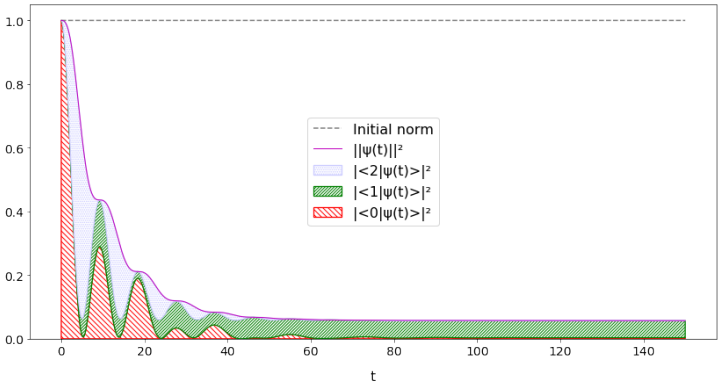

"Asymptotic" fidelity for $|1\rangle$

```
times_extended[-1]
```

```
150.0
```

```
norms_extended[-1]**2
```

```
0.05684539507975811
```

```
(np.abs(evolution_extended[1])**2)[-1] / norms_extended[-1]**2
```

```
0.9414855990054901
```

Detection probability

```
_detection_prob = -np.gradient(norms_extended**2, times_extended)
fig, ax = plt.subplots(figsize=(14, 7))
ax.set_xlabel('t')
ax.set_ylabel('Detection␣probability␣density␣␣=␣␣-␣d||\u03C8(t)||\u00B2␣/␣dt')
ax.plot(times_extended, _detection_prob, c='y', linewidth=3)
plt.savefig('_img/detect3.021/loss_ext.pdf', bbox_inches='tight', pad_inches=0)
```

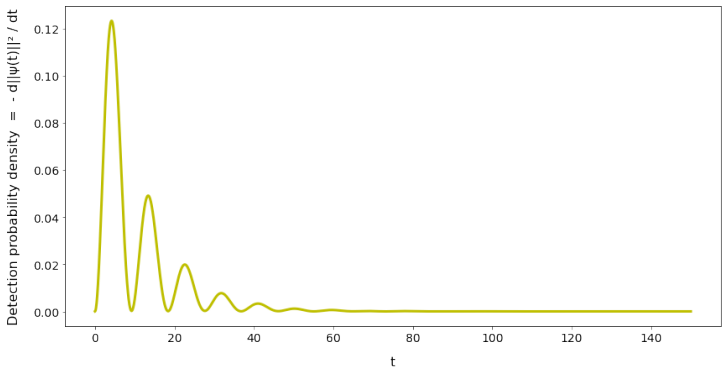

"3D"

```
# 3D parametric plot

for (vertical_angle,horizontal_angle,height,width,lloc,view) in (15,-80,15,15,'
    center␣left','side'), (90, -80, 15, 15,'center␣left','top'):
    fig = plt.figure(figsize=(width, height))

    ax = fig.gca(projection='3d')

    ax.view_init(vertical_angle, horizontal_angle) # rotate 3d point of view

    ax.set_xlabel('Re␣<0,1,2|\u03C8>')
    ax.set_ylabel('Im␣<0,1,2|\u03C8>')
    ax.set_zlabel('t')

    ax.scatter(
        np.zeros(NPLOTPOINTS, dtype=np.float),
        np.zeros(NPLOTPOINTS, dtype=np.float),
        times,

        c = np.array([
            np.abs(evolution[0])**2,
            np.abs(evolution[1])**2,
            np.abs(evolution[2])**2
        ]).T,
        s = 24,
```

```
        marker='o'
    )
    _c = ['r', 'g', 'b']

    for i in 0, 1, 2:
        ax.plot(
            np.real(evolution[i]),
            np.imag(evolution[i]),
            times,
            #depthshade=False,
            c = _c[i],
            linewidth=2,
            label = PROB_AMP_LABELS[i]
        )
        ax.legend(loc=lloc)
    plt.savefig('_img/detect3.021/NonHermitianSpaceTime_%s.pdf' % view,
        bbox_inches='tight', pad_inches=0)
```

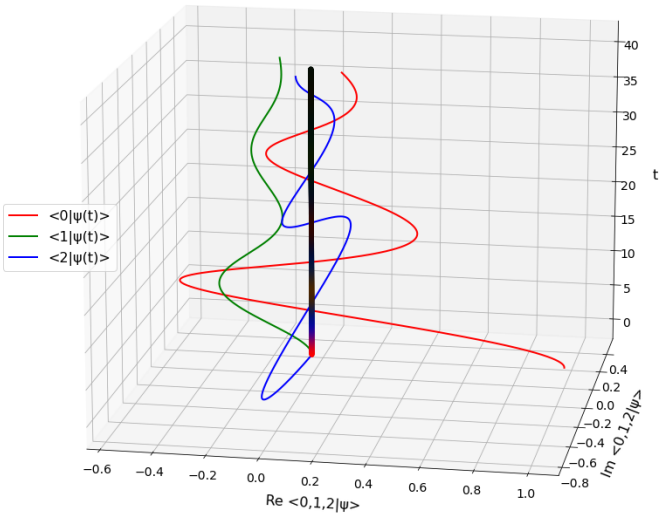

A.1.5 Page-Wootters

```
from scipy.linalg import dft, norm, expm, det, inv
```

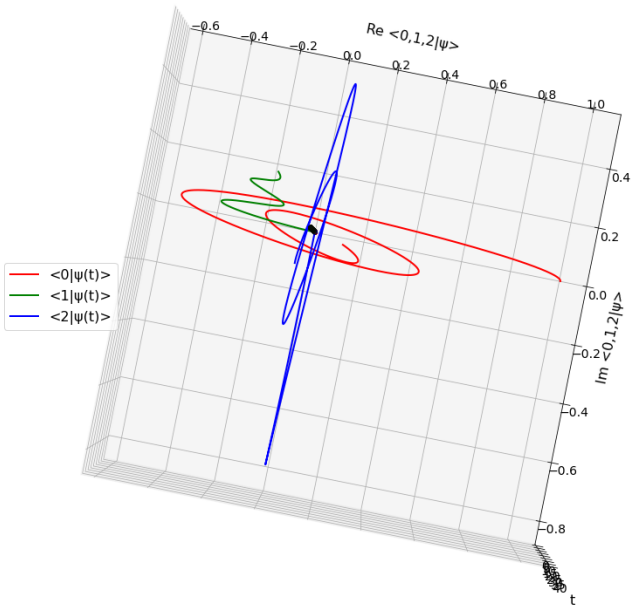


```
# Dimension of the system, or the spatial/"ordinary" Hilbert space
NS = 3
# Number of levels of the clock aka dimension of Time Hilbert space
NT = 60
# "Period"
DT = TMAX_N  # assume we start with time 0

T = DT * np.diag(np.arange(NT)) / NT
```

```
F = dft(NT, scale='sqrtn')
F_dagger = F.conj().T
```

```
Omega = F_dagger @ T @ F * 2*np.pi * NT / DT**2
```

```
J = np.kron(Omega, np.eye(3)) + np.kron(np.eye(NT), K())
```

```
eigenvalues, eigenvectors = np.linalg.eig(J)
```

```
eigenvectors = eigenvectors.T
```

```
eigenvectors_normalized_in_S = np.empty((NT*NS, NT*NS), dtype=complex)

for i in range(NT*NS):
    eigenvectors_normalized_in_S[i] = eigenvectors[i] / norm(eigenvectors[i
        ][:3])
```

```
histories = np.empty((NT*NS, NT*NS), dtype=complex)

for i in range(NT*NS):
    histories[i] = \
        expm(np.kron( -1j*T*eigenvalues[i], np.eye(NS) )) @ \
        eigenvectors_normalized_in_S[i]
```

```
# Only implemented for NS=3
def find_linear_independent_initial(eigenvectors=eigenvectors_normalized_in_S):
    best_i, best_j, best_k = -1, -1, -1
    best_det = 0
    best_states = np.array([
        [0, 0, 0],
        [0, 0, 0],
        [0, 0, 0]
    ])
    for i in range(NT*NS):
        for j in range(i, NT*NS):
            for k in range(j, NT*NS):
                # this normalization is not necessary if default
                # eigenvectors=eigenvectors_normalized_in_S
                # is given
                si = eigenvectors[i][:3]
                si = si / norm(si)
                sj = eigenvectors[j][:3]
                sj = sj / norm(sj)
                sk = eigenvectors[k][:3]
                sk = sk / norm(sk)
                states = np.array([
                    si,
                    sj,
                    sk
                ])
                _det = det(states)
                if abs(abs(_det)-1.0) < abs(abs(best_det) - 1.0):
                    best_det = _det
                    best_i, best_j, best_k = i, j, k
                    best_states = states
                if abs(abs(_det)-1.0) == 0:
                    return best_i, best_j, best_k, best_det
        percent = int(100 * (i + 1) / (NT*NS))
        print(
            str(percent) + '%␣scanned' + "\tabs(best_det)␣=␣" + str(abs(best_det
```

```
                )),
            end="\r", flush=True)

    return best_i, best_j, best_k, best_det
```

```
best_i, best_j, best_k, best_det = find_linear_independent_initial()
```

```
100% scanned    abs(best_det) = 0.9893579012772128
```

```
states = np.array([
    histories[best_i][:NS],
    histories[best_j][:NS],
    histories[best_k][:NS]
])
#assert(np.round(abs(det(states)), decimals=2) == 1.0)
# Find what linear combination would bring to the desired initial state psi_0_n
coeffs = inv(states.T) @ psi_0
```

```
history = coeffs.dot(np.array([
    histories[best_i],
    histories[best_j],
    histories[best_k]
]))
```

```
# 3D parametric plot

times_discrete = np.diag(T)

psi = history.reshape((-1,NS)).T

for (vertical_angle,horizontal_angle,height,width,lloc,view) in ((10,-120,15,25,
    'center␣right','side'), (80,-100,15,25,'center␣right','top')):
    fig = plt.figure(figsize=(width, height))


    ax = fig.gca(projection='3d')

    ax.view_init(vertical_angle, horizontal_angle) # rotate 3d point of view

    ax.set_xlabel('Re␣<t|\u2297<0,1,2|\u03A8>>')
    ax.set_ylabel('Im␣<t|\u2297<0,1,2|\u03A8>>')
    ax.set_zlabel('t')

    ax.scatter(
        np.zeros(NT, dtype=np.float),
        np.zeros(NT, dtype=np.float),
        times_discrete,
```

```
        c = np.round((abs(psi.T)**2), 8), # rounding, to avoid number
            instability causing out-of-range rgb vals
        s = 75,
        marker='o'
    )
    _c = ['r', 'g', 'b']

    for i in range(NS):
        ax.scatter(
            np.real(
                psi[i]
            ),
            np.imag(
                psi[i]
            ),
            times_discrete,

            marker = 's',
            #depthshade=False,
            #s = abs(_psi[i]**2)*60,
            s = 60,
            edgecolor = _c[i],
            facecolor = (0, 0, 0, 0),
            linewidth = 1,

            label = PROB_AMP_LABELS_PW[i]
        )
    ax.legend(loc=lloc)
    plt.savefig('_img/detect3.021/PWSpaceTime_%s.pdf' % view, bbox_inches='tight
        ', pad_inches=0)
```

```
norm(psi)**2
```

```
18.550562258122728
```

```
norm(psi)
```

```
4.307036366008851
```

Overlapping PW and QM continuous

```
# 3D parametric plot

times_discrete = np.diag(T)
```

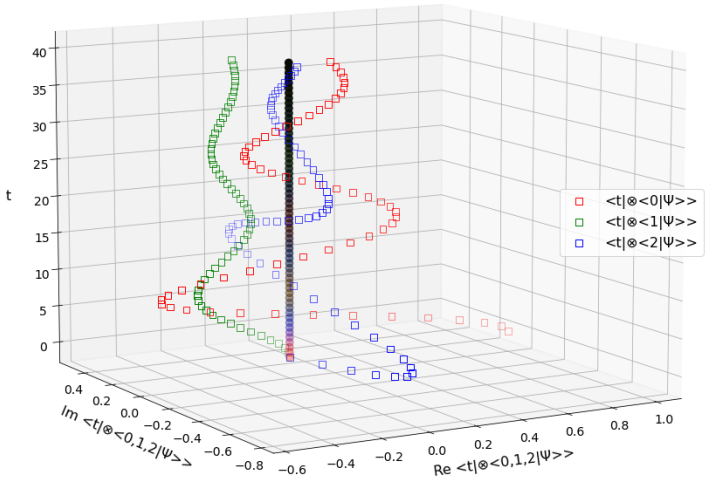
t
Im <t|⊗<0,1,2|Ψ>>
Re <t|⊗<0,1,2|Ψ>>
<t|⊗<0|Ψ>>
<t|⊗<1|Ψ>>
<t|⊗<2|Ψ>>

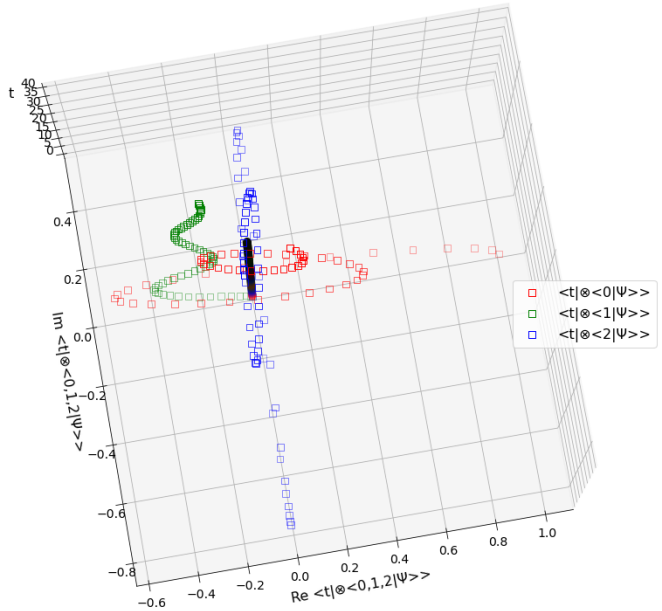
t
Im <t|⊗<0,1,2|Ψ>>
Re <t|⊗<0,1,2|Ψ>>
<t|⊗<0|Ψ>>
<t|⊗<1|Ψ>>
<t|⊗<2|Ψ>>

```
psi = history.reshape((-1,NS)).T

for (vertical_angle,horizontal_angle,height,width,view) in (15,-80,15,15,'side')
    , (90,-80,15,15,'top'):
    # fig = plt.figure(figsize=(width, height), dpi=300)
    fig = plt.figure(figsize=(width, height))

    ax = fig.gca(projection='3d')

    ax.view_init(vertical_angle, horizontal_angle) # rotate 3d point of view

    ax.set_xlabel('Re')
    ax.set_ylabel('Im')
    ax.set_zlabel('t')

    ax.scatter(
        np.zeros(NT, dtype=np.float),
        np.zeros(NT, dtype=np.float),
        times_discrete,

        c = np.round((abs(psi.T)**2), 8), # rounding, to prevent numeric
            instability from causing out-of-range RGB values
        s = 75,
        marker='o'
    )
    _c = ['r', 'g', 'b']
    for i in range(NS):
        ax.scatter(
            np.real(
                psi[i]
            ),
            np.imag(
                psi[i]
            ),
            times_discrete,

            marker = 's',
            #depthshade=False,
            #s = abs(_psi[i]**2)*60,
            s = 80,
            edgecolor = _c[i],
            facecolor = (0, 0, 0, 0),
            linewidth = 0.8,
            label = PROB_AMP_LABELS_PW[i]
        )

    # QM continuous
    for i in 0, 1, 2:
        ax.plot(
            np.real(evolution[i]),
```

```
            np.imag(evolution[i]),
            times,
            #depthshade=False,
            c = _c[i],
            linewidth=1.5,
            label = PROB_AMP_LABELS[i]
        )
    ax.legend(loc='center␣left')
    plt.savefig('_img/detect3.021/PWSpaceTimeFit_%s.pdf' % view, bbox_inches='
        tight', pad_inches=0)
```

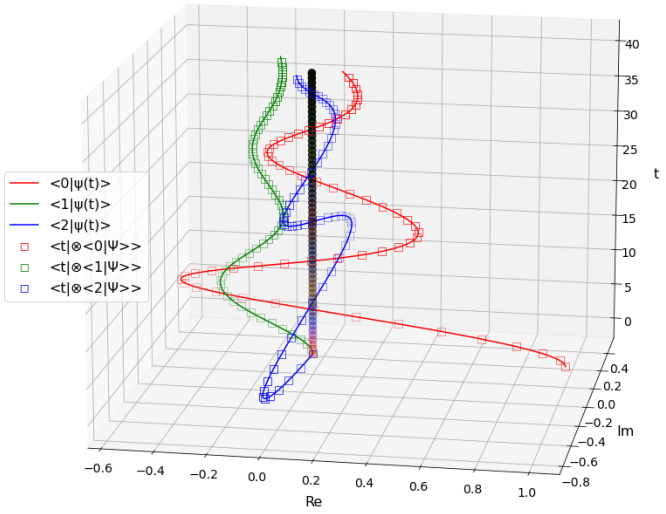

A.1.6 TOA prob as in Maccone/Sacha arXiv:1810.12869

Adapted from § "Time of arbitrary event".

```
def t_eigenstate(n):
    v = np.zeros(NT, dtype=np.complex)
    v[n] = 1
    return v
```

```
arrived_state = np.array([0, 0, 1])
```

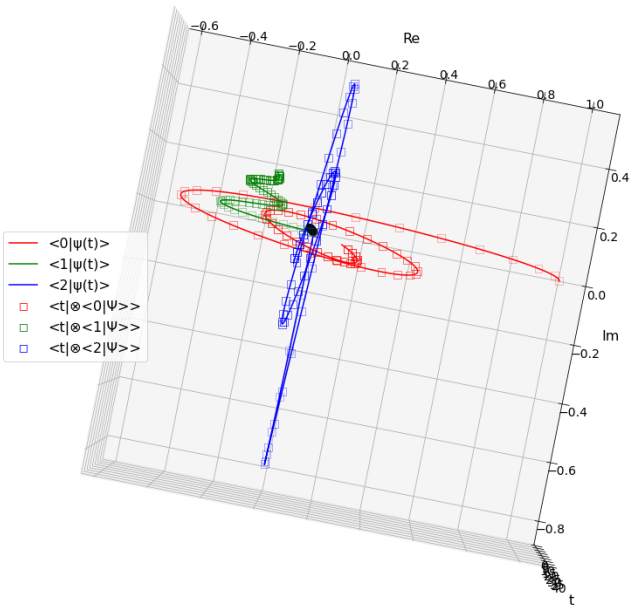


```
def tn_ox_arrived(n):
    return np.kron(t_eigenstate(n), arrived_state)
```

```
history_normalized = history / norm(history)  ## normalized in H_T \otimes H_S
```

```
def joint_prob(n):
    return np.abs(tn_ox_arrived(n) @ history_normalized)**2
```

```
X = np.arange(NT)

iterable = (joint_prob(n) for n in X)
Y = np.fromiter(iterable, float)
```

```
dT  = DT / (NT)
```

```
# A "time bin"
X = X * dT # real time
Y = Y / dT # probability _density_
```

```
bayes_denominator = np.sum(Y * dT)
```

```
Y = Y / bayes_denominator
```

```
# fig, ax = plt.subplots(figsize=(12, 8), dpi=300)
fig, ax = plt.subplots(figsize=(12, 8))
ax.set_xlabel('t')
ax.set_ylabel('Detection probability density')
ax.plot(X, Y, 'bs', label='Page-Wootters (Maccone / Sacha -- Bayesian / conditional)')
ax.plot(times, -np.gradient(norms**2, times) / bayesian_denominator_nonpw,
        c='y', linewidth=2, label='Detector model (normalization loss)')
ax.legend()
plt.savefig('_img/detect3.021/conditionalProbFit.pdf', bbox_inches='tight', pad_inches=0)
plt.show()
```

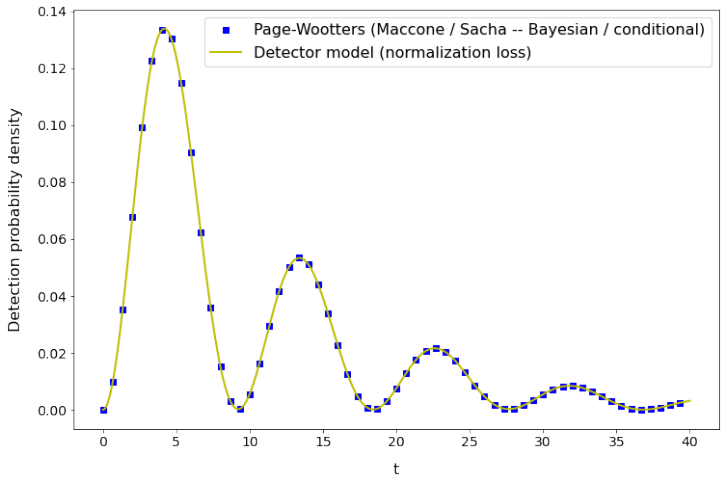


```
nonpw_probs = -np.gradient(norms**2, times) / bayesian_denominator_nonpw
```

```
np.sum(nonpw_probs*times[1])
```

```
1.0000197507624184
```

```
np.sum(Y*dT)
```

```
1.0
```

Appendix B

Mathematica notebooks[1]

Preliminary note

Here we just report the necessary Mathematica commands and suppress some intermediate outputs, using `TeXForm[]` otherwise, in lack of a viable export functionality available for whole notebooks.

Minimal edit on expressions has been performed for formatting purposes only.

B.1 Page–Wootters model: `NN`-level clock + 2-level system[2]

```
NN := 32
```

```
T := DiagonalMatrix[Range[0,NN-1]] * \[Pi] / 16
```

```
F := FourierMatrix[NN]
```

[1] Ref.: Wolfram Research, Inc. 2018.

[2] Here the symbol `NN` is used instead of `N` to avoid confusion with Mathematica's *function* `N[]` which is used to convert symbolic expressions to their numerical value.

For simplicity, $\hbar = \omega = 1$.

Also, note that Mathematica uses a different sign convention[3] than Python[4], hence F and $F^\dagger$ have a swapped role in the two platforms:

```
\[CapitalOmega] := F.T.F\[ConjugateTranspose]  * 16 / \[Pi]
```

Hamiltonian in "ordinary" space

```
Hs := \[ImaginaryI]{{0, 1}, {-1, 0}}
```

```
MatrixForm[Hs]
```

$$\begin{pmatrix} 0 & i \\ -i & 0 \end{pmatrix}$$

Matrix representation of Giovannetti et al. 2015, eq. 1. We turn it into numeric (`N[ ]`) as treating it symbolically onward would be unfeasible:

```
J := N[KroneckerProduct[\[CapitalOmega],IdentityMatrix[2]] + KroneckerProduct[
    IdentityMatrix[NN],Hs]]
```

```
Chop[Eigenvalues[J]]
```

```
Eigenvalues[J][[40]]

Out[ ] = 12.

Eigenvalues[J][[41]]

Out[ ] = 11.

chosenEigenvector := Eigenvectors[J][[ 40]]
```

[3] See https://reference.wolfram.com/language/ref/FourierMatrix.html

[4] See https://github.com/sympy/sympy/blob/77f1d79c705da5e9b3dee456a14b1b4e92dd620c/sympy/matrices/expressions/fourier.py#L52

```
chosenEigenvectorB := Eigenvectors[J][[41]]

Normalization := Sqrt[Abs[chosenEigenvector[[1]]^2] + Abs[chosenEigenvector
    [[2]]^2] ]

NormalizationB := Sqrt[Abs[chosenEigenvectorB[[1]]^2] + Abs[chosenEigenvectorB
    [[2]]^2] ]

chosenEigenvectorNormalized  := chosenEigenvector / Normalization

chosenEigenvectorNormalizedB := chosenEigenvectorB / NormalizationB

probability := Abs[chosenEigenvectorNormalized ^2]

probabilityB := Abs[chosenEigenvectorNormalizedB^2]

ListPlot[probability,
  GridLines ->{Range[0,NN*2, 2], Range[0, 1, 0.1]},
  AxesLabel->{n, "P(0), P(1)"},
  LabelStyle->Directive[16],
  PlotMarkers->{Automatic, 16},
  ImageSize->1024
```

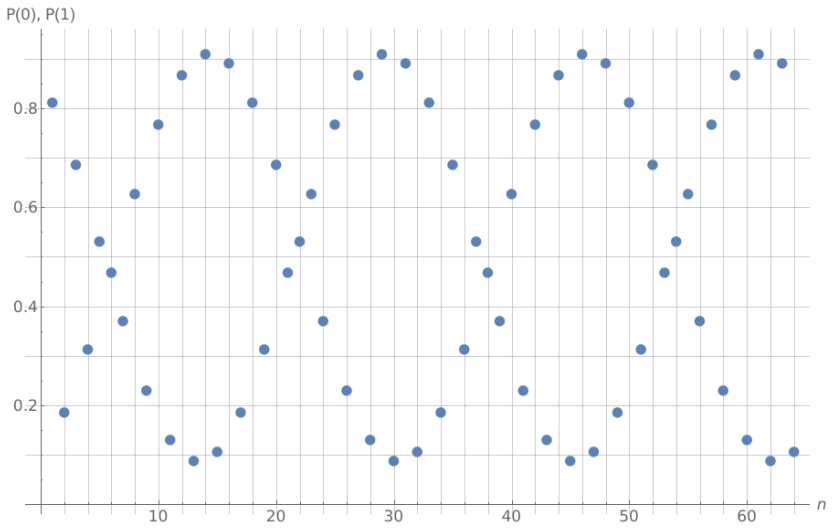

Figure B.1: png
P-W "evolution" for $\hat{\mathbb{J}}$ eigenvalue $= 12$

```
ListPlot[probabilityB,
  GridLines ->{Range[0,NN*2, 2], Range[0, 1, 0.1]},
```

```
  AxesLabel->{n, "P(0), P(1)"},
  LabelStyle->Directive[16],
  PlotMarkers->{Automatic, 16},
  ImageSize->1024
```

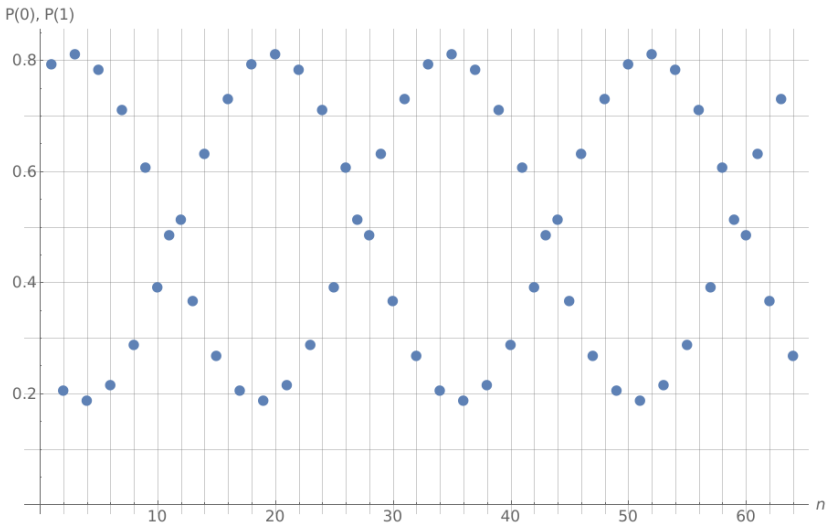

Figure B.2: png
P-W "evolution" for $\hat{\mathbb{J}}$ eigenvalue = 11

B.1.1 Consistency of PW with ordinary QM (discrete approximation)

```
psi0 :=  chosenEigenvectorNormalizedB[[{1,2}]]
```

```
psi[t_] := MatrixExp[-I Hs t, psi0 ]
```

```
Plot[(Abs[psi[t]]^2)[[1]],{t,0,2\[Pi]},
  AxesLabel->{t, "P(0)"},
  LabelStyle->Directive[16],
  ImageSize->900
```

```
Plot[(Abs[psi[t]]^2)[[2]],{t,0,2\[Pi]},
  AxesLabel->{t, "P(1)"},
  LabelStyle->Directive[16],
  ImageSize->900
```

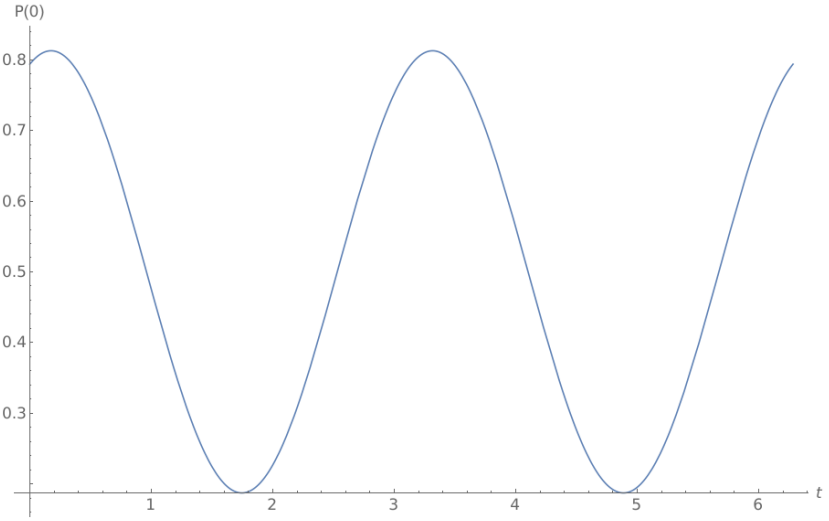

Figure B.3: png
Schrödinger evolution of $|\langle 0|\psi(t)\rangle|^2$, $t \in (0, 2\pi)$ picking the first two components of an eigenvector of $\hat{\mathbb{J}}$ as the two components of $\psi_{t=0}$ in ordinary Hilbert space. Related eigenvalue of $\hat{\mathbb{J}}$ is 11

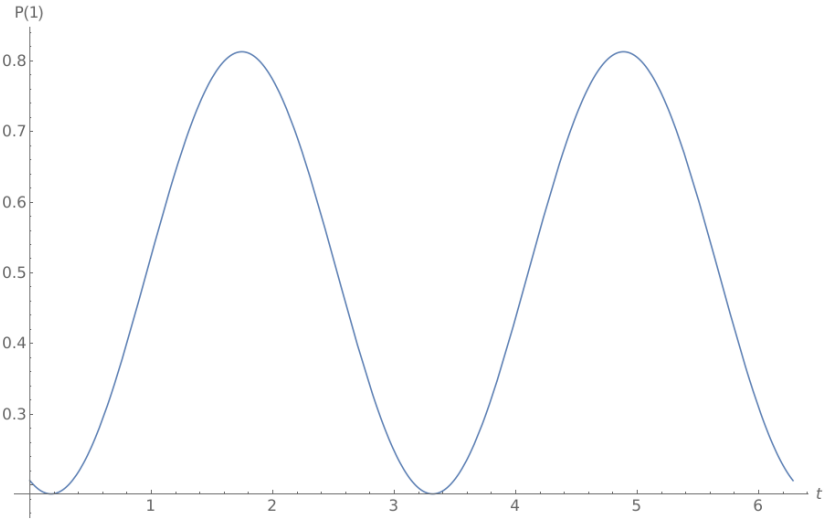

Figure B.4: png
Schrödinger evolution of $|\langle 1|\psi(t)\rangle|^2$, $t \in (0, 2\pi)$ picking the first two components of an eigenvector of $\hat{\mathbb{J}}$ as the two components of $\psi_{t=0}$ in ordinary Hilbert space. Related eigenvalue of $\hat{\mathbb{J}}$ is 11

Complex evolution of ψ (not just $|\psi|^2$)

Please note index count is $1, 2$ (cells above) but refers, respectively, to computational base elements $|0\rangle, |1\rangle$ in ordinary Hilbert space.

```
re0psi[t_] := Simplify[Re[psi[t][[1]]], Assumptions->Element[t, Reals]]
im0psi[t_] := Simplify[Im[psi[t][[1]]], Assumptions->Element[t, Reals]]
re1psi[t_] := Simplify[Re[psi[t][[2]]], Assumptions->Element[t, Reals]]
```

```
zAxis := ParametricPlot3D[{0,0,t}, {t,0,2\[Pi]}, PlotStyle->{Gray}]
psi0plot := ParametricPlot3D[{re0psi[t], im0psi[t], t}, {t, 0, 2\[Pi]},
    PlotStyle->{Red} ]
```

```
Show[zAxis, psi0plot,psi1plot, ImageSize->Medium,
  AxesLabel -> {
    Style[Re["<0,1|\[Psi]>"], Bold],
    Style[Im["<0,1|\[Psi]>"], Bold],
    Style[t, Bold]
  }
```

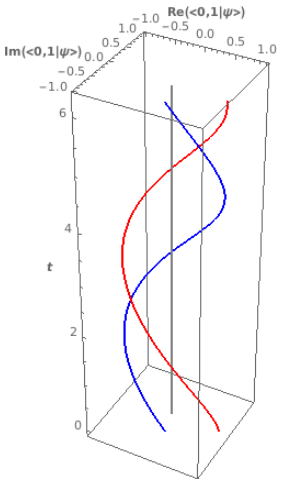

Figure B.5: png
Schrödinger full complex evolution of components $\langle 0|\psi(t)\rangle$ (red) and $\langle 1|\psi(t)\rangle$ (blue) for $t \in (0, 2\pi)$. The initial state has been chosen as the first two components of an eigenstate of $\hat{\mathbb{J}}$, related to eigenvalue = 11.

```
pi = N[\[Pi]]
```

```
rephased[k_] := chosenEigenvectorNormalizedB [[k]] * Exp[-\[ImaginaryI]*pi*11*(k
    -1)/NN]
```

```
rephased1[k_] := chosenEigenvectorNormalizedB [[k]] * Exp[-\[ImaginaryI]*pi*11*(
    k-2)/NN]

scatter[k_] := {Re[ rephased[k]], Im[ rephased[k]], pi*(k-1)/NN}

scatter1[k_] := {Re[ rephased1[k]], Im[ rephased1[k]], pi*(k-2)/NN}

scatterPoints = Map[scatter, Range[1,2*NN, 2]]

Out[ ] = {{0.891003,-0.00706481,0.}, {0.896671,-0.0925068,0.19635},
    {0.86788,-0.174394,0.392699}, {0.805737,-0.249579,0.589049},
    {0.71263,-0.315173,0.785398}, {0.592137,-0.368655,0.981748},
    {0.448889,-0.40797,1.1781}, {0.28839,-0.431607,1.37445},
    {0.116809,-0.438657,1.5708}, {-0.0592618,-0.42885,1.76715},
    {-0.233055,-0.402563,1.9635}, {-0.397892,-0.360805,2.15984},
    {-0.547438,-0.305182,2.35619}, {-0.675946,-0.237831,2.55254},
    {-0.778478,-0.16134,2.74889}, {-0.851094,-0.0786487,2.94524},
    {-0.891003,0.00706481,3.14159}, {-0.896671,0.0925068,3.33794},
    {-0.86788,0.174394,3.53429}, {-0.805737,0.249579,3.73064},
    {-0.71263,0.315173,3.92699}, {-0.592137,0.368655,4.12334},
    {-0.448889,0.40797,4.31969}, {-0.28839,0.431607,4.51604},
    {-0.116809,0.438657,4.71239}, {0.0592618,0.42885,4.90874},
    {0.233055,0.402563,5.10509}, {0.397892,0.360805,5.30144},
    {0.547438,0.305182,5.49779}, {0.675946,0.237831,5.69414},
    {0.778478,0.16134,5.89049}, {0.851094,0.0786487,6.08684}}

scatterPoints1 = Map[scatter1, Range[2,2*NN, 2]]
```

```
scatterPlot = ListPointPlot3D[scatterPoints, PlotStyle->{Red, PointSize[Large]}]
```

```
scatterPlot1 = ListPointPlot3D[scatterPoints1, PlotStyle->{Blue, PointSize[Large
    ]}]
```

```
Show[zAxis, psi0plot,psi1plot,scatterPlot, scatterPlot1, ImageSize->Large,
  AxesLabel->{
    Style[Re["<0,1|\[Psi]>"], Bold],
    Style[Im["<0,1|\[Psi]>"], Bold],
    Style[t, Bold]
  }
```

See Figure 4.2.

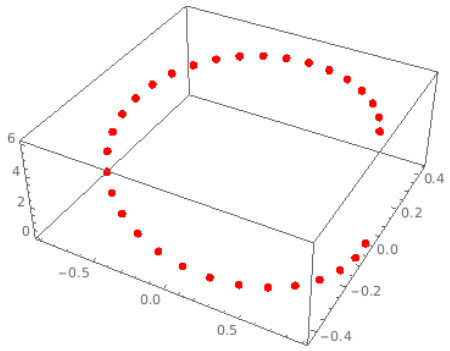

Figure B.6: png
Page–Wootters discrete-time evolution of $\langle 0|\psi(t)\rangle$ in 32 points between $t \in (0, 2\pi)$. From an eigenstate of $\hat{\mathbb{J}}$ related to eigenvalue $\epsilon = 11$. The evolution has been "corrected" via a phase oscillation factor $e^{-i\epsilon t}$ as explained in Giovannetti et al. 2015, *"The Zero-eigenvalue"*.

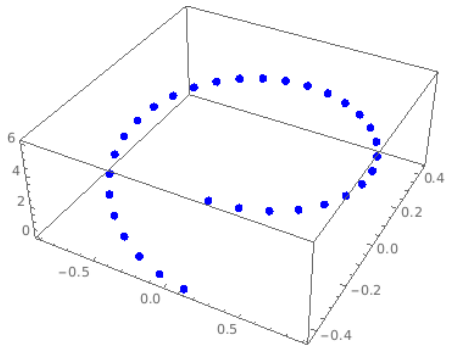

Figure B.7: png
Page–Wootters discrete-time evolution of $\langle 1|\psi(t)\rangle$ in 32 points between $t \in (0, 2\pi)$. From an eigenstate of $\hat{\mathbb{J}}$ related to eigenvalue $\epsilon = 11$. The evolution has been "corrected" via a phase oscillation factor $e^{-i\epsilon t}$ as explained in Giovannetti et al. 2015, *"The Zero-eigenvalue"*.

Bibliography

Adlam, Emily (2022). "Watching the Clocks: Interpreting the Page–Wootters Formalism and the Internal Quantum Reference Frame Programme". In: *Foundations of Physics* 52.5. DOI: 10.1007/s10701-022-00620-7. arXiv: 2203.06755.

Aharonov, Y. and D. Bohm (1961). "Time in the Quantum Theory and the Uncertainty Relation for Time and Energy". In: *Phys. Rev.* 122 (5), pp. 1649–1658. DOI: 10.1103/PhysRev.122.1649.

Allcock, G. R. (1969a). "The time of arrival in quantum mechanics I. Formal considerations". In: *Annals of Physics* 53.2, pp. 253–285. DOI: 10.1016/0003-4916(69)90251-6.

— (1969b). "The time of arrival in quantum mechanics II. The individual measurement". In: *Annals of Physics* 53.2, pp. 286–310. DOI: 10.1016/0003-4916(69)90252-8.

— (1969c). "The time of arrival in quantum mechanics III. The measurement ensemble". In: *Annals of Physics* 53.2, pp. 311–348. DOI: 10.1016/0003-4916(69)90253-X.

Appleby, D M (1998). "Maximal accuracy and minimal disturbance in the Arthurs-Kelly simultaneous measurement process". In: *Journal of Physics A: Mathematical and General* 31.30, pp. 6419–6436. DOI: 10.1088/0305-4470/31/30/009. arXiv: quant-ph/9803047.

ATLAS, Collaboration (2012). "Observation of a new particle in the search for the Standard Model Higgs boson with the ATLAS detector at the LHC". In: *Physics Letters B* 716.1, pp. 1–29. DOI: 10.1016/j.physletb.2012.08.020.

Ballentine, Leslie E. (1998). *Quantum Mechanics: A Modern Development*. 2nd ed. World Scientific. ISBN: 981-02-4105-4.

Bederián, Carlos S and Axel D Dente (2011). "Boosting quantum evolutions using Trotter-Suzuki algorithms on GPUs". In: *Proceedings of HPCLatAm-11, 4th High-Performance Computing Symposium, Córdoba, Argentina*. Citeseer. URL: http://citeseerx.ist.psu.edu/viewdoc/download?doi=10.1.1.705.3488&rep=rep1&type=pdf.

Beneduci, Roberto (2014). "Mathematical Structure of Positive Operator Valued Measures and Applications". PhD thesis. University of Debrecen, Hungary. URL: https://dea.lib.unideb.hu/dea/bitstream/handle/2437/200830/thesis_t.pdf.

Berberian, Sterling K (1966). *Notes on spectral theory*. Vol. 5. Van Nostrand Princeton, NJ.

Blum, K. (2013). *Density Matrix Theory and Applications*. Physics of Atoms and Molecules. Springer. ISBN: 9781475749311.

Bryan, K. L. H. and A. J. M. Medved (2017). *Realistic clocks for a Universe without time*. arXiv: 1706.02531.

Chen, Xi, I. Lizuain, A. Ruschhaupt, D. Guéry-Odelin, and J. G. Muga (2010). "Shortcut to Adiabatic Passage in Two- and Three-Level Atoms". In: *Phys. Rev. Lett.* 105 (12), p. 123003. DOI: 10.1103/PhysRevLett.105.123003. arXiv: 1003.2515.

Choi, Soonwon et al. (2017). "Observation of discrete time-crystalline order in a disordered dipolar many-body system". In: *Nature* 543, pp. 221–225. DOI: 10.1038/nature21426. arXiv: 1610.08057.

CMS, Collaboration (2012). "Observation of a new boson at a mass of 125 GeV with the CMS experiment at the LHC". In: *Physics Letters B* 716.1, pp. 30–61. DOI: 10.1016/j.physletb.2012.08.021.

Cohen-Tannoudji, C., B. Diu, and F. Laloë (1977). *Quantum Mechanics*. Wiley.

Corbin, Vincent and Neil J. Cornish (2009). "Semi-classical limit and minimum decoherence in the Conditional Probability Interpretation of Quantum Mechanics". In: *Found. Phys.* 39, pp. 474–485. DOI: 10.1007/s10701-009-9298-5. arXiv: 0811.2814.

Damborenea, J. A., Íñigo L. Egusquiza, Gerhard C. Hegerfeldt, and J. Gonzalo Muga (2002). "Measurement-based approach to quantum arrival times". In: *Phys. Rev. A* 66 (5), p. 052104. DOI: 10.1103/PhysRevA.66.052104. arXiv: quant-ph/0209027.

De Rosa, Guido (2022). *Jupyter notebooks: quantum models of time*. Git repository: https://github.com/gderosa/timeq/tree/main/comp/jupyter.

Dirac, P. A. M. (1933). "The Lagrangian in Quantum Mechanics". In: *Physikalische Zeitschrift der Sowjetunion, Band 3, Heft 1*. 2005. World Scientific. DOI: 10.1142/9789812567635_0003.

Egusquiza, Íñigo L. and J. Gonzalo Muga (1999). "Free-motion time-of-arrival operator and probability distribution". In: *Phys. Rev. A* 61 (1), p. 012104. DOI: 10.1103/PhysRevA.61.012104. arXiv: quant-ph/9905023.

— (2000). "Erratum: Free-motion time-of-arrival operator and probability distribution [Phys. Rev. A 61, 012104 (2000)]". In: *Phys. Rev. A* 61 (5), p. 059901. DOI: 10.1103/PhysRevA.61.059901.

Englert, F. and R. Brout (1964). "Broken Symmetry and the Mass of Gauge Vector Mesons". In: *Phys. Rev. Lett.* 13 (9), pp. 321–323. DOI: 10.1103/PhysRevLett.13.321.

Esposito, Giampiero (2011). "An Introduction to quantum gravity". In: *Section 6.7.17 of the EOLSS Encyclopedia by UNESCO*. arXiv: 1108.3269.

Fano, U. (1957). "Description of States in Quantum Mechanics by Density Matrix and Operator Techniques". In: *Rev. Mod. Phys.* 29 (1), pp. 74–93. DOI: 10.1103/RevModPhys.29.74.

Fleischhauer, Michael, Atac Imamoglu, and Jonathan P. Marangos (2005). "Electromagnetically induced transparency: Optics in coherent media". In: *Rev. Mod. Phys.* 77 (2), pp. 633–673. DOI: 10.1103/RevModPhys.77.633.

Fock, V. and N. Krylov (1947). "On two main interpretations of the uncertainty relation for energy and time". In: *J. of Phys.(USSR)* 11, pp. 112–120.

Folland, G.B. (1992). *Fourier Analysis and Its Applications*. Wadsworth & Brooks/Cole Advanced Books & Software.

Galapon, Eric (2002). "Pauli's theorem and quantum canonical pairs: the consistency of a bounded, self–adjoint time operator canonically conjugate to a Hamiltonian with non–empty point spectrum". In: *Proceedings of the Royal*

Society of London A: Mathematical, Physical and Engineering Sciences 458.2018, pp. 451–472. DOI: 10.1098/rspa.2001.0874. arXiv: quant-ph/9908033.

Giovannetti, Vittorio, Seth Lloyd, and Lorenzo Maccone (2015). "Quantum Time". In: *Physical Review D* 92.4, p. 045033. DOI: 10.1103/PhysRevD.92.045033. arXiv: 1504.04215v3.

— (2022). *Geometric Event-Based Relativistic Quantum Mechanics*. arXiv: 2206.08359.

Greiner, Walter (2000). *Relativistic quantum mechanics. Wave equations*. Springer-Verlag.

Guralnik, G. S., C. R. Hagen, and T. W. B. Kibble (1964). "Global Conservation Laws and Massless Particles". In: *Phys. Rev. Lett.* 13 (20), pp. 585–587. DOI: 10.1103/PhysRevLett.13.585.

Halliwell, J. J. (1999). "Arrival Times in Quantum Theory from an Irreversible Detector Model". In: *Progress of Theoretical Physics* 102.4, pp. 707–717. DOI: 10.1143/PTP.102.707. arXiv: quant-ph/9805057.

Haroche, Serge and Jean-Michel Raimond (2006). *Exploring the Quantum: Atoms, Cavities, and Photons*. Oxford University Press.

Hawton, Margaret (2019). "Covariant photon quantum mechanics". In: *Phys. Rev. A* 100 (1), p. 012122. DOI: 10.1103/PhysRevA.100.012122. arXiv: 1902.10537.

Hawton, Margaret and Vincent Dabierre (2015). *Photon position observable*. arXiv: 1512.06067.

Heisenberg, W. (1927). "The physical content of quantum kinematics and mechanics". In: *Quantum theory and measurement*. Ed. by J. A. Wheeler and W. H. Zurek. (Originally appeared as "Über den anschaulichen Inhalt der quantentheoretischen Kinematik und Mechanik" in *Zeitschrift fur Physik* 43). Princeton University Press. ISBN: 9781400854554.

Higgs, Peter W. (1964). "Broken Symmetries and the Masses of Gauge Bosons". In: *Phys. Rev. Lett.* 13 (16), pp. 508–509. DOI: 10.1103/PhysRevLett.13.508.

Hunter, J. D. (2007). "Matplotlib: A 2D Graphics Environment". In: *Computing in Science Engineering* 9.3, pp. 90–95. DOI: 10.1109/MCSE.2007.55.

Jacobs, K. (2014). *Quantum Measurement Theory and its Applications*. Cambridge University Press. ISBN: 9781139992190.

Jones, Eric, Travis Oliphant, Pearu Peterson, et al. (2001). *SciPy: Open source scientific tools for Python*. URL: http://www.scipy.org/.

Josset, Thibaut (2017). "The Second Law of Thermodynamics at the Microscopic Scale". In: *Foundations of Physics* 47.9, pp. 1185–1190. DOI: 10.1007/s10701-017-0104-5. arXiv: 1702.07706.

Kennard, E. H. (1927). "Zur Quantenmechanik einfacher Bewegungstypen". In: *Zeitschrift für Physik* 44.4, pp. 326–352. DOI: 10.1007/BF01391200.

Kijowski, Jerzy (1974). "On the time operator in quantum mechanics and the Heisenberg uncertainty relation for energy and time". In: *Reports on Mathematical Physics* 6.3, pp. 361–386. DOI: 10.1016/S0034-4877(74)80004-2.

Kiukas, Jukka, Andreas Ruschhaupt, Piet O Schmidt, and Reinhard F Werner (2012). "Exact energy–time uncertainty relation for arrival time by absorption". In: *Journal of Physics A: Mathematical and Theoretical* 45.18, p. 185301. DOI: 10.1088/1751-8113/45/18/185301. arXiv: 1109.5087.

Kluyver, Thomas et al. (2016). "Jupyter Notebooks — a publishing format for reproducible computational workflows". In: *Ebook: Positioning and Power in Academic Publishing: Players, Agents and Agendas. Proceedings of the 20th International Conference on Electronic Publishing*. Ed. by Fernando Loizides and Birgit Schmidt. Jupyter homepage: http://jupyter.org/. IOS Press, pp. 87–90. DOI: 10.3233/978-1-61499-649-1-87.

Landau, L. and R. Peierls (1965). "6 - Extension of the uncertainty principle to relativistic quantum theory". In: *Collected Papers of L.D. Landau*. Ed. by D. Ter Haar. Originally appeared as "Erweiterung des Unbestimmtheitsprinzips für die relativistische Quantentheorie" in: *Z. Phys.* 69, 56 (1931). Pergamon, pp. 40–51. ISBN: 978-0-08-010586-4. DOI: 10.1016/B978-0-08-010586-4.50011-0.

Leon, Juan and Lorenzo Maccone (2017). "The Pauli objection". In: *Foundations of Physics* 47.12, pp. 1597–1608. DOI: 10.1007/s10701-017-0115-2. arXiv: 1705.09212.

Maccone, Lorenzo (2018). *A fundamental problem in quantizing general relativity*. arXiv: 1807.01307.

Maccone, Lorenzo and Krzysztof Sacha (2020). *Quantum measurements of time*. DOI: 10.1103/PhysRevLett.124.110402. arXiv: 1810.12869v2.

Mandelstam, L. and I. Tamm (1945). "The Uncertainty Relation Between Energy and Time in Non-relativistic Quantum Mechanics". In: *J. Phys. (USSR)* 9, pp. 249–254. DOI: 10.1007/978-3-642-74626-0_8.

Marletto, Chiara and Vlatko Vedral (2017). "Evolution without evolution, and without ambiguities". In: *Physical Review D* 95.4, p. 043510. DOI: 10.1103/PhysRevD.95.043510. arXiv: 1610.04773.

Melo e Souza, Reinaldo de, François Impens, and Paulo A. Maia Neto (2016). "Decoherence by spontaneous emission: A single-atom analog of superradiance". In: *Physical Review A* 94.6. DOI: 10.1103/physreva.94.062114.

Meurer, Aaron et al. (2017). "SymPy: symbolic computing in Python". In: *PeerJ Computer Science* 3, e103. DOI: 10.7717/peerj-cs.103.

Moreva, Ekaterina, Giorgio Brida, Marco Gramegna, Vittorio Giovannetti, Lorenzo Maccone, and Marco Genovese (2014). "Time from quantum entanglement: An experimental illustration". In: *Phys. Rev. A* 89 (5), p. 052122. DOI: 10.1103/PhysRevA.89.052122. arXiv: 1310.4691.

— (2015). "The time as an emergent property of quantum mechanics, a synthetic description of a first experimental approach". In: *Journal of Physics: Conference Series*. Vol. 626. 1. IOP Publishing, p. 012019. DOI: 10.1088/1742-6596/626/1/012019. arXiv: 1502.03264.

Moreva, Ekaterina, Marco Gramegna, Giorgio Brida, Lorenzo Maccone, and Marco Genovese (2017). *Quantum time: experimental multi-time correlations*. arXiv: 1710.00707.

Muga, J. Gonzalo, S. Brouard, and D. Macias (1995). "Time of Arrival in Quantum Mechanics". In: *Annals of Physics* 240.2, pp. 351–366. DOI: 10.1006/aphy.1995.1048.

Muga, J. Gonzalo and C. R. Leavens (2000). "Arrival time in quantum mechanics". In: *Physics Reports* 338.4, pp. 353–438. DOI: 10.1016/S0370-1573(00)00047-8.

Muga, J. Gonzalo, C. R. Leavens, and J. P. Palao (1998). "Space-time properties of free-motion time-of-arrival eigenfunctions". In: *Phys. Rev. A* 58 (6), pp. 4336–4344. DOI: 10.1103/PhysRevA.58.4336. arXiv: quant-ph/9807066.

Muga, J. Gonzalo, J. P. Palao, J. P. Navarro, and Íñigo L. Egusquiza (2004). "Complex absorbing potentials". In: *Physics Reports* 395.6, pp. 357–426. DOI: 10.1016/j.physrep.2004.03.002.

Muga, J. Gonzalo, Andreas Ruschhaupt, and Adolfo del Campo, eds. (2009). *Time in Quantum Mechanics – Vol. 2*. Lecture Notes in Physics 789. Springer Berlin Heidelberg.

Muga, J. Gonzalo, Rafael Sala Mayato, and Íñigo L. Egusquiza, eds. (2007). *Time in Quantum Mechanics – Vol. 1*. 2nd ed. Lecture Notes in Physics 734. Springer Berlin Heidelberg.

Nakahara, Mikio and Tetsuo Ohmi (2008). *Quantum computing: from linear algebra to physical realizations*. Lecture notes available at http://www.math.wm.edu/~ckli/qc2011/taiyuan.pdf. CRC press.

Nakatsugawa, Keiji, Toshiyuki Fujii, and Satoshi Tanda (2017). *Effective Quantum Time Crystal by Decoherence*. arXiv: 1703.04002.

Neumann, J. von (1955). *Mathematical Foundations of Quantum Mechanics*. Originally published as *Mathematische Grundlagen der Quantenmechanik*, Springer-Verlag (1932). Princeton University Press.

Nielsen, Michael A. and Isaac L. Chuang (2011). *Quantum Computation and Quantum Information: 10th Anniversary Edition*. Cambridge University Press. URL: http://www.cambridge.org/9780521635035.

Oberthaler, Markus K., Roland Abfalterer, Stefan Bernet, Jörg Schmiedmayer, and Anton Zeilinger (1996). "Atom Waves in Crystals of Light". In: *Phys. Rev. Lett.* 77 (25), pp. 4980–4983. DOI: 10.1103/PhysRevLett.77.4980.

Oliphant, Travis E. (2015). *Guide to NumPy*. 2nd. USA: CreateSpace Independent Publishing Platform. ISBN: 151730007X.

Oppenheim, Alan V. and Ronald W. Schafer (1989). *Discrete-Time Signal Processing*. 1st, International. Prentice Hall. ISBN: 0-13-216771-9.

— (2014). *Discrete-Time Signal Processing*. 3rd, International. Pearson. ISBN: 1-292-02572-7.

Page, Don N. and William K. Wootters (1983). "Evolution without evolution: Dynamics described by stationary observables". In: *Phys. Rev. D* 27 (12), pp. 2885–2892. DOI: 10.1103/PhysRevD.27.2885.

Palao, J. P., J. Gonzalo Muga, and R. Sala (1998). "Composite Absorbing Potentials". In: *Phys. Rev. Lett.* 80 (25), pp. 5469–5472. DOI: 10.1103/PhysRevLett.80.5469. arXiv: quant-ph/9805035.

Paris, M. G. A. (2012). "The modern tools of quantum mechanics". In: *The European Physical Journal Special Topics* 203.1, pp. 61–86. DOI: 10.1140/epjst/e2012-01535-1. arXiv: 1110.6815.

Pauli, W (1933). "Die allgemeinen Prinzipien der Wellenmechanik". In: *Handbuch der Physik*. English translation: "General Principles of Quantum Mechanics", 1980. Berlin: Springer. Chap. 4.

Peskin, Michael E. and Daniel V. Schroeder (1995). *An Introduction to Quantum Field Theory*. Perseus Books.

Petiziol, Francesco, Ennio Arimondo, Luigi Giannelli, Florian Mintert, and Sandro Wimberger (2020). "Optimized three-level quantum transfers based on frequency-modulated optical excitations". In: *Scientific Reports* 10.1. DOI: 10.1038/s41598-020-59046-8.

Preskill, John (2015). *Lecture notes on Quantum Computation*. Updated version. California Institute of Technology. URL: http://www.theory.caltech.edu/~preskill/ph219/.

Proakis, John G. and Dimitris G. Manolakis (1996). *Digital Signal Processing: principles, algorithms, and applications*. 3rd. Prentice Hall.

Prvanovic, Slobodan (2017). *Operator of Time and Generalized Schroedinger Equation*. arXiv: 1701.05244.

Roncallo, Simone, Krzysztof Sacha, and Lorenzo Maccone (2023). "When does a particle arrive?" In: *Quantum* 7, p. 968. DOI: 10.22331/q-2023-03-30-968. arXiv: 2205.02219.

Rovny, Jared, Robert L. Blum, and Sean E. Barrett (2018a). "^{31}P NMR study of discrete time-crystalline signatures in an ordered crystal of ammonium dihydrogen phosphate". In: *Phys. Rev. B* 97 (18), p. 184301. DOI: 10.1103/PhysRevB.97.184301. arXiv: 1802.00457.

— (2018b). "Observation of Discrete-Time-Crystal Signatures in an Ordered Dipolar Many-Body System". In: *Phys. Rev. Lett.* 120 (18), p. 180603. DOI: 10.1103/PhysRevLett.120.180603. arXiv: 1802.00126.

Ruschhaupt, A, J G Muga, and M G Raizen (2006). "Improvement by laser quenching of an 'atom diode': a one-way barrier for ultra-cold atoms". In: *Journal of Physics B: Atomic, Molecular and Optical Physics* 39.6, pp. L133–L138. DOI: 10.1088/0953-4075/39/6/l05. arXiv: quant-ph/0601213.

Sazonov, V. V. (2002). "Measure". In: *Encyclopaedia of Mathematics*. Kluwer Academic Publishers. ISBN: 1402006098. URL: http://www.encyclopediaofmath.org/index.php?title=Measure&oldid=18607.

Sakurai, J. J. and Jim Napolitano (2011). *Modern Quantum Mechanics*. 2nd. Addison-Wesley.

Scully, Marlan O. and M. Suhail Zubairy (1997). *Quantum Optics*. Cambridge University Press.

Shore, Bruce W. and Peter L. Knight (1993). "The Jaynes-Cummings Model". In: *Journal of Modern Optics* 40.7, pp. 1195–1238. DOI: 10.1080/09500349314551321.

Smith, Alexander R. H. and Mehdi Ahmadi (2019). "Quantizing time: Interacting clocks and systems". In: *Quantum* 3, p. 160. DOI: 10.22331/q-2019-07-08-160.

Srednicki, Mark (2007). *Quantum Field Theory*. Cambridge University Press. URL: http://web.physics.ucsb.edu/~mark/qft.html.

Syrwid, Andrzej, Jakub Zakrzewski, and Krzysztof Sacha (2017). *Time crystal behavior of excited eigenstates*. arXiv: 1702.05006.

Szriftgiser, Pascal, David Guéry-Odelin, Markus Arndt, and Jean Dalibard (1996). "Atomic Wave Diffraction and Interference Using Temporal Slits". In: *Phys. Rev. Lett.* 77 (1), pp. 4–7. DOI: 10.1103/PhysRevLett.77.4.

Thaller, Bernd (1992). *The Dirac Equation*. Springer-Verlag.

Tong, David (2011). *Physics and the Integers*. Is Reality Digital or Analog? Essay Contest. URL: https://fqxi.org/community/forum/topic/897.

Torosov, Boyan T., Giuseppe Della Valle, and Stefano Longhi (2014). "Non-Hermitian shortcut to stimulated Raman adiabatic passage". In: *Phys. Rev. A* 89 (6), p. 063412. DOI: 10.1103/PhysRevA.89.063412. arXiv: 1405.7503.

Vourdas, A (2004). "Quantum systems with finite Hilbert spaces". In: *Reports on Progress in Physics* 67.3, p. 267. DOI: 10.1088/0034-4885/67/3/R03.

Walls, D. F. and Gerard J. Milburn (2008). *Quantum Optics*. 2nd. Springer.

Webber, Bryan (2006). *Gauge Field Theory*. URL: http://www.hep.phy.cam.ac.uk/theory/webber/GFT/.

Weyl, Hermann (1950). "Commutation Rules. Canonical Transformations". In: *The theory of groups and quantum mechanics*. Translated from *Gruppentheorie und Quantenmechanik* (1931). Mineola, NY: Dover Publications. Chap. II, p. 95.

Wiebe, Nathan, Dominic Berry, Peter Høyer, and Barry C Sanders (2010). "Higher order decompositions of ordered operator exponentials". In: *Journal of Physics A: Mathematical and Theoretical* 43.6, p. 065203. DOI: 10.1088/1751-8113/43/6/065203. arXiv: 0812.0562.

Wilczek, Frank (2012). "Quantum Time Crystals". In: *Phys. Rev. Lett.* 109 (16). DOI: 10.1103/PhysRevLett.109.160401. arXiv: 1202.2539.

Wolfram Research, Inc. (2018). *Wolfram Development Platform, Version 11.3*. URL: https://www.wolframcloud.com/.

Wootters, William K. (1984). "'Time' replaced by quantum correlations". In: *International Journal of Theoretical Physics* 23 (8). The Loyola Conference, pp. 701–711. DOI: 10.1007/BF02214098.

Zhang, J. et al. (2017). "Observation of a Discrete Time Crystal". In: *Nature* 543, pp. 217–220. DOI: 10.1038/nature21413. arXiv: 1609.08684.